# DIFFERENTIALLY EXPRESSED GENES IN OESOPHAGEAL CANCER:

## RETINOIC ACID RECEPTOR-ß2, TRIO AND ABL-RELATED GENE

**Katie Emma Hadley**



Thesis submitted in fulfilment of the degree of M.Sc (med)

MRC/ UCT Oesophageal Cancer Research Group
Division of Medical Biochemistry
Faculty of Health Sciences
University of Cape Town

**DECEMBER 2003**

## DECLARATION

I, Katie Emma Hadley, hereby declare that this dissertation is my own unaided work, except where acknowledgements indicate otherwise. Neither the whole work, nor part thereof has been, is being, or is to be submitted for any degree or examination at any other university.

I empower the University of Cape Town to reproduce for the purposes of research, either the whole, or any part of this dissertation, in any manner whatsoever.

Signed by candidate

Katie Emma Hadley
December 2003

## ACKNOWLEDGEMENTS

I wish to express my sincere thanks to the following individuals:

- Dr Denver Hendricks for his excellent supervision, support and enthusiasm
- Prof Bo Wang for his expert instruction and help with sequencing
- Prof Parker, Dr Sharon Prince, Dr Robea Ballo, Dr Collet Dandara, Dr Fred Wamunyokoli for insightful discussions and providing an excellent research environment
- My fellow students Catherine Arendse, Widaad Zemanay, Amaal Abrahams, Dongping Li, Jacquie Bracher, Anna Chen, Tandi Matsha, Michelle Skelton for all the help, laughs and friendship
- All the staff of the division of Medical Biochemistry, especially Hajira Karjiker and Ridwaan Majiet
- Ingrid Baumgarten, who helped with mycoplasm testing
- Heidi de Wet, who helped with real time PCR
- Heather, Nafiesa and Crystal assisted with immunohistochemistry
- Susanne Schmidt, Anthony Koleske, Pierre Chambon and Cecile Rochette-Egly provided antibodies
- Len Neckers, John Moss, Karen Orpitz and Novartis Pharmaceuticals provided drugs
- Arieh Katz, Dharmarai Pillay and Patsy Burger provided cell lines
- MRC and UCT provided funding

## TABLE OF CONTENTS

## LIST OF ABBREVIATIONS

| | |
|---|---|
| 5Aza-dC | 5-Aza-2'-deoxycytidine |
| 5'UTR | 5' Untranslated region |
| 9-cis-RA | 9-cis retinoic acid |
| 17-AAG | 17-Allylamino geldanamycin |
| ADC | Adenocarcinoma |
| ARG | Abl-related gene |
| ASIR | Age standardised incidence rate |
| ATRA | All-*trans*-retinoic acid |
| BCA | Bicinchoninic acid |
| BCR | Breakpoint cluster region |
| CDDP | cis-diamminedichloroplatinum |
| CDK4 | Cyclin dependent kinase 4 |
| CML | Chronic myelogenous leukaemia |
| Cp | Crossing point |
| DAB | Diaminobenzene |
| Dbl | Diffuse B-cell lymphocyte |
| DH | Dbl homology |
| DMEM | Dulbecco's modified Eagle medium |
| DMSO | Dimethyl sulfoxide |
| ECL | Enhanced chemiluminescence |
| EGF | Epidermal growth factor |
| EGFR | Epidermal growth factor receptor |
| FA | Focal adhesion |
| F-actin | Filamentous actin |
| FAK | Focal adhesion kinase |
| GAP | GTPase activating protein |
| GAPdH | Glyceraldehyde-3-dehydrogenase |
| GDI | GDP dissociation inhibitor |
| GDP | Guanine diphosphate |
| GEF | Guanine nucleotide exchange factor |
| GIST | Gastrointestinal stromal tumour |
| GTP | Guanine triphosphate |
| HIF1-α | Hypoxia-inducible factor 1-alpha |
| HNSCC | Head and neck squamous cell carcinoma |
| HPV | Human papilloma virus |
| HRP | Horseradish peroxidase |

| | |
|---|---|
| Hsp90 | Heat shock protein 90 |
| LAR | Leukocyte antigen receptor |
| LDL | Low density lipoprotein |
| LDL-R | Low density lipoprotein receptor |
| MMP | Matrix metalloproteinase |
| MSP | Methylation specific polymerase chain reaction |
| MTT | (3-(4,5-dimethylthiazol-2-yl)-2,5-diphenyl tetrazolium bromide |
| NGF | Nerve growth factor |
| NSCLC | Non-small cell lung cancer |
| OC | Oesophageal cancer |
| OD | Optical density |
| ONPG | o-Nitrophenyl ß-D-Galactopyranoside |
| OSCC | Oesophageal squamous cell carcinoma |
| PBS | Phosphate buffered saline |
| PH | Pleckstrin homology |
| PIPES | Piperazine-*N*,*N*'-bis(2-ethanesulfonic acid) |
| RA | Retinoic acid |
| RAR | Retinoic acid receptor |
| RARE | Retinoic acid response element |
| RIPA buffer | Radioimmunoprecipitation assay buffer |
| RXR | Retinoid X receptor |
| RARß2 | Retinoic acid receptor beta2 |
| Rb | Retinoblastoma |
| RT-PCR | Reverse transcription polymerase chain reaction |
| SCC | Squamous cell carcinoma |
| $sdH_2O$ | Sterile, distilled water |
| SH | Spectrin homology |
| SNP | Single nucleotide polymorphism |
| TBS | Tris buffered saline |
| TGF-α | Transforming growth factor alpha |
| TGF-ß | Transforming growth factor beta |
| TKI | Tyrosine kinase inhibitor |
| UDG | Uracil DNA glycosylase |
| VEGF | Vascular endothelial growth factor |

## ABSTRACT

Oesophageal cancer (OC) is one of the most frequent causes of cancer death in Black South Africans. The molecular mechanisms underlying this disease are poorly understood, although several differentially expressed genes have been identified in oesophageal squamous cell carcinoma (OSCC) tissue compared to normal tissue. These include the genes encoding Retinoic acid receptor ß2 (RARß2), Trio and Abl-related gene (ARG). This study aimed to determine the role played by the products of each of these genes in the development of OC with the objective of identifying potential diagnostic markers or therapeutic targets.

RARß2 expression was found to be downregulated in OSCC cell lines by hypermethylation of the promoter region of the gene. In primary tissue samples, however, hypermethylation of the RARß2 promoter region was observed in only one out of 11 patients. It also seems unlikely that the expression of alternative, less transcriptionally active isoforms of RARß is responsible for the decreased expression in oesophageal cancer (OC), since western blot analysis revealed the presence of a single isoform. However, point mutations were identified in the regulatory regions of the gene, which may be important in the transcriptional downregulation of the gene.

Two anticancer agents that have not previously been used in the treatment of OSCC were tested on OSCC cell lines. 17-Allylamino geldanamycin (17-AAG), an inhibitor of the HSP90 chaperone, was found to inhibit cell growth of eight OSCC cell lines at concentrations in the nanomolar range. However, the cell lines were relatively resistant to Gleevec™, a specific inhibitor of the ARG tyrosine kinase. Although Gleevec was tested in combination with other anti-cancer drugs, no synergistic activity was observed. It was concluded that 17-AAG would be an interesting candidate for further trials in the treatment of OC, but that Gleevec would be of little value as a chemotherapeutic agent for the majority of OC patients.

# CHAPTER 1

# Introduction

## 1.1 Oesophageal cancer

Oesophageal cancer (OC) is the most common cause of cancer death among Black males, and the third most common cancer among Black females in South Africa (Mqoqi *et al.*, 2003). Patients typically have a very low survival rate because the development of the cancer can go undetected until a very late stage. A better understanding of molecular events involved in carcinogenesis is needed to provide efficient screening for the disease, early detection and more effective treatment.

### 1.1.1 Epidemiology

The global distribution of oesophageal cancer is peculiar in that it occurs at a high frequency in very defined geographical regions. For instance, a high incidence of OC is reported in China, Iraq, Iran, and some areas in South America as well as South and Eastern Africa, as shown in figure 1.1. However, in places like North America and Western Europe, the incidence is low. The gradient of incidence is extremely sharp in many cases, with different regions in close proximity having very different levels of disease incidence (Day, 1984). In Africa the occurrence is much more frequent in countries along the East coast of the continent, in a belt stretching from Kenya to South Africa (Day, 1984; Hendricks and Parker, 2002). Countries in Western Africa, such as Mali and the Gambia have a much lower incidence of OC, with age standardised incident rates (ASIR) among males estimated at 1.7 and 0.9 per 100,000 respectively (Bayo *et al.*, 1990; Bah *et al.*, 1990). The prevalence of oesophageal cancer in South Africa is second only to Zimbabwe and Uganda, with an ASIR of 11.6 and 4.9 per 100,000 for males and females respectively (Sitas *et al.*, 1997). OC incidence is especially high in the Black population in the Transkei region

(Dietzsch and Parker, 2002). In the Centane district of the Transkei, the ASIR was reported as 89.0 per 100,000 for males (Marasas, 2001). A population based cancer register of the Umtata region of the Transkei between 1996 and 1999 indicated that the ASIR for OC was 95.3 per 100,000 for males and 54.4 per 100,000 for females (Mugwanya *et al.*, 2001). The reasons for the confined geographical distribution are not well understood at present.

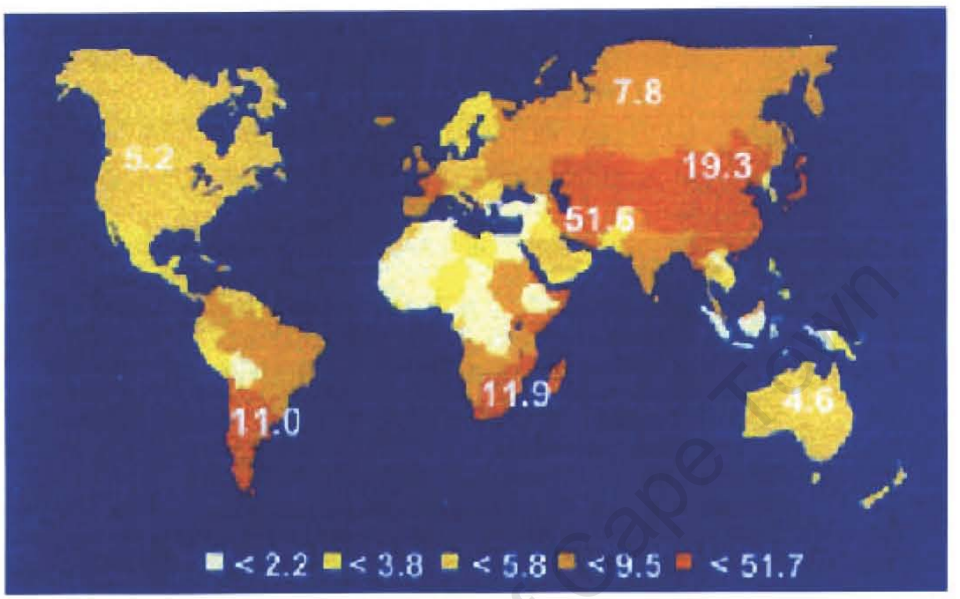


Fig 1.1. Geographic distribution and annual incidence of OC per 100 000 males. Numbers on the map indicate region specific averages (Hamilton and Aaltonen, 2000)

The two main histological subtypes of OC are adenocarcinoma (ADC) and squamous cell carcinoma (SCC). Other types such as mucoepidermoid carcinoma, small cell carcinoma, sarcomatoid carcinoma and melanoma occur infrequently (Lam, 2002). Correct histological classification of cancers is very important, since their development is influenced by different aetiological factors. ADC is associated with gastric reflux and Barrett's oesophagus, a condition in which the normal squamous cells lining the oesophagus are replaced by metaplastic columnar epithelium. ADC is not related to smoking or alcohol. It occurs primarily in developed countries and is much less common than SCC (Meltzer, 1996; Kim *et al.*, 1997). ADC develops mostly in the lower region of the oesophagus and at the gastro esophageal junction, whereas SCC is most

common in the mid- to upper oesophagus. SCC develops from the epithelial cells lining the oesophagus, and occurs mainly in the middle third of the oesophagus (Glickman, 2002). This research focuses on the latter subtype.

### 1.1.2 Aetiology

A number of risk factors have been identified that dramatically increase a person's chances of developing OC. The most significant of these is smoking. In a study carried out in Johannesburg between 1995 and 1999 (Pacella-Norman *et al.*, 2002) it was found that smoking resulted in a three-fold increase in risk for light smokers and a six-fold increase for heavy smokers. Alcohol consumption, weekly or frequently, also doubled the risk of developing the cancer. The combined use of alcohol and tobacco significantly increased the odds ratio for OC in males and females alike.

The risk of OC has a clear link to age. Males most commonly present with the disease between the ages of 55 and 64 years, with females most often presenting with OC over the age of 65 years (Pacella-Norman *et al.*, 2002). The ratio of males to females with the disease is roughly 2:1 (Marasas, 2001; Mugwanya *et al.*, 2001). An association has also been found between education and development of OC. In both males and females, having no education doubled the odds ratio for OC (Pacella-Norman *et al.*, 2002). This may be a reflection of the effect of low socioecomomic status. It has been shown that a poor diet lacking in fresh fruit and vegetables may be a risk factor for OC, as well as deficiencies in various micronutrients (Mettlin *et al.*, 1981). Members of a rural community, with no formal education and low income are most likely to suffer an inadequate diet, predisposing them to the disease. This type of community is representative of most regions of the Transkei, where OC incidence is highest in South Africa (Day, 1984).

Another risk factor shown to have a strong association to OC is the consumption of maize that is infected with fungus of the *Fusarium* species. *Fusarium*

*verticilioides* has been shown to produce toxins called fumonisins that can deregulate the cell cycle and promote cancer (reviewed in Marasas, 2001). Infectious agents such as human papilloma virus (HPV) may also play a role in oesophageal carcinogenesis. HPV is clearly implicated in the development of cervical cancer (Ursic-Vrscaj *et al.*, 1996), and has also been detected in 26-71% of South African OC patients (reviewed in Hendricks and Parker, 2002). The most common types of HPV identified in oesophageal samples are those which are categorized as low-risk for cervical cancer (types 11 and 39) (Matsha *et al.*, 2002).

Other factors that have been suggested to be linked to OC development include any practices that damage the oesophageal epithelium such as the consumption of scalding hot beverages (Nakachi *et al.*, 1988). The consumption of pickled fruit and vegetables, practiced in Iran and China, may also promote OC development, as these foods have been found to contain a number of harmful chemicals, including nitroso compounds, which are thought to act as promoters of OC, at high levels (Li *et al.*, 1981).



### 1.1.3 Treatment

Treatment for OC depends on the age and condition of the patient at presentation with the disease. Oesophagectomy is generally the favoured approach (Linden and Sugarbaker, 2003). Besides a 50% morbidity rate associated with the operation, surgical cure rates are often poor, owing to the high rate of tumour metastasis. In a study of autopsy results of patients who had undergone oesophagectomies, recurrence or residual cancer was observed in 62.8% of patients, as well as frequent metastasis to thoracic, abdominal and cervical lymph nodes (Katayama *et al.*, 2003). The five-year survival rate for patients undergoing oesophagectomy is 20% (Linden and Sugarbaker, 2003).

Neither radiotherapy nor chemotherapy are effective treatments if used individually. However, either of these treatments or a combination thereof may be

used prior to surgery, a technique referred to as "neoadjuvant therapy". This has the benefit of earlier treatment of remote micrometastases, and can give some idea of a patient's prognosis, indicating which patients may not benefit from surgical resection. It is recommended that this treatment be reserved for locally advanced malignancies, and that small, early-stage tumours be surgically removed (Kukreja and Jaklitsch, 2003).

In inoperable cases, the combination of radiotherapy and drugs such as cisplatin can be reasonably effective at slowing the advancement of cancer. However, serious side effects such as nausea and neutropenia (reduction in number of white blood cells, chiefly neutrophils) are seen in some patients (Kumar *et al.*, 2002). Other chemotherapeutic agents used to treat OC include 5-fluorouracil, which is commonly used in combination with cisplatin (Kleinberg *et al.*, 2003). The development of new chemotherapeutic agents to combat OC could result in a greater efficacy of treatment, or reduced negative side effects, which would be of tremendous benefit to patients.



## 1.2 Molecular events in cancer development

The change of a cell from a normal to a malignant state is a multistep process, involving a number of sequential genetic changes (Farber, 1984). Each step confers a new property to the transforming cell, but may result from a variety of different genetic alterations. An excellent review by Hanahan and Weinberg (2000) outlines the minimal characteristics a cell must acquire for transformation to the malignant phenotype. These are discussed below.

Probably the earliest alterations occur in genes that control cellular responses to growth factors and growth-inhibitory factors. While normal cells rely on growth signals from their tissue microenvironment in order to proliferate, most cancer cells have the ability to produce the growth factors necessary to proceed through the cell cycle. For instance, expression of the autocrine growth factors Epidermal growth factor (EGF) and Transforming growth factor alpha (TGF-α) by OC cells is

associated with poor prognosis (Yoshida *et al.*, 1990). Another mechanism by which cells can reduce their reliance on exogenous growth factors, is through increased expression of the growth factor receptors or by altered expression of proteins further downstream in the signaling cascade. One example is the receptor for EGF (EGFR), which is frequently overexpressed in OC through gene amplification (Hollstein *et al.*, 1988; Lu *et al.*, 1988)

In addition to growth factors, cells are exposed to a variety of growth inhibitory factors. In most cases, the response to these growth inhibitory signals involves the Transforming growth factor ß (TGFβ) / Retinoblastoma (Rb) pathway (Hanahan and Weinberg, 2000). When hypophosphorylated, Rb prevents the cell from dividing by sequestering E2F transcription factors necessary for the cell to proceed into the S phase. Cyclin D1, together with Cyclin dependent kinase 4 (CDK4), is involved in phosphorylating the Rb protein, thereby allowing progression through the cell cycle (reviewed in Sherr, 1996). There are a number of ways in which this pathway may be disrupted. In OC, the Cyclin D1 gene is frequently amplified, with simultaneous reduction in the levels of Rb protein (Jiang *et al.*, 1993; Mandard *et al.*, 2000). This allows the cell to grow and divide, by overriding growth inhibitory signals from the environment.

Apoptosis is the ordered breakdown of a cell, in response to physiological stimuli. An important step in cellular transformation is the ability to avoid this process, which can be achieved in two main ways: reducing the cell's sensitivity to apoptotic stimuli, or reducing the cell's ability to undergo apoptosis by disruption of the necessary cellular machinery and signaling cascades. Receptors to survival signaling molecules may be overexpressed and receptors to death signals may be downregulated. The tumour suppressor molecule p53 acts in response to DNA damage to elicit DNA repair or the onset of apoptosis. The p53 gene is mutated in a wide variety of cancers, and mutations in this gene are reported in 50% of cases of OC (Hollstein *et al.*, 1991; reviewed in Lam, 2002; Mandard *et al.*, 2000). This allows the cell to evade apoptosis and contributes to

the accumulation of gross genetic abnormalities in the genome, which may in turn contribute to the cell acquiring more of the critical characteristics of a cancer cell.

A cell's ability to produce its own growth factors and evade apoptosis is not sufficient to confer limitless replication potential. The number of divisions which a cell can undergo is limited by the length of the telomeres, which are shortened by 50-100 bp with each division. Most cancer cells overcome this limitation by overexpression of telomerase, a polymerase which adds hexanucleotide repeats at the ends of the chromosomes to protect them from degeneration, and inevitable cell death (reviewed in Kim, 1997).

Later steps in the transformation process include the ability to nourish the growing tumour by developing a network of capillaries to carry blood to the cells. The overexpression of Cyclin D1 by oesophageal tumour cells is reported to increase the expression of Vascular endothelial growth factor (VEGF), which is necessary for the formation of blood vessels into the tumour tissue (Shintani *et al.*, 2002).

Invasion of surrounding tissue is a common problem associated with OC (reviewed in Hendricks and Parker, 2002). A number of molecular alterations may jointly be responsible for this feature of OC. One example is the frequent deregulation of Matrix metalloprotease (MMP) expression. These enzymes digest proteins in the extracellular matrix, allowing the tumour cells to break through surrounding tissue. Expression of several MMPs in OC has been studied by immunohistochemistry and most are detected in at least half of OC patients (reviewed in Lam, 2002).

The precise mutations within a cell and the sequence in which they are attained may vary dramatically, even within otherwise histologically identical tumours. However they all serve to accomplish the same biological endpoints.

## 1.3 Aims of Research

Management of OC in South Africa presents a serious burden to the health sector, which faces the problems of limited resources, and sometimes extremely rural settings (reviewed in Hendricks and Parker, 2002). Screening for the disease at an early stage is not feasible, and better prognostic and diagnostic measures need to be instituted if patient survival is to be improved. Better understanding of the process and events involved in oesophageal carcinogenesis could reveal new targets for therapy. It could also allow the identification of protein markers of cells, allowing for early detection of cellular transformation, or measurement of factors reflecting metastatic potential, prognosis, or responsiveness to different therapies.

The molecular changes discussed in section 1.2 have been identified using techniques such as differential display reverse transcription polymerase chain reaction (RT-PCR) and microarray hybridisation. These techniques only serve to identify a large cohort of genes that have altered levels of transcription. A more detailed investigation into the cellular effect of molecular changes is necessary for this information to be beneficial.

This project aims to investigate a few of the molecular changes that have been identified in OC by microarray analysis (carried out by Wamunyokoli, 2002). Of a large cohort of differentially expressed genes, three genes of interest were selected for a more indepth analysis. They are Retinoic Acid Receptor β2 (RARß2), a putative tumour suppressor gene; Trio, a multidomain signalling protein which has been implicated in cell motility; and Abl-related gene (ARG), a tyrosine kinase which is reported to be a target of the newly developed anti-cancer drug Gleevec™.

# CHAPTER 2

## Hypermethylation of the RARβ2 promoter region

### 2.1 Introduction

Loss of expression of Retinoic Acid Receptor ß (RARß) is an early event in the progression of oesophageal carcinogenesis (Qiu *et al.*, 1999). Microarray analysis has shown that expression of RARβ2 is reduced in tumour tissue to almost half the level of normal tissue (Wamunyokoli, 2002). However, the cause of the altered expression levels has not been determined. In breast and cervical cancers, decreased expression of this gene has been attributed to hypermethylation of the promoter region of the gene. The aim of this research was to determine whether a similar mechanism is responsible for RARß2 suppression in OC.

#### 2.1.1 Retinoid receptors in cancer development

The term retinoid encompasses all natural and synthetic vitamin A analogues and metabolites (Sun and Lotan, 2001). The endogenous retinoids play an important role in regulating fundamental biological processes including cell differentiation, proliferation and apoptosis. The effects of these retinoids are mediated by a family of retinoid receptors, that belong to the steroid hormone receptor superfamily. Retinoid receptors are transcriptionally active when complexed to their ligand, and are categorised as either retinoic acid receptors (RARs) or rexinoid receptors (RXRs) on the basis of their different ligand specificity. RARs can complex with either all-*trans*-retinoic acid (ATRA) or 9-cis-retinoic acid (9-cis-RA), while RXRs can only complex with 9-cis-RA. These two types of receptors usually function as heterodimers. Each type of receptor (RAR or RXR) includes three subtypes: α, β, and γ. These differ in their amino- and carboxy-terminal domains (reviewed in Altucci and Gronemeyer, 2001).

Genes that are transcriptionally regulated by retinoids have a conserved sequence in the promoter region called the retinoic acid response element (RARE). The RARE usually consists of two directly repeated half-sites of the sequence AGGTCA separated by 2 or 5 bases (Chambon, 1996). When not complexed to a ligand, the heterodimers of RAR and RXR bind to the RARE. This creates a complex with a corepressor that binds Histone deacetylase. The removal of acetyl groups from the histone proteins stabilises the DNA in a condensed form and the gene is not transcribed. However, binding of RA to the RAR-RXR complex induces a conformational change in the ligand-binding domain. This destablises the interaction with the corepressor, allowing coactivators of the p160 family (PIC1, TIF2, and AIB1) to bind to the complex instead. These co-activators recruit Histone acetyltransferase, which acetylates histone proteins, allowing the chromatin to decondense and thus be transcribed (Altucci and Gronemeyer, 2001).

Four isoforms of RARβ have been identified, which arise from differential usage of promoters and alternative splicing. These are designated RARβ1 to 4 (Sun and Lotan, 2002). All four transcripts of RARβ were identified in a mouse model (Nagpal *et al.*, 1992; Zelent *et al.*, 1991) and only RARβ2 and RARβ4 have been reported to be expressed in normal human adult cells (de The *et al.*, 1989). The ß2 and ß4 transcripts differ by 357 bases in exon 5, which are present in RARβ2, but spliced out of RARβ4. RARß' is an antagonistic isoform that has been identified in breast cancer. It is the product of translation from an alternative start site in the ß2 or ß4 mRNA downstream of the start site used to generate the ß2 and ß4 proteins (Chen *et al.*, 2002). The different transcripts and isoforms are depicted in figure 2.1.

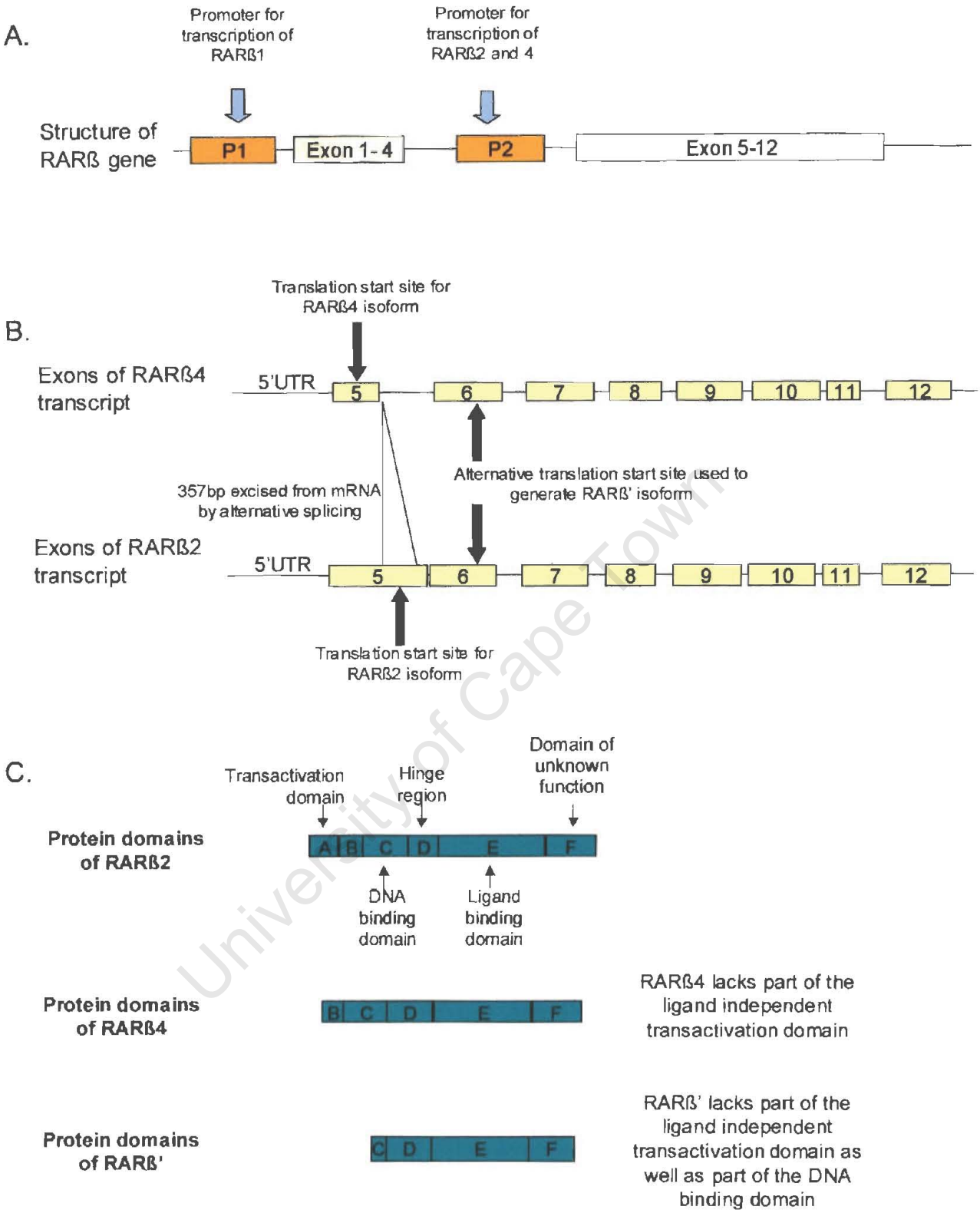


Fig. 2.1. Schematic representation of the generation of different isoforms of human RARß, including (A) gene structure, (B) the different transcripts transcribed from P2 (C) the structural differences between RARß2, ß4 and ß' (modified from Toulouse *et al.*, 1996; Chen *et al.*, 2002)

The RARβ gene has a conserved RARE site in the P2 promoter region. The RAR-RXR heterodimers bind to this consensus sequence to mediate transcription of RARß in response to ligand binding (Widschwendter *et al.*, 2000). Thus the expression of RARβ2 is autoregulated, and is induced by the presence of retinoic acid.

Genes under the control of RARβ2 regulation were identified using subtractive hybridization and DNA array analysis in a teratocarcinoma model. These genes encode transcription factors, cell surface signal transducing proteins and metabolic enzymes such as *c-myc*, *FOG1*, glutamate dehydrogenase, glutathione S-transferase homologue (p28) and Platelet derived growth factor-α receptor (Zhuang *et al.*, 2003).

Expression of RARβ2 has been shown to be reduced in the development of a wide range of cancers. As early as 1985, before the identification of the different classes of RARs, de Bolla *et al.* reported that RAR expression in bladder tumours was inversely related to tumour stage and grade. They also linked high incidence of tumour recurrence and lower survival rate to reduced expression of this receptor. In breast cancer, a progressive decrease in the level of RARβ mRNA throughout the stages of carcinogenesis was observed by *in situ* hybridization (Xu *et al.*, 1997). Expression was detected in 98% of adjacent normal tissues, with the frequency decreasing to just 35.7% in poorly differentiated invasive carcinomas. A very similar pattern was observed in head and neck squamous cell carcinoma (HNSCC). About 70% of adjacent normal and hyperplastic lesions were found to express RARβ. This level decreased to 56% for dysplastic lesions and 35% for HNSCC (Xu *et al.*, 1994).

Significant reduction in RARβ expression occurs even in premalignant oral lesions (Lotan *et al.*, 1995; Chakravarti *et al.*, 2000). Although the receptor was detected in 100% of normal specimens by *in situ* hybridization, only 40% of premalignant oral tissue samples were found to express the receptor. While

RARβ is expressed in normal lung tissue, it has been shown that most epidermoid (squamous cell) lung cancer cell lines do not express RARβ mRNA, although the gene is intact. Transfection of such cells with RARβ resulted in reduced growth rate and a marked reduction in tumourigenicity when injected into nude mice (Houle *et al.*, 1993). RARβ mRNA was undetectable in 50% of non-small-cell lung cancers (Khuri *et al.*, 2000), with similar patterns of expression observed in cervical, prostate and pancreatic carcinomas (Ivanova *et al.*, 2002; Lotan *et al.*, 2000; Xu, 2001 respectively). A large body of evidence strongly suggests that RARβ may function as a tumour suppressor gene in a number of different cancers.

A study in China has shown that RARβ expression was lost in nearly 50% of invasive oesophageal cancers and 43% of moderate to severe dysplastic lesions (Qiu *et al.*, 1999). While the study suggested that loss of RARβ was an early event in oesophageal carcinogenesis, the cause of the reduced expression was not determined. Interestingly, there is evidence to suggest that in some cancers, DNA hypermethylation plays a role in reducing expression of this receptor. The possibility that RARß2 promoter hypermethylation occurs in OC is addressed in this study. An overview of how DNA methylation is associated with gene silencing follows.



### 2.1.2 DNA methylation

The frequency of the CpG dinucleotide in the eukaryotic genome has been steadily declining over the course of evolution (Ng and Bird, 1999). In the vertebrate genome the CpG doublet occurs at a frequency of only 20% of what would be expected from the proportion of GC base pairs (Lewin, 1997). However short segments of CpG repeats (0.5- several kb long) known as CpG islands are associated with at least half of all cellular genes (Baylin and Bestor, 2002). There are about 45 000 CpG islands in the human genome, located in regions proximal to gene promoters (Lewin, 1997). Addition of a methyl group to these cytosine

residues, as shown in figure 2.2, is an important regulator of gene expression, since gene silencing due to methylation can be inherited by daughter cells (Baylin and Herman, 2000). Examples of methylated DNA may be found in the inactivated X chromosome, imprinted genes, and genes that are regulated by methylation during the course of development (Smiraglia *et al.*, 2001).

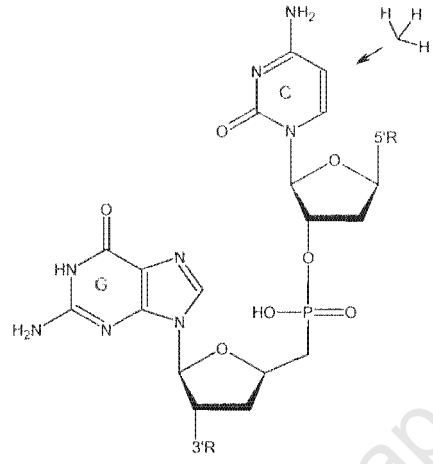


Fig. 2.2. Methylation of the cytosine residue in a CpG dinucleotide

It has long been recognised that methylation patterns in tumour cells differ from those of normal cells. The general trend in cancer genomes is widespread hypomethylation with regions of very dense hypermethylation (Costello *et al.*, 2000). Whether these aberrant methylation patterns are a direct cause of cellular transformation, or arise as a consequence of a cell becoming tumorigenic is still an area of considerable debate (Baylin and Bestor, 2002). However, recent evidence has shown that removal of methylation by genetic, rather than chemical means (i.e. mutational inactivation of methyltransferase enzymes) resulted in re-expression of the epigenetically silenced gene which was accompanied by decreased methylation of the surrounding histones. Over time these cells exhibited a re-silencing of the gene with methylation of the histones, but no DNA methylation. This suggests that methylation does not initiate gene silencing, but can serve to cement the transcriptional repression initiated by another route (Bachman *et al.*, 2003).

Alterations in DNA methylation can have a variety of effects which could all contribute to the development of cancer. For example, methylation of a promoter region is associated with chromatin condensation, which prevents transcription factors from binding to the DNA, resulting in failure to initiate transcription. In instances where the silenced genes are involved in control of cellular proliferation, this could lead to cancer formation or progression. Furthermore, although methylation is an epigenetic event, unlike mutation, it has been shown that areas of dense CpG methylation act as hotspots for acquired somatic mutations. A good example of this phenomenon is demonstrated by the observed mutation in the genes encoding the Low density lipoprotein receptor (LDL-R) and p53 (Rideout *et al.*, 1990). 5-methylcytosine functions as an endogenous mutagen (Robertson and Jones, 2000). Deamination of unmethylated cytosine results in uracil. Since uracil is not a naturally occurring residue in DNA, the change is readily detected and repaired by uracil DNA glycosylase (UDG). However, spontaneous deamination of methyl cytosine results in the formation of thymine. This base is not as easily detected by DNA repair enzymes, resulting in a high frequency of C to T transversions in methylated CpG islands. The rate of spontaneous deamination in CpG islands is sufficient to account for all mutations in double stranded DNA (Shen, Rideout and Jones, 1994). The rate of cell division is also important in determining the stability of 5-methylcytosine. It has been shown in bacteria that cell division can determine the level of mutagenicity of the base (Lieb and Rehmat, 1997), and it has also been documented that the level of CpG mutation is higher in cancers where hormones stimulate cell division (such as breast cancer) or where tissues are damaged and undergoing repair (Greenblatt *et al.*, 1994). The multistep model of cancer development accommodates all the above factors, although they may be of varying importance in different cancers during the course of transformation.

The methyltransferase inhibitor 5-Aza-dC has been used successfully in the treatment of human cancers (Karpf and Jones, 2002). It is incorporated into

genomic DNA during DNA replication, and binds covalently to the active site of DNA methyl transferase I, the enzyme responsible for maintenance of DNA methylation in the genome. By inactivation of this enzyme, treatment with 5-Aza-dC leads to reactivation of epigenetically silenced genes and gradual chromatin decondensation over time. The drug has some cytotoxic effects which are thought to be a result of widespread genomic DNA demethylation. This may be a primary result of the covalent trapping of the methyltransferase, with subsequent expression of previously silenced genes being a secondary effect (Jutterman *et al.*, 1994).

Since it has been found that RARß2 expression is reduced in OC, this study was conducted to investigate the involvement of DNA methylation in this event. The specific aims of this study were:

- To determine whether hypermethylation of the RARß2 P2 promoter is involved in downregulation of RARß2 expression in OC cell lines
- To establish the role of RARß2 promoter hypermethylation in cancer development in vivo
- To investigate the role played by expression of different isoforms of the RARß protein in reduced RARß2 expression

## 2.2 Methodology

### 2.2.1 Cell culture and treatment

Four OC cell lines of South African origin (WHCO1, WHCO3, WHCO5, WHCO6) (Veale and Thornley, 1989) and three cell lines of Japanese origin (KYSE30, KYSE70, KYSE520) (Shimada *et al.*, 1992) were used in this study. Routine cell culture methods and cell line characteristics are detailed in Appendix 1.

5-aza-2'-deoxycytidine (5-Aza-dC) (Sigma), a DNA demethylating agent, and all-*trans*-retinoic acid (ATRA) (Sigma) were dissolved in DMSO (Sigma) to make

stocks of 2.5mM and 1mM respectively. Cells were treated as described in table 2.1.

Table 2.1. Treatment of cell lines prior to extraction of RNA for RT-PCR

| | Treatment | Duration | Expected result |
|---|---|---|---|
| 5-Aza-dC | 2.5µM 5-Aza-dC | 5 days | Demethylation of genomic DNA |
| ATRA | 1µM ATRA | 1 day | Induction of RARß2 |
| 5-Aza-dC + ATRA | 2.5µM 5-Aza-dC 1µM ATRA | 5days 1day | Demethylation of genomic DNA with subsequent induction of RARß2 |
| Control | DMSO to 0.1% final volume | 1 day | No effect |

All cells were exposed to the same concentration of DMSO solvent (0.1% final volume). Previous studies performed in the laboratory have shown that DMSO has an inhibitory effect on cell growth only at concentrations higher than 0.5% (Marian Brennan, personal communication).

### 2.2.2 Reverse transcription PCR

RNA was extracted using the TRI-zol reagent (Invitrogen Corp., CA) as per manufacturer's instructions. This is a widely used reagent that allows the extraction of total RNA from cultured cells or tissues without ultracentrifugation steps. The isolated RNA was run on a 1% agarose gel containing formaldehyde to check the quality of the RNA by comparing the ratio of 18S:28S bands and any smearing of the bands. Only RNA of high quality was used in subsequent experiments.

One-step reverse transcription PCR was carried out using the GeneAmp EZ rTth RNA PCR Kit (Applied Biosystems, New Jersey). rTth is a recombinant thermostable enzyme that has both reverse transcriptase and polymerase activity. Hot start multiplex PCR was used to amplify a 721bp region of the RARβ2 transcript and a 276bp region of the low density lipoprotein receptor (LDL-R) transcript, with the latter transcript serving as an internal control for the PCR reaction and RNA integrity. The primers used for the amplification were described by Widschwendter *et al.* (2000) (sequences are included in appendix 1). They spanned introns to eliminate the possibility of amplification of contaminating genomic DNA, and the forward primer for RARß2 lay within the 357bp region that is spliced from the RARß4 transcript, in order to make the reaction specific for the amplification of RARß2. The location of primer sequences is shown schematically by the position of red arrows in figure 2.3.

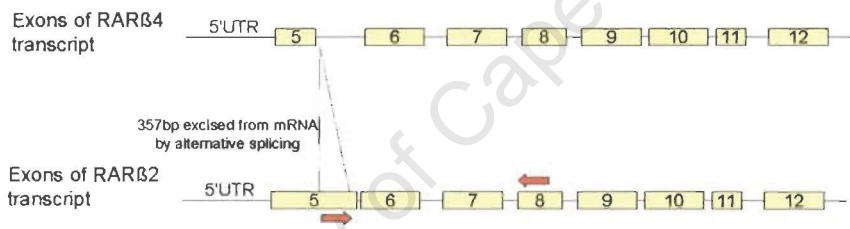


Fig. 2.3. Transcripts of RARß4 and RARß2, showing position of primers (red arrows) as described in text (Widschwendter *et al.*, 2000)



The RT-PCR reaction was carried out in a total volume of 50μl including 1μg RNA, 5μl 10x EZ buffer, 300μM of each dNTP, 0.45μM of each primer, 2.5mM manganese acetate, and 5 units of rTth polymerase. The thermocycling was carried out in a GeneAmp PCR system 2700 (Applied Biosystems) under the following conditions:

Reverse transcription at 65°C for 40 minutes; denaturation at 94°C for 90s; eighteen cycles of 94°C for 45s, 65°C for 30s, 72°C for 60s; five cycles in which the elongation step was increased to 75s, followed by five cycles in which the

elongation step was 90s. PCR products were run on a 2% agarose gel and viewed by ethidium bromide staining. A lane of molecular weight marker VIII (Promega) was run to indicate the size of the product generated.

### 2.2.3 Northern blot analysis

RNA extracted from the treated and untreated cells was run on a 1% agarose gel containing 20mM MOPS and 5.4% formaldehyde. The RNA was transferred to a Hybond $N^+$ membrane (Amersham Pharmacia Biotech, UK) and baked at 80°C for three hours. The blots were incubated with a $^{32}P$ labeled probe (described below) at 42°C overnight in ULTRAHyb™ hybridization solution (Ambion), and exposed to autoradiographic film (Agfa) at –70°C for up to two weeks.

Several different probes were used. The first (hRARß) was specific for the entire 3' region of the transcript, encoding domains A-F, which would largely be common to all isoforms (Brand *et al.*, 1988). The second was designed to be specific for the RARß2 transcript. This probe was generated by isolating the 721bp RT-PCR product shown in figure 2.3 using a QIAquick spin column purification according to the manufacturer's protocol (Qiagen, CA), and cutting it with the SphI restriction enzyme (Boehringer Mannheim) at 37°C overnight. This yielded a 170bp fragment, which was purified as previously. This fragment was from the 5' end of the PCR product, and was unique to the RARß2 transcript. The third probe was generated by PCR of genomic DNA using primers that annealed within the 357bp region unique to the RARß2 transcript, to yield a 330bp PCR product as described by Sommer *et al.* (1999).

The blots were then stripped to remove radioactivity, by shaking in stripping buffer at 90°C for 3 minutes, and probed with a $^{32}P$ labeled 18S probe (prepared by standard PCR using primers described in Uray *et al.*, 2002) as an internal standard. The density of bands on the autorads was determined on a densitometer (Chemi-Imager 5500, Alpha Innotech). Values for RARß calculated

as a ratio of 18S. Background readings were automatically calculated as an average of the 10 least dense pixels in a given band.

### 2.2.4 Sodium bisulfite genomic sequencing

The treatment of DNA and subsequent PCR were carried out as described by Widschwendter *et al.* (2000). Briefly, 8µl of 3M NaOH was added to 4µg of DNA in a volume of 70µl. This was incubated at 37°C for 15 minutes, heated to 95°C for 3 minutes, and put directly onto ice. 1ml of bisulfite reagent (freshly prepared by adding 8.1g of sodium metabisulfite to 15ml water, adding 1ml of 40mM hydroquinone and adjusting pH to 5.0 with 3M NaOH) was added. The DNA was then incubated at 55°C in the dark for 16 hours. The DNA was recovered using the GENECLEAN III kit (Qbiogene) and eluted in 100µl of water. 11µl of 3M NaOH was added, before incubation at 37°C for 15 minutes. 110µl 6M Ammonium acetate (pH7.0) was added, and DNA was recovered by ethanol precipitation with 1ml absolute ethanol. The DNA pellet was washed with 70% ethanol, air dried and resuspended in 80µl of water. 1µl of this solution was used as template for each PCR reaction.

Nested PCR was carried out using the primers that amplified a fragment from RARß2 P2 and part of exon 5, as detailed in Appendix 1. The PCR products were cloned into the pGEM T-Easy vector (Promega). Sequencing was performed either (i) manually using the Sequenase Quick-denature Plasmid Sequencing kit (USB Corp.) according to the manufacturer's instructions (with $^{32}$P dCTP); or (ii) using the DNA Sequencing Kit Big Dye Terminator V3.0 Cycle Sequencing Ready Reaction Mix (Applied Biosystems, CA), and an automated sequencer.

Cells grown in culture may display altered methylation patterns compared to the primary tissue from which they were derived (Smiraglia *et al.*, 2001). It was therefore important to investigate the level of methylation of the RARß2 promoter

in primary oesophageal tumour tissue compared to normal. DNA extracted from the tissue was treated in the same way as described for cell line DNA, and sequenced manually.

### 2.2.5 Methylation Specific PCR (MSP)

MSP was carried out as described by Kuroki *et al.* (2003) with modifications. DNA was treated with sodium bisulfite as described in section 2.2.4. Sodium bisulfite modified DNA was amplified in two separate reactions using primers specific for methylated and unmethylated DNA. PCR was performed in a final volume of 25µl containing 1x PCR buffer (50mM KCl; 10mM Tris.HCl, pH 8.4), 2mM $MgCl_2$, 0.2mM each dNTP, 10pmol each primer, 1µl Taq polymerase, and approximately 50ng template DNA.

PCR cycling conditions were as follows: 10 minutes at 94°C; 35 cycles of 30s at 94°C, 30s at 55°C, and 30s at 72°C; followed by a final 5 minute extension at 72°C. Primers specific for ß-actin (Matsha *et al.*, 2002) were used as a positive control for DNA integrity.

### 2.2.6 Western Blot Analysis

Cells were grown in 60mm dishes until ~80% confluent. Media was collected and floating cells were pelleted by centrifugation for 5 minutes at maximum speed in a Spinnette desktop centrifuge (IEC). Adherent cells were washed three times with cold PBS, and collected in 200µl RIPA solution containing the protease inhibitors pepstatin, aprotinin and leupeptin, by scraping with the plunger of a 1ml syringe. The pellet of cells from the media was resuspended in this solution. Cell solution was sonicated for 10 seconds to break up cell material, and quantitated using the bicinchoninic acid (BCA) assay kit (Pierce). An equal amount of each sample was mixed with 2x loading dye and heated to 95°C for 10 minutes, before loading on a 15% polyacrylamide gel. The gel was run at 200V for 1 hour. The

protein from the gel was transferred to Hybond ECL nitrocellulose membrane (Amersham Pharmacia Biotech) for 1 hour at 100V. The blot was blocked in TBS-tween with 5% fat-free milk powder for 1 hour at room temperature, and then incubated overnight at 4°C in primary mouse monoclonal antibody (RARß F region Ab8ß(F)2 (8ß-10ß2)) provided by Chambon and Rochette-Egly, at a dilution of 1:5000, as described in Rochette-Egly *et al.* (1991). The membrane was then washed twice in TBS-tween for 10 minutes each, followed by two 10 minute washes in 5% fat-free milk powder solution. The blot was incubated in secondary antibody (HRP conjugated goat- anti-mouse) (Bio-Rad) at a dilution of 1:5000 for 1 hour, followed by four 10 minute washes in TBS-tween. Signal detection was carried out using the SuperSignal West Dura Extended Duration Substrate Kit (Pierce).

## 2.3 Results and discussion

### 2.3.1 Reverse transcription PCR

Reverse transcription PCR (RT-PCR) was employed to detect the presence of RARß2 mRNA in 5-Aza-dC and ATRA treated cells. 5-Aza-dC covalently binds to DNA methyltransferase I, thus treating cells with this agent results in a gradual reduction in methylation in genomic DNA over a number of cell divisions. ATRA, on the other hand, was used to induce expression of RARß2.

Cells treated with DMSO alone served as a control for the effects of the solvent, as constitutive RARß2 expression is expected to be low in OSCC cell lines. A water blank without RNA was used to monitor possible contamination of the RT-PCR reaction. As a positive internal control, primers specific for mRNA of the Low density lipoprotein receptor (LDL-R) gene were included in each reaction. LDL-R is a housekeeping gene, and its expression is not affected by methylation (Widschwendter *et al.*, 2000). Amplification of a product by these primers indicated that the template RNA was intact and that the RT-PCR reaction was

free of inhibitors. It was also used to give a semi-quantitative indication of equal loading of RNA in each reaction.

This experiment, including plating and treatment of cells, harvesting of RNA and RT-PCR, was repeated three times. Figure 2.4 shows representative results of the three independent experiments.

The absence of bands in the water blank lanes indicates that there was no contamination, and no false-positive amplification. In all the other lanes, the amplification of a 276bp region of the LDL-R transcript indicates that no inhibitors of PCR were present in the reaction. It also serves as a loading control. In three out of the seven cell lines tested (WHCO1, WHCO6, and KYSE70) a band of 721bp is amplified from cells treated with 5-Aza-dC and ATRA. This is a portion of the RARß2 transcript, indicating that the gene is expressed only when methyl groups have been removed from DNA (by 5-Aza-dC treatment) and the gene is induced (by treatment with ATRA).

Amplification of RARß2 mRNA is seen in WHCO6 cells following treatment with 5-Aza-dC, as evidenced by the presence of a weak band in lane 1. This indicates that removal of methyl groups is sufficient to initiate transcription of RARß2 in this cell line, without induction by ATRA.

We hypothesise that promoter hypermethylation was responsible for gene silencing in three out of seven cells lines, and that yet another mechanism was responsible for the low level of RARß2 expression observed in the other cell lines.

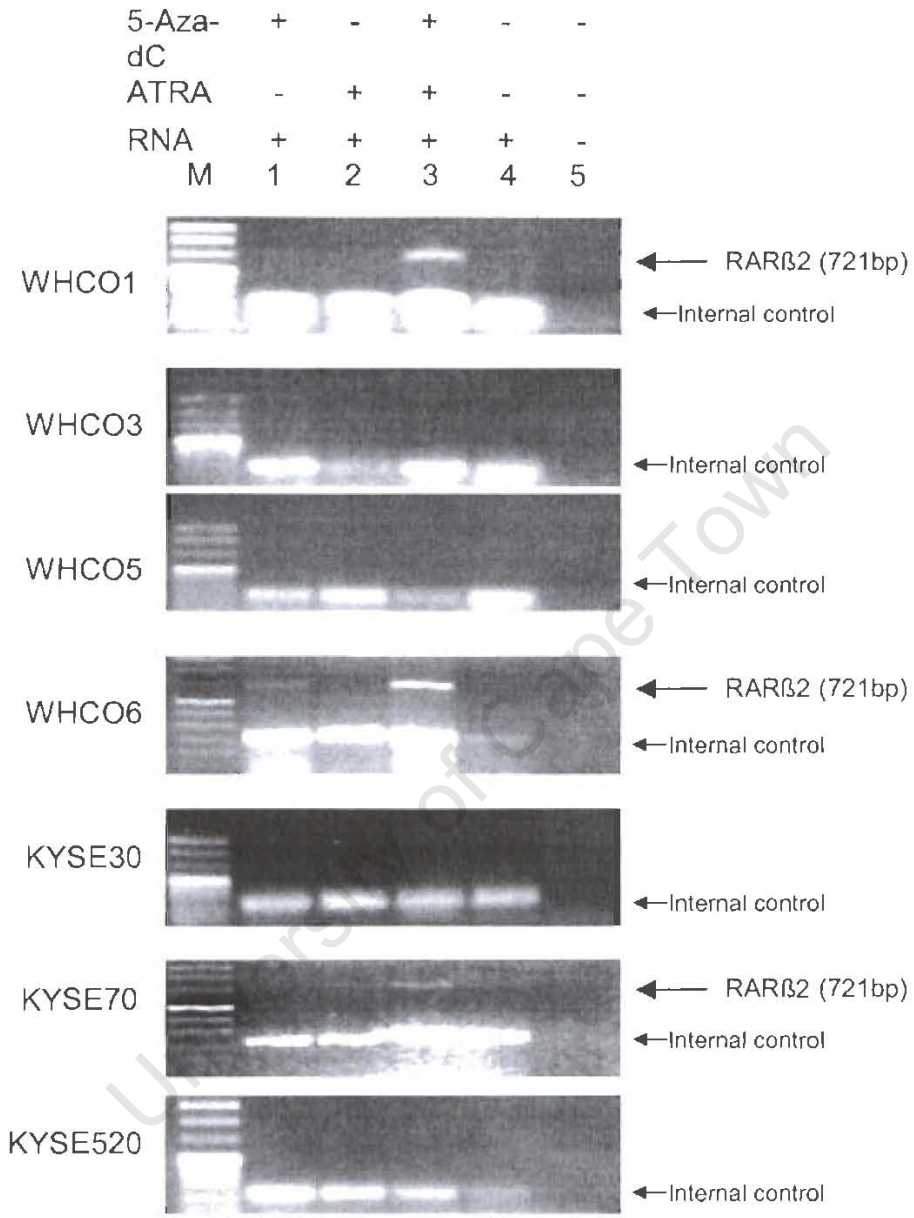


Fig. 2.4. Quantitation of RARß2 RNA in OSCC cell lines. RT-PCR was carried out as described in section 2.2.2, and the PCR products were separated on 2% agarose gel. Cells had been treated as follows: lane 1: 5-Aza-dC for five days; lane 2: ATRA for 1 day; lane 3: 5-Aza-dC for five days followed by ATRA for 1 day; lane 4: DMSO for 1 day; lane 5: No RNA control. The 721bp band is the amplification product of RARß2. The internal control is a 276bp fragment of the LDL-R transcript. The lane marked M contains molecular weight marker VIII (Promega).

## 2.3.2 Northern blot analysis

In order to confirm the results of the RT-PCR experiment, Northern blot analysis was employed. The primary data are shown in figure 2.5.

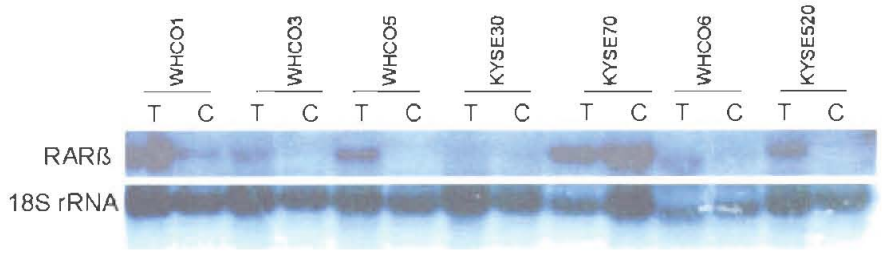


Fig. 2.5. Northern blot analysis of RARß expression in untreated (C) , or 5-Aza-dC and ATRA treated (T) OSCC cells. 10µg of RNA was separated on a gel, transferred to nitrocellulose and probed with an RARß2-specific DNA probe. The blot was subsequently probed for 18S rRNA levels for normalization.

In almost all the cell lines, the signal was stronger in the treated lane than the control lane. The only exception was KYSE70, where 18S rRNA levels show that unequal loading is responsible for the apparent decrease in RARß expression on treatment. In KYSE30, the signal was extremely weak for both 5-Aza-dC treated and untreated cells, which made accurate quantitation difficult.

Values generated by densitometric quantitation of the RARß signals on autoradiographs were divided by the values obtained for an 18S loading control on the same blots to standardize for loading. The results are presented graphically in figure 2.6.

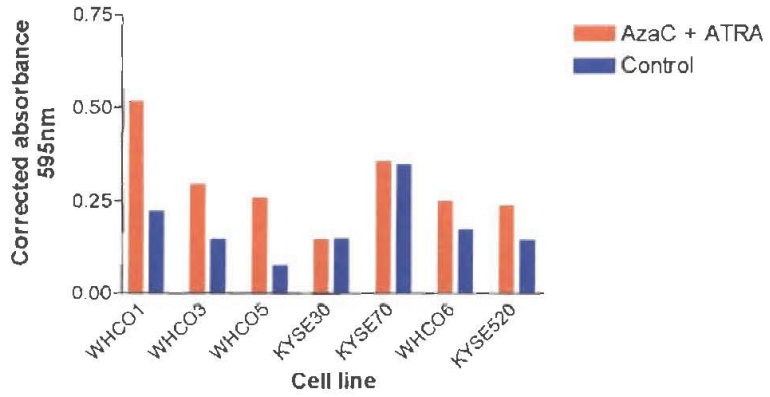


Fig. 2.6. Results of Northern blot analysis of OSCC cell lines for RARß

Expression of RARß was increased following treatment with 5-Aza-dC and ATRA in all cell lines except KYSE 30 and KYSE70. These results do not support those obtained by RT-PCR. Upon investigation, it was found that the structure of the probe used in this study (Brand *et al.*, 1988) included the coding sequence for all domains of the RARß mRNA, from A to F. Therefore, an alternative explanation for the discrepancy between the two data sets is that the probe was able to anneal to the RARß4 transcript as well as that of RARß2. This may account for the disparity in the results obtained by Northern blotting compared to RT-PCR. Constitutive expression detected by Northern blot analysis that was not observed with RT-PCR, could be due to the presence of another transcript generated by alternative splicing. This would not be detected by RT-PCR due to the specificity of the primers.

The blot was therefore stripped and probed with the probe specific for RARß2 transcript. The results obtained were, however, inconclusive and this experiment was not repeated due to time constraints.

### 2.3.3 Sodium bisulfite genomic sequencing

Bisulfite treatment of single stranded DNA converts unmethylated cytosines to uracil but has no effect on cytosines that are methylated. When amplified by PCR, Taq polymerase recognises uracil residues as thymine, and adds a complimentary adenine accordingly. At the end of several rounds of PCR, the only cytosine residues that will remain are those that were protected by methylation in the initial sequence (Zeschnigk *et al.*, 1997).

In order to confirm that the increase in RARß2 expression observed on treatment with 5-Aza-dC (as shown by RT-PCR) could in fact be attributed to demethylation of the P2 region of RARß2, DNA from WHCO1 and KYSE70 was subjected to sodium bisulfite treatment and nested PCR. After this, the PCR product was cloned into pGEM-T-Easy vector (see appendix 1) and sequenced manually.

This method revealed that a number of CpG dinucleotides in the promoter region were methylated, as shown in figure 2.7. Furthermore, similar treatment of DNA from cells that had been treated with 5-Aza-dC confirmed that the 5-Aza-dC treatment had effectively removed all the methyl groups from the DNA.

-357 GCAGGCGGAA CACCGTTTTC CAAGCTAAGC CGCCGCAAAT AAAAAGGCGT
-307 AAAGGGAGAG AAGTTGGTGC TCAACGTGAG CCAGGAGCAG CGTCCCGGCT
-257 CCTCCCCTGC TCATTTTAAA AGCACTTCTT GTATTGTTTT TAAGGAGAGA
-207 AATAGGAAAG AAAACGCC*GG CTTGTGC*GCT CGCTGCCTGC CTCTCTGGCT
-157 GTCTGCTTTT GCAGGGCTGC TGGGAGTTTT TAAGCTCTGT GAGAATCCTG
-107 GGAGTTGGTG ATGTCAGACT AGTTGGGTCA TTTGAAGGTT AGCAGCCCGG
-57 GTAGGGTTCA CCGAAAGTTC ACTC*GCA*TAT AT*TAGGCAAT TCAATCTTTC
-7 ATTCTGTGTG ACAGAAGTAG TAGGAAGTGA GCTGTTCAGA GGCCAGGAGG
43 GTCTATTCTT TGCCAAAGGG GGGACCAGAA TTCCCCCATG C*GAGCTGTTT
93 GAGGACTGGG ATGCC*GAGAA C*GC*GAGC*GAT CC*GAGCAGGG TTTGTCTGGG
143 CACC*GTC*GGG GTAGGATCC*G GAAC*GCATTC* GGAAGGCTTT TTGCAAGCAT
193 TTACTTGGAA GGAGAACTTG GGATCTTTCT GGGAACCCCC C*GCCCC*GGCT
243 GGATTGGCCG AGCAAGCCTG GAAAATGGTA AATGATC

Fig. 2.7. Promoter P2 region of RARß gene from cultured OSCC cells showing cytosine methylation. C=methylated in WHCO1; C*= methylated in KYSE70; C*= methylated in both WHCO1 and KYSE70. TATA box is shown in italics.

This finding supported the results obtained by RT-PCR, which indicated that expression of RARß2 was inducible for these two cell lines (WHCO1 and KYSE70). However, Northern blot analysis indicated that expression of RARß2 was increased following treatment with 5-Aza-dC and ATRA, in other cell lines as well. Sodium bisulfite genomic sequencing was used to verify that this was a reflection of removal of gene suppression through promoter hypermethylation. DNA from WHCO3, which did not display inducible expression by RT-PCR, was subjected to sodium bisulfite treatment, nested PCR and automated sequencing. This revealed that nine cytosines in the promoter region were methylated, as shown in figure 2.8 below.

-357 GCAGGCGGAA CACCGTTTTC CAAGCTAAGC CGCCGCAAAT AAAAAGGCGT
-307 AAAGGGAGAG AAGTTGGTGC TCAACGTGAG CCAGGAGCAG CGTCCCGGCT
-257 CCTCCCCTGC TCATTTTAAA AGCACTTCTT GTATTGTTTT TAAGGAGAGA
-207 AATAGGAAAG AAAACGCCGG CTTGTGCGCT CGCTGCCTGC CTCTCTGGCT
-157 GTCTGCTTTT GCAGGGCTGC TGGGAGTTTT TAAGCTCTGT GAGAATCCTG
-107 GGAGTTGGTG ATGTCAGACT AGTTGGGTCA TTTGAAGGTT AGCAGCCCGG
-57 GTAGGGTTCA CCGAAAGTTC ACTCGC*ATAT ATTA*GGCAAT TCAATCTTTC
-7 ATTCTGTGTG ACAGAAGTAG TAGGAAGTGA GCTGTTCAGA GGCCAGGAGG
43 GTCTATTCTT TGCCAAAGGG GGGACCAGAA TTCCCCCATG CGAGCTGTTT
93 GAGGACTGGG ATGCCGAGAA CGCGAGCGAT CCGAGCAGGG TTTGTCTGGG
143 CACCGTCGGG GTAGGATCCG GAACGCATTC GGAAGGCTTT TTGCAAGCAT
193 TTACTTGGAA GGAGAACTTG GGATCTTTCT GGGAACCCCC CGCCCCGGCT

Fig. 2.8. Sodium bisulfite genomic sequencing of WHCO3 RARß2 promoter region. Methylated cytosines shown in red, underlined

Sodium bisulfite genomic sequencing was also used to determine the methylation status of the RARß2 promoter in primary OC samples compared to normal tissue samples. Out of 11 primary tissue samples, only one patient showed methylation of cytosine bases in the promoter region of RARß2, as shown in figure 2.9.

-357 GCAGGCGGAA CACCGTTTTC CAAGCTAAGC CGCCGCAAAT AAAAAGGCGT
-307 AAAGGGAGAG AAGTTGGTGC TCAACGTGAG CCAGGAGCAG CGTCCCGGCT
-257 CCTCCCCTGC TCATTTTAAA AGCACTTCTT GTATTGTTTT TAAGGAGAGA
-207 AATAGGAAAG AAAACGCCGG CTTGTGCGCT CGCTGCCTGC CTCTCTGGCT
-157 GTCTGCTTTT GCAGGGCTGC TGGGAGTTTT TAAGCTCTGT GAGAATCCTG
-107 GGAGTTGGTG ATGTCAGACT AGTTGGGTCA TTTGAAGGTT AGCAGCCCGG
-57 GTAGGGTTCA CCGAAAGTTC ACTCGCA*TAT ATTA*GGCAAT TCAATCTTTC
-7 ATTCTGTGTG ACAGAAGTAG TAGGAAGTGA GCTGTTCAGA GGCCAGGAGG
43 GTCTATTCTT TGCCAAAGGG GGGACCAGAA TTCCCCCATG CGAGCTGTTT
93 GAGGACTGGG ATGCCGAGAA CGCGAGCGAT CCGAGCAGGG TTTGTCTGGG
143 CACCGTCGGG GTAGGATCCG GAACGCATTC GGAAGGCTTT TTGCAAGCAT
193 TTACTTGGAA GGAGAACTTG GGATCTTTCT GGGAACCCCC CGCCCCGGCT

Fig. 2.9. Sodium bisulfite genomic sequencing of DNA from tumour samples. The TATA box is shown in italics; point mutations of four different patients are shown in red (each mutation being observed in one patient only); and methylated cytosine bases observed in one patient are underlined.

Although it is a small sample group, the frequency is lower than previously reported by Kuroki *et al.* (2003). A likely explanation for this is contamination of tumour samples with normal cells. When taking a tissue sample from a tumour that has been removed by oesophagectomy, it is difficult to ensure that every cell in the sample is neoplastic. Even a sample from what appears to be tumour tissue at a macroscopic level, may be contaminated with large numbers of normal cells. DNA from these normal cells could therefore also be amplified by the PCR reaction. Cloning the DNA into *E. coli* before sequencing increases the chances of sequencing a fragment from a minor population of normal cells, giving a false result. A preferable technique is the sequencing of the PCR product directly. However, this method yielded very poor sequencing results, which were difficult to interpret. Although cell lines are known to develop spontaneous alterations in DNA methylation patterns during culture (Smiraglia *et al.*, 2001), in this case, the data obtained from cell lines may in fact give more accurate information than primary tissue because of the confounding problem of contaminating normal cells in tumour specimens. It is clear that a better assay is needed for the detection of methylation in DNA from primary tissue samples.

An unexpected but noteworthy finding was the occurrence of point mutations in the DNA of four out of 11 patients. These four mutations are indicated in red in figure 2.9. Single nucleotide polymorphisms (SNPs) in the promoter region of genes have been reported to decrease transcriptional activity (Yoshida *et al.*, 2003; Hoogendoorn *et al.*, 2003). We hypothesised that this could be an important factor in RARß2 gene regulation, in the absence of methylation. This novel discovery was not analysed further in this study, but definitely warrants further investigation.

### 2.3.4 Methylation Specific PCR (MSP)

MSP was used as an alternative method to determine the frequency of promoter methylation observed in primary tissue samples, thus avoiding the pitfalls associated with cloning DNA prior to sequencing. This technique involves the use of primers that are specific for either methylated or unmethylated DNA after sodium bisulfite modification. Optimisation of the PCR reaction was performed on DNA from cell lines, before using valuable DNA from tumour and normal oesophageal specimens.

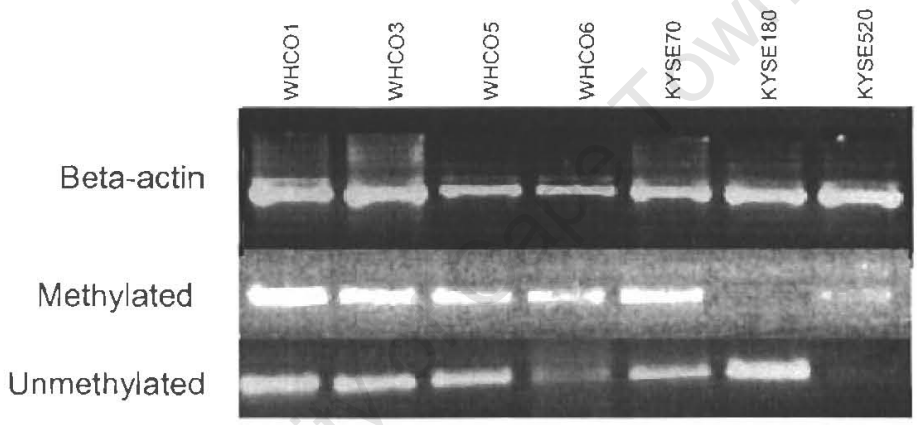


Fig. 2.10. Ethidium bromide stained agarose gel of PCR products generated by MSP. MSP was performed on sodium bisulfite treated DNA, using primers specific for either methylated or unmethylated DNA as described in section 2.2.5. Beta-actin was used as a positive control.



For most of the cell lines (except KYSE180 and KYSE520) both methylated (M) primers and unmethylated (U) primers amplified the 146bp region of the RARß2 promoter. Although one would not expect both methylated and unmethylated promoters to exist within a cell line, epigenetic regulation is a very variable mechanism of transcriptional control. The levels of methyl transferases vary throughout the cell cycle (Szyf and Detich, 2001). The variation between methylated and unmethylated DNA may therefore be a reflection of differences between individual cells. Since the PCR reaction was not quantitative, even a

small fraction of cells displaying a certain methylation pattern could give a positive result.

A number of experimental factors could also underlie this inconclusive result. Firstly, the primer sequences are very important, since they control the selectivity between methylated (M) and unmethylated (U) DNA. However, the selection takes place on the basis of the short region to which they anneal. The methylation status of this particular stretch of DNA may not necessarily reflect the overall methylation status of the entire promoter region. This was seen in some of the cell lines which were subjected to sodium bisulfite genomic sequencing. It was found necessary to combine the different primers, since the cells did not show methylation in the region of the reverse U primer. This approach therefore proved to be a poor technique for differentiating between methylated and unmethylated DNA.

Secondly, the nature of the PCR reaction requires that primer annealing maintains a high degree of specificity. Since the primers differ in only a few bases (those at which unmethylated cytosines are replaced with thymines), it is important that the annealing temperature be high. Although the temperature was varied over quite a broad range, and thus allowed differentiation between true and false positives for some of the cell lines (data not shown), it could not be standardised for all the cell lines. Thus, in some cell lines, even though ß-actin primers generated a product, the annealing temperature did not allow for amplification by either M or U primers.

In cases where promoter methylation has been identified as a prognostic indicator for cancer development, MSP provides a powerful tool for screening. MSP can be employed to specifically amplify DNA from body fluids, obtained by non-invasive means. It has been widely discussed in the literature (reviewed in Laird, 2003) and has been used to successfully detect aberrant methylation of the p16 promoter in serum of liver and colorectal cancer patients (Wong *et al.*,

1999; Zou *et al.*, 2002 respectively). In breast cancer, methylation of RAR-ß, amplified from cells contained in ductal lavage, has been used as a marker for cancer development and progression (Evron *et al.*, 2001). This technique could be a very useful screening procedure for early detection of OC, if properly optimised for amplification from peripheral blood. However, for the purposes presented here, MSP was found to be an unsatisfactory technique. It was decided that MSP would be an unsatisfactory assay for RARß2 promoter methylation in primary tissues.

### 2.3.5 Western Blot analysis

It has been suggested in the literature that overexpression of other isoforms of RARß could interfere with RARß2 gene transcription. In breast cancer, it has been shown that translation of the RARß mRNA from a downstream start codon results in a peptide called RARß' that lacks the transactivation domain, as well as the DNA binding domain of RARß2 (Chen *et al.*, 2002). Furthermore, the RARß4 isoform is very similar to RARß2, but with weaker transactivational ability (Sommer *et al.*, 1999). Since RARß2 is autoregulated, we hypothesised a scenario in which RARß' or RARß4 may be translated and bind to the P2 promoter, but fail to transactivate transcription of the gene. This would prevent RARß2 from binding and thus reduce expression of the RARß2 isoform.

In order to test this hypothesis, we obtained an antibody specific for the F domain of the RARß protein which is conserved in all the isoforms (kindly provided by C. Rochette-Egly and P. Chambon). By separating the proteins on a polyacrylamide gel, it was hoped to detect all isoforms of the protein that were expressed in the cells.

The results of the Western blot shown in figure 2.11 indicate that only one RARß isoform of 66kDa was present in the cells. The size corresponds to that of RARß2. It is interesting that the levels of mRNA (determined by Northern blot

analysis) and protein (determined by Western blot analysis) do not correlate. Chen *et al.* (2002) reported a similar finding in breast cancer cell lines. The Western blot analysis demonstrated that involvement of other RARß isoforms did not play a role in the downregulation of RARß2 in these OSCC cell lines.

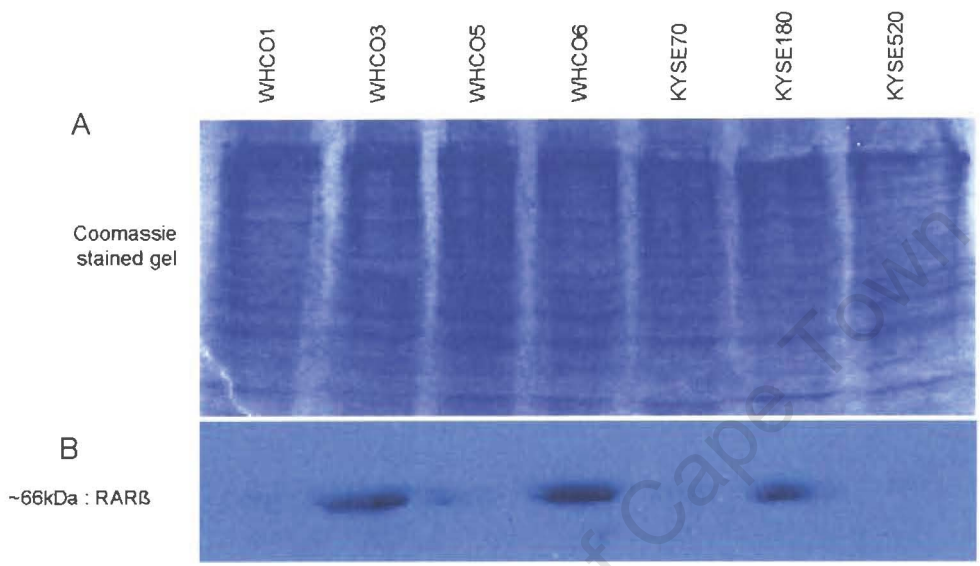


Fig. 2.11. Western blot staining for RARß F domain in OSCC cell lines. Western blot was carried out as described in section 2.2.6. Coomassie stained gel (A) shows equal loading of protein in all lanes, while Western blot with an antibody specific for the F domain of RARß, conserved in all isoforms (B) shows expression of a single RARß isoform in three OSCC cell lines.



Another mechanism that could possibly play a role in the downregulation of RARß2 is the deacetylation of histones in the region of RARß2 P2. Sirchia *et al.* (2002) reported that RARß2 can be reactivated by histone acetylation in breast cancer. However, this possibility was not examined further in this project.

## 2.4 Summary

Hypermethylation of the RARß2 promoter region was found to play a role downregulating the expression of this gene in a number of OSCC cell lines. This finding was supported by sodium bisulfite genomic sequence analysis of the promoter. Primary tumour samples did not display the same frequency of promoter hypermethylation, possibly due to contamination of tumour samples with normal cells. A better assay needs to be developed for methylation detection in primary samples, since sequencing of clones may not be entirely accurate. The expression of alternative isoforms of RARß was not responsible for reducing the gene's expression, since only one isoform was present as indicated by Western blot analysis. A novel finding in this study was the presence of point mutations in the promoter region of RARß2 in DNA from tumour samples. This could provide a interesting alternate method of RARß2 regulation in OC.

# CHAPTER 3

## Trio Expression in Oesophageal cancer

### 3.1 Introduction

The Trio guanine nucleotide exchange factor has been implicated in signalling pathways leading to cell migration (Seipel *et al.*, 1999) and may therefore play a role in metastasis. Microarray analysis of oesophageal tumour samples has shown that Trio is expressed at a level 2.3 fold higher than in normal oesophageal tissue (Wamunyokoli, 2002). Given that a high rate of metastasis is a hallmark of oesophageal tumours, this study was conducted to determine the role of Trio in OC metastasis.

#### 3.1.1 The Dbl family of oncoproteins

The Dbl family (from diffuse B-cell lymphocyte) is a group of Guanine nucleotide exchange factors (GEFs), and includes a number of oncoproteins such as Trio, Sos, Vav, Tiam-1, and Dbl, of which the latter was the first to be characterised. These proteins play a role in the regulation of cell growth through interactions with Guanine nucleotide binding proteins (G proteins). G proteins can exist in two states, bound either to GDP, or to GTP. In the GDP-bound state they are inactive, but when they bind GTP they adopt an active conformation and can interact with a variety of downstream effectors, bringing about a range of physiological and morphological changes (reviewed in Bateman and van Vactor, 2001).

A number of proteins regulate the transition between active and inactive complexes, as represented in figure 3.1. The GAPs (GTPase activating proteins) reduce the activity of G proteins, by promoting the intrinsic GTPase activity of the G protein, resulting in hydrolysis of GTP and returning it to the inactive GDP-

bound state. GDIs (GDP dissociation inhibitors) also decrease G protein activity. They bind to the G protein in the GDP-bound state and prevent it from releasing the GDP. They thereby prevent the G protein from reaching the active GTP-bound state. In contrast, the GEFs favour the active complex by binding to the GDP-bound protein, and inducing a conformational change that favours the release of GDP. This allows the molecule to bind with GTP and enhances signalling to downstream effectors (reviewed in Bateman and van Vactor, 2001).

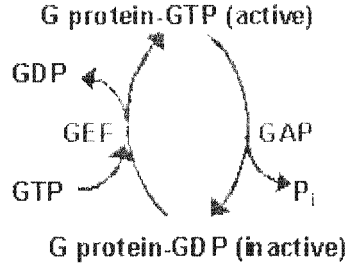


Fig. 3.1. The role of GEFs and GAPs in transition of G proteins between an active and inactive state

The common characteristic feature of the Dbl family members is a Dbl-homology domain (DH) in tandem with a pleckstrin homology domain (PH). The DH domain is the active site at which interaction with small G proteins occurs and the release of GDP is catalysed. All members of the family display specific activity and will catalyse the GTPase activity of a particular, limited set of G proteins. The PH domain does not interact directly with the DH domain, or the G protein, however it is thought to play a role in targeting the protein to a specific cellular location. Although DH and PH domains are the most significant features of the group as a whole, many Dbl family proteins also have other signalling domains and are involved in a diverse range of other signalling pathways (Cerione and Zheng, 1996).

### 3.1.2 Trio function

Trio was given its unusual name on account of its three important characteristic functional domains. These are two DH domains, designated DH1 and DH2, and a C terminal serine/threonine kinase domain, as shown in figure 3.2. In addition, it has several spectrin-like repeats, a PH domain and an SH3-like domain in tandem with each DH, and an immunoglobulin-like domain (Ig). The assortment of functional domains in Trio has lead to the hypothesis that Trio may be involved in a number of signaling pathways (Bateman and Van Vactor, 2001).

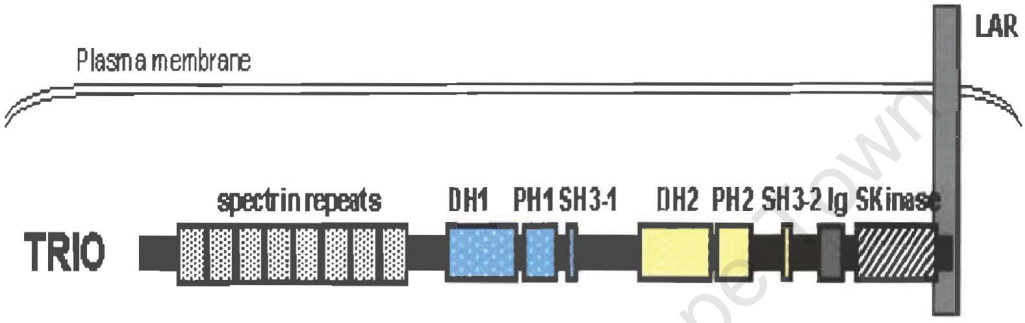


Fig. 3.2. Depiction of Trio protein showing important domains, including those from which its name is derived: DH1 and 2 (Dbl-homology domains) and SKinase (serine/threonine kinase domain) (Debant *et al.*, 1996).



Trio has been shown to play a vital role in the outgrowth of neurons and guiding the direction of the neuron to its target (Bateman and Van Vactor, 2001). Mice that do not express Trio die during late embryogenesis. The embryos exhibit skeletal muscle defects as well as disorganization of cells within the hippocampus and olfactory bulb of the brain, although overall brain structure is not affected. This suggests that Trio is involved in the control of neural development on a fine scale, once the gross morphology of the brain has been established (O'Brien *et al.*, 2000).

Estrach *et al.* (2002) clearly implicated Trio as a component of the nerve growth factor (NGF) signalling pathway, when they found that treatment of cultured cells

with NGF resulted in an accumulation of Trio protein within the cell. The regulation appears to occur at a post-transcriptional level, since no increase in levels of mRNA was detected. Furthermore, Estrach *et al.* (2002) found that while expression of the full-length Trio resulted in the growth of neurites, different deletion mutants had very different effects on cell morphology. For instance, expression of the DH1 domain caused cells to develop broad lamellipodia, and expression of the DH2 domain caused cell retraction. The production of long thin neurite structures depended on the simultaneous expression of both domains, suggesting that a regulatory mechanism exists between the two domains. To identify the downstream effectors, Estrach *et al.* (2002) experimented with various G proteins. Mutant RhoG was shown to completely abolish neurite outgrowth from the cell. Rac1 and CDC42 mutants were shown to have a similar effect, but to a lesser extent. They therefore propose that RhoG is the direct target of Trio, and that the GTP-bound RhoG subsequently acts on Rac1 and CDC42 via an unknown pathway to produce lamellipodia and filopodia. Effectors further downstream of Trio also play important roles in cell mobility, suggesting that Trio may be a component of a signaling pathway involved in metastasis.

Trio associates with the membrane through its interaction with Leukocyte antigen receptor (LAR), a widely expressed transmembrane tyrosine phosphatase. It was this association which lead to its isolation by interaction trap assay (Debant *et al.*, 1996). It has been hypothesized that the interaction between Trio and LAR may play a regulatory role in protein phosphorylation (Seipel *et al.*, 1999). The observation that LAR is localised to the ends of focal adhesions (FAs) lead to the hypothesis that it may be integral in the process of FA disassembly (Debant *et al.*, 1996). It has been observed in *Drosophila* that Dlar, the homologue of LAR, interacts directly with the tyrosine kinase Abl and the tyrosine phosphorylated protein Ena, the homologue of mammalian Mena. Ena binds to profilin which is involved in actin dynamics, leading to the formation of long profilin filaments by preventing capping of the ends (Liebl *et al.*, 2000).

The N-terminal serine/threonine domain and SH3 domain of Trio interacts with Focal adhesion Kinase (FAK), activating it by bringing about its autophosphorylation (Medley *et al.*, 2003). FAK and Trio have been shown to form stable complexes at the cell periphery in vivo. This suggests that Trio plays a role in the dynamics of focal adhesion formation, as well as in the regulation of cell motility via Rho family proteins. Another Trio-interacting protein that affects actin dynamics, is Tara, which consists of an N terminal PH domain and a C terminal coiled-coil region. Tara binds to the Trio DH1 domain, and also binds and stabilises F-actin, although it lacks conventional actin-binding domains. When Tara is overexpressed in a cell, it co-localises with myosin II and leads to an increase in cell spreading and a flattened morphology (Seipel *et al.*, 2001).

Trio expression has not previously been associated with cancer. The novel finding that it is upregulated in OC (Wamunyokoli, 2002) was especially interesting considering the role of Trio in modulating cell motility. The aims of this research were therefore:

- To confirm microarray findings of increased Trio expression in OC using Northern blots and real time PCR
- To establish whether Trio is overexpressed in a large sample of OC patients compared to normal using immunohistochemical staining of tumour and normal sections
- To assess the role that Trio plays in advancement of the metastatic phenotype through the creation of a knock-out mutant by si-RNA. Various properties of wild type and knock-out cells can be compared by motility, invasion and adhesion assays.

## 3.2 Methodology

### 3.2.1 Northern blot analysis

Initial Northern blots of paired tumour and normal RNA were carried out as described in chapter 2 using 2-5μg of RNA. Because of the large size of the trio transcript (> 9Kb), the RNA used for Northern blots had to be electrophoresed for more than 4 hours at 50V. These blots were probed as described in the previous chapter, using one of two Trio-specific probes. The first, pSRαDH1, encoding the DH1 domain of Trio, was provided by Anne Debant (CNRS, Montpelier, France). The other was a 445bp probe generated by standard PCR using primers to exon 4 of Trio, designed using Primer3 software (Rosen and Skaletsky, 2000). Following PCR, the product was purified using QIAquick spin columns (QIAgen), cloned into pGEM T-Easy (Promega) and sequenced manually using the Sequenase Quick-denature Plasmid sequencing Kit (USB Corp.) to confirm the sequence. For normalisation, an 18S rRNA probe was prepared using standard PCR primers described by Uray *et al.* (2002).

It was necessary to select an appropriate cell line, with relatively abundant Trio expression as a model for subsequent experiments involving RNA interference. In order to determine the relative levels of Trio expression in 12 cancer cell lines Northern blot analysis was performed using 10μg of RNA per lane.

### 3.2.2 Real time PCR

RNA was extracted using TRI-zol reagent (Invitrogen) according to the manufacturers instructions, and quantified spectrophotometrically. A small quantity was run on a gel to check its integrity, based on the ratio of 18S: 28S, and the absence of smearing in the lanes. The RNA was then treated with RNase-free DNase I (Boehringer Mannheim) to remove contaminating DNA, and the RNA was recovered by phenol-chloroform extraction and subsequent ethanol

precipitation. PCR with Taq polymerase lacking RT activity (Takara Biomedicals) was used to confirm the efficiency of the DNase treatment. First strand cDNA synthesis was carried out using the ProtoScript™ First strand cDNA synthesis kit (New England Biolabs). As a control for the efficiency of the RT step, PCR was carried out to check that amplifiable cDNA had been produced.

Real time PCR reactions were carried out using the LightCycler System (Roche). One sample was selected as a calibrator for generation of a standard curve. Serial dilutions of this sample were made from 1 to 1:100 000. The other samples were diluted 1:100 for use in the PCR reaction. Each dilution was amplified in triplicate, using primers for Glyceraldehyde-3-dehydrogenase (GAPdH) kindly provided by Heidi de Wet (Stellenbosch University, South Africa). The same dilutions were then amplified using primers for Trio. A typical 10µl reaction included 0.5µM primers, 3-5mM $MgCl_2$, depending on the primer set, 0.5µl of SYBR green Reaction Mix (Roche) and 1µl of cDNA at the appropriate dilution. The PCR protocol included an activation step of 95°C for 600s; 40 amplification cycles of 95°C for 10s, 57°C for 3s, and 72°C for 9s, with a single fluorescence reading at 81°C (above the melting temperature of the primer dimers, but below that of the expected PCR product); melting curve analysis from 65°C to 95°C at 0.1°C/sec with continous fluorescence reading; and cooling of the carousel to 40°C for 30sec.

Data were analysed using the LightCycler software (Roche), $2^{nd}$ derivative maximum method, with arithmetic baseline adjustment.

### 3.2.3 Immunohistochemistry

Slides of paraffin-embedded samples of oesophageal resections from OC patients were used. The samples were collected at Groote Schuur Hospital. Slides were heated and washed in xylol and then ethanol to dewax. Antigen retrieval was performed by heating to 95°C in a pressure cooker for 2 minutes in

citrate buffer. Endogenous Peroxidase activity was blocked treating cells with a 1% hydrogen peroxide solution, before being incubated for 10 minutes in a 1:20 dilution of normal goat serum in PBS. Polyclonal anti-Trio antibody was diluted 1:3000 in antibody diluent (DAKO), and used to submerge the section for 1 hour or overnight in a humidity chamber at room temperature. The sections were rinsed in water and PBS, and then covered in Envision (DAKO) for 30 minutes. Slides were rinsed as previously and covered in diaminobenzene (DAB) (DAKO) for 5 minutes. The slides were then rinsed, immersed in a 1% copper sulfate solution for two minutes, counterstained in haemotoxylin for 10 seconds and immersed in Scott's blueing agent for 10 seconds. Dehydration was subsequently performed by immersing slides in 96% ethanol, absolute ethanol and finally xylol before mounting in Entellan (Merck).

### 3.2.4 Transfection of OSCC cell lines

In order to optimise the protocol for transfection of the KYSE cell lines, FuGENE 6 transfection reagent (Roche) was used in varying ratios to DNA. COS1 cells were included as a positive control, since they are known to transfect well using FuGENE reagent (FuGENE 6 Package insert). Transfection optimisation was performed using a plasmid encoding the ß-galactosidase gene, and transfection efficiency was measured using an assay for β-gal activity (described in Sambrook *et al.*, 1989 with modifications). Briefly, cells were plated in 2 mls media in 6 well plates at a density of 1.5-2 x $10^5$ cells per well. FuGENE reagent was added to unsupplemented DMEM. This was mixed with the plasmid DNA in the following ratios: 3:1, 3:2, and 6:1 to give a final volume of 100µl, which was added to the cells dropwise. The cells were incubated at 37°C for 48 hours. Cells were washed three times on ice with cold PBS. 200µl TEN buffer was added to each well, and plates were incubated at room temperature for 5 minutes. The solution was collected with scraping, transferred to a 1ml eppendorf and centrifuged at 13000rpm in a Heraeus Sepatech Biofuge (model 13R) centrifuge for 10 minutes at 4°C. The supernatant was carefully removed with a Pasteur pipette, and the

pellet was resuspended in 0.25M Tris-Cl pH8. The suspension was subjected to three freeze thaw cycles in liquid nitrogen and a 37°C waterbath. 10µl of this lysate was used in the β-gal assay as detailed below, while the rest was frozen at –70°C. To the 10µl cell extract were added 500µl Z buffer and 100µl 4mg/ml o-Nitrophenyl ß-D-Galactopyranoside (ONPG) (Sigma). This reaction was incubated at 37°C in a waterbath until a yellow colour, the product of breakdown of ONPG by ß-galactosidase activity, was observed, at which point the reaction was stopped by adding 250µl of 1M $Na_2CO_3$. The optical density (OD) of the samples was determined at 420nm using untransfected control samples as a blank. The transfection efficiency was calculated in β-gal units using the following equation :

β-gal units = (380 x $OD_{420}$) / incubation time (minutes)

### 3.2.5 Western blot analysis

Cells were plated in 150mm dishes at a density of 3.5 x $10^6$ cells per dish, and grown for 2 days or until roughly 80% confluent. They were washed with ice cold PBS, collected in 1 ml protein lysis buffer including protease inhibitors and stored at -20°C. Protein quantitation was carried out using the BCA assay kit (Pierce). In some instances it was necessary to reduce the volume of the protein in order to load more. In such cases protein was aliquoted, frozen in liquid nitrogen and vacuum dried to reduce the volume to approximately half. An equal volume of 2x loading dye was added and the samples were incubated at 95°C for 10 minutes, before being loaded onto a 5% to 15% gradient gel (Gallagher, 1999) alongside a lane of Rainbow marker (AEC Amersham). Cell lysate of transiently transfected COS cells was provided by Susanne Schmidt (CNRS, Montpelier, France) for use as a positive control for the antibody. The protein was electrophoresed at 30mA for 3-4 hours, and then proteins were transferred to nylon ECL membrane (Amersham Pharmacia biotech) at 200mA for 2 hours at 4°C. The blot was blocked for 1hr at room temperature in 1% blocking solution (Roche Diagnostics).

Rabbit polyclonal anti-Trio antibody was the kind gift of Susanne Schmidt. This was diluted 1:3000 in TBS for overnight incubation of the blot at 4°C with shaking. The blot was then thoroughly rinsed and incubated with Peroxidase-labelled secondary antibody (Roche Diagnostics) for 1 hour at room temperature. The blot was rinsed again before chemiluminescent detection was carried out using the BM Chemiluminescence Western Blotting Kit (mouse/rabbit) (Roche Diagnostics).

## 3.3 Results and discussion

### 3.3.1 Northern blot analysis

Trio was shown to be overexpressed in tumour tissue by DNA microarray analysis (Wamunyokoli, 2002) and Northern blots of RNA from tumour and adjacent normal tissue was performed to verify this. Although a band was present at approximately the expected molecular weight of the Trio transcript (~10kb), as shown in figure 3.3, the signal intensity observed was very weak, suggesting low abundance of the Trio transcript. Northern blot analysis of tissue RNA was therefore not conclusive. Owing to the small amount of tissue that is obtained from patients, RNA from tissue samples is very precious. It was decided not to repeat Northern blot analysis with patient RNA, but rather to explore other quantitative techniques that would require the use of smaller quantities of RNA, such as real time PCR.

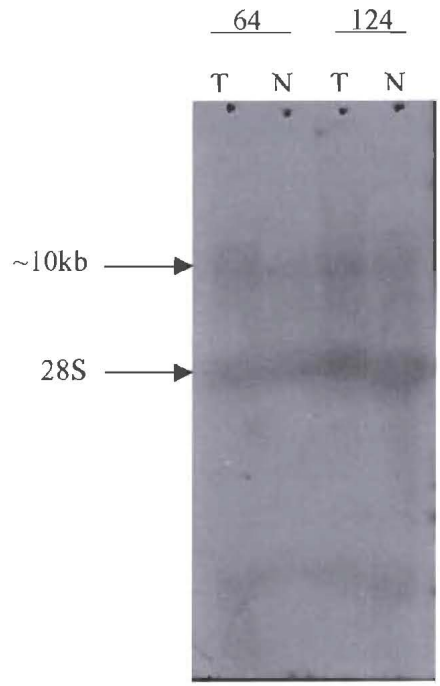


Fig. 3.3. Northern blot of RNA isolated from tumour (T) or adjacent normal (N) tissue samples probed with Trio-specific probe. 5μg of total RNA from patients number 64 and 124 was immobilised on the membrane.

Northern blot analysis of OSCC cell line RNA was performed in order to optimise the technique, and investigate the relative abundance of Trio in different cell lines. 10μg of RNA was run on a gel, blotted and probed as described in Appendix 1. OSCC cell lines and cell lines of other cancers were used. Three cervical cancer cell lines (SiHa, a squamous cell carcinoma; HeLa, adenocarcinoma; and ME180, an epidermoid carcinoma) a breast epithelial adenocarcinoma cell line (MDA-MB-231) and a neuroblastoma cell line (SK-N-SH) were included in the study. KYSE520 was run again on the second blot to facilitate comparison across the different membranes, as shown in figure 3.4 A. Notes on cell culture techniques are included in Appendix 1.

Using 18S to correct for loading differences, the autoradiographic data was quantified using a densitometer (Chemi-Imager 5500, Alpha Innotech Corp.) and analysed using Prism software. Figure 3.4 (B) below shows a graphical representation of the normalised data.

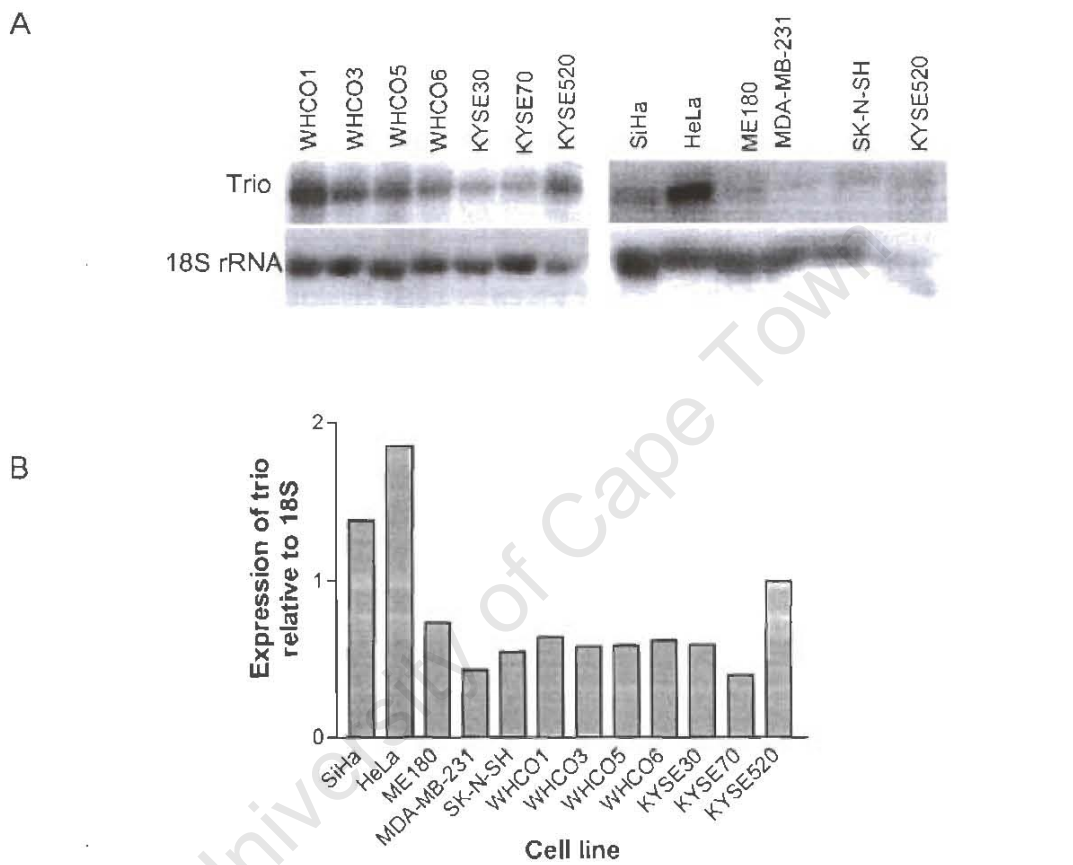


Fig. 3.4. Northern blot of 10µg cell line RNA probed with Trio-specific probe, and an 18S rRNA specific probe, for normalisation. Autoradiographic data shown in (A) was quantitated by densitometer and the normalised data are represented graphically in (B).

From this result it was determined that KYSE520 would be a good candidate cell line for RNAi experimentation since it expressed the highest levels of Trio of all the OSCC cell lines tested. However, HeLa and SiHa also expressed Trio at quite high levels and could also provide interesting results in Trio knock-out analysis.

It was planned to transiently transfect the cells with the pSilencer plasmid (Ambion) to prevent translation of Trio mRNA by the generation of siRNA molecules. Assays would then be carried out to compare the motility and cell adhesion properties of transfected and untransfected cells.

### 3.3.2 Transfection of OSCC cells

Previous experiments performed in the lab have shown that OSCC cell lines do not transfect as efficiently as other cell lines. Methods such as calcium phosphate transfection, lipofectamine, and eletroporation have all yielded very poor transfection efficiencies (Bo Wang, personal communication). Although the FuGENE transfection reagent had been tested on the WHCO cell lines, and been unsuccessful in transient transfection experiments, it had not been tested on the KYSE cell line series. For this reason, the transfection protocol was optimised for the KYSE cell lines, by varying cell density at the transfection step and the ratio of DNA to transfection reagent.

Unfortunately, transient transfection of the KYSE cell lines also proved to be very inefficient. Representative results of FuGENE transfection of the KYSE cell lines are shown in table 3.1 below. COS1 was used as a positive control, and was shown to express transfected DNA approximately $10^4$ times more efficiently than KYSE70.



Table 3.1. Results of transient FuGENE transfection of KYSE OSCC cell lines. Averages are calculated for 6 replicates (COS1, KYSE520, KYSE30) or 2 replicates (KYSE70).

| Cell line | Average absorbance at 420nm | Average length of incubation for yellow colour to develop (min) | Average ß-gal units |
|---|---|---|---|
| COS1 | 0.61845 | 3 | 78.3 |
| KYSE520 | 0.03455 | 1080 | 0.0143 |
| KYSE30 | 0.0434 | 430 | 0.1106 |
| KYSE70 | 0.02335 | 1080 | 0.0082 |

Due to time constraints and the extremely problematic nature of transfecting these cell lines, it was decided not to pursue this line of investigation. Trials are currently underway to generate stable transfectants of these cell lines, which, if successful, would permit investigation into the role of Trio in the development and progression of OC.

### 3.3.3 Immunohistochemistry

In order to determine the frequency of Trio overexpression in OC patients, immunohistochemical staining of paraffin-embedded sections of oesophageal cancer samples was undertaken. Initial steps taken to optimise staining included varying the concentration and length of incubation time of the primary antibody. It was noted that even at high dilutions of antibody (1:1500), with short incubation time (1hour), high background staining was seen. Both cytoplasm and cell nuclei stained under these conditions. Very intense staining of muscle tissue was also observed. Very little difference could be observed between the staining of normal and tumour samples. Figure 3.5 shows some immunohistochemically stained sections using this antibody.

The high nonspecific staining caused concern about the specificity of the antibody. This antibody was provided by Susanne Schmidt and Anne Debant (CNRS, Montpelier, France), and had not previously been used for immunohistochemistry. In order to check the specificity of the antibody for Trio, Western blot analysis of cell line protein lysate was performed.

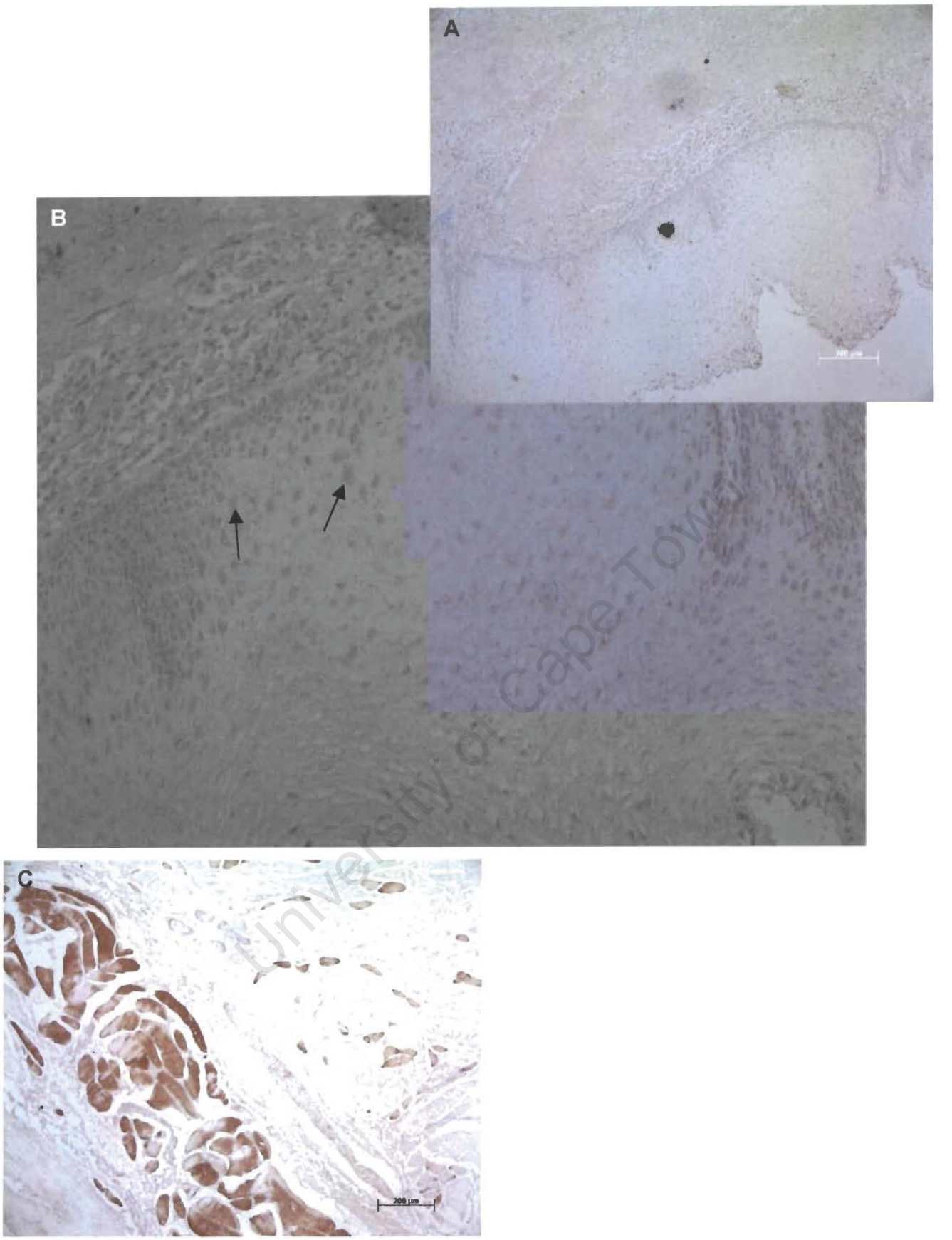


Fig. 3.5. Oesophageal tissue sections stained with Trio antibody. (A) shows a section of normal epithelial tissue, magnified in (B). Some normal cells exhibit cytoplasmic staining with the Trio antibody, as indicated with arrows. (C) shows a section through smooth muscle of the oesophageal wall. Muscle stains very strongly compared to the surrounding connective tissue.

### 3.3.4 Western blot analysis

Western blot analysis was used to detect Trio protein in cell line lysates, and determine the specificity of the anti-Trio antibody. A positive control for the antibody consisted of lysate of COS1 cells that had been transiently transfected with the Trio gene (supplied with the antibody). Western blot analysis revealed a number of very strong bands in each lane on the autorad, shown in figure 3.6 below. The band corresponding to Trio, as indicated by the positive control, was extremely weak in all three of the cell lines tested.

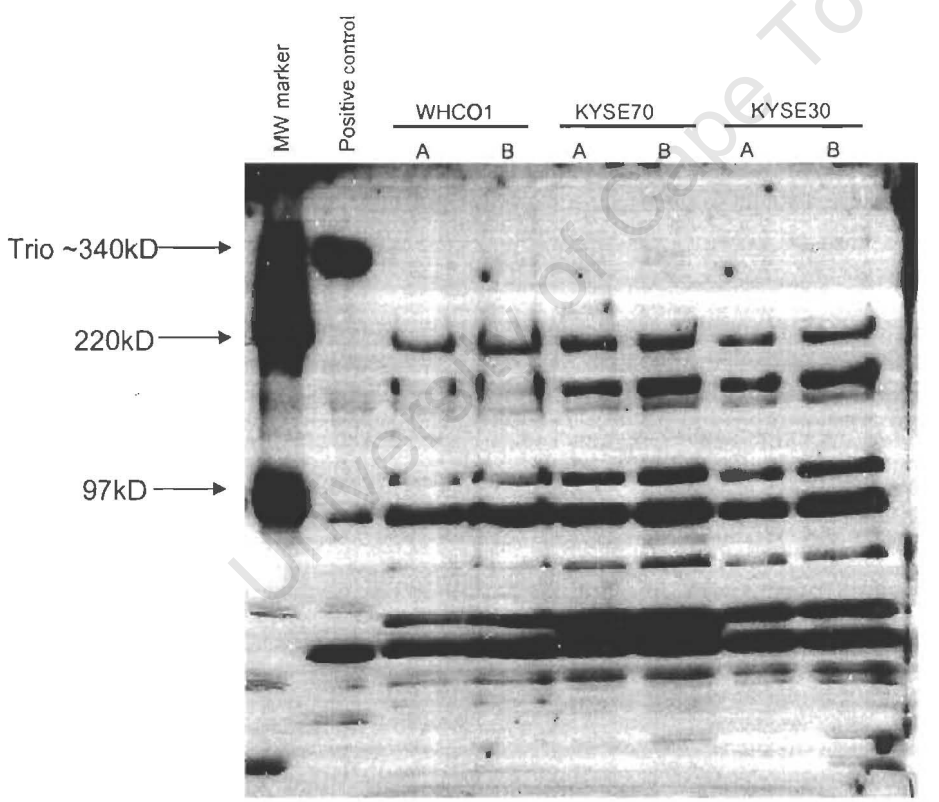




Fig. 3.6. Western blot of cell lysate from 3 OSCC cell lines with anti-Trio antibody. Protein was separated on a 5-15% gradient polyacrylamide gel. Different quantities of protein were loaded in each lane to optimise the level needed for Trio detection. The amount of protein loaded are as follows: WHCO1 (A) 71µg (B) 142µg; KYSE30 (A) 47µg (B) 94µg; KYSE70 (A) 61µg (B) 122µg. In each AB pair, B was subjected to freeze-drying to reduce the volume loaded, while A was not.

The high number of bands visualised by Western blot could suggest either that the antibody had low specificity for the Trio protein, or that the Trio protein was highly unstable and degraded into a number of smaller products. Although the blot clearly shows that the freeze-drying process has not caused an increase in such degradation, it is possible that other factors during protein collection could have allowed such degradation to occur. In order to preclude this possibility, protein collection was repeated using 2x Boiling blue (see Appendix 2) which stabilises proteins at the point of collection due to the addition of ß-mercaptoethanol. This sample was then run alongside a sample from the blot above. The results (data not shown) indicated low levels of Trio protein and high numbers of other bands for both sets of protein, irrespective of the collection procedure. This suggests that the anti-Trio antibody was not very specific, and would not be suitable for use in immunohistochemistry.

### 3.3.5 Real time PCR

In the study of gene expression, reverse transcription of mRNA to cDNA followed by PCR has become an invaluable tool, especially in instances where the transcript of interest is present at low levels. In order to quantify the amount of mRNA produced by a cell, ordinary RT-PCR is not sufficient, since the PCR reactions reach a plateau after a number of cycles. Real time PCR is now commonly used in the quantification of gene expression, since it uses the exponential phase of the reaction for quantification.

Real time PCR relies on the production of fluorescent signal in relation to the amount of DNA in the sample. This can be achieved by the use of quenchers (e.g. TaqMan probes) or minor groove binders (e.g. SYBR green). Quantitative PCR requires a housekeeping gene in order to standardise the amount of gene of interest in each sample. The level of expression of the housekeeping gene should be the same in normal and tumour samples.

Since PCR is an exponential process, the amount of product produced in n cycles ($T_n$) will be dependent on the amount of starting template ($T_o$), the efficiency of the PCR reaction (E), and the cycle number (n).

$T_n = T_o \times E^n$

The relationship is linearised by taking logs:
$\log T_n = \log T_o + n.\log E$

In a perfect PCR reaction, every copy of the template would be doubled in each cycle. The maximum theoretical efficiency (E) of a reaction is therefore 2. A standard curve is generated by PCR of a serial dilution of template. At a hypothetical crossing point (Cp) the amount of product in each reaction is the same. The cycle number at which the PCR reaches the Cp (when the Cp is extrapolated to the x axis) can be compared for different samples. It gives an indication of the relative amount of PCR template in a sample. Another method to quantify the increase in PCR product throughout the reaction is based on the difference in Cp for the gene of interest and the housekeeping gene in different samples ($2^{-\Delta\Delta Ct}$ Method) (Livak and Schmittgen, 2001)

The relative concentration of PCR product can be read off the standard curve of cycle number at crossing point versus log concentration. The slope of the standard curve gives an indication of PCR efficiency (E) (Reviewed in Bustin, 2002).

Real time PCR successfully suggested that Trio mRNA was overexpressed in 3 out of four patients, as shown in figure 3.7. This sample size is too small to draw an accurate conclusion about the status of Trio in the general population of OC patients. However, this technique is too time-consuming and expensive to

efficiently screen a large sample size. A technique such as immunohistochemistry would be preferable for this purpose.

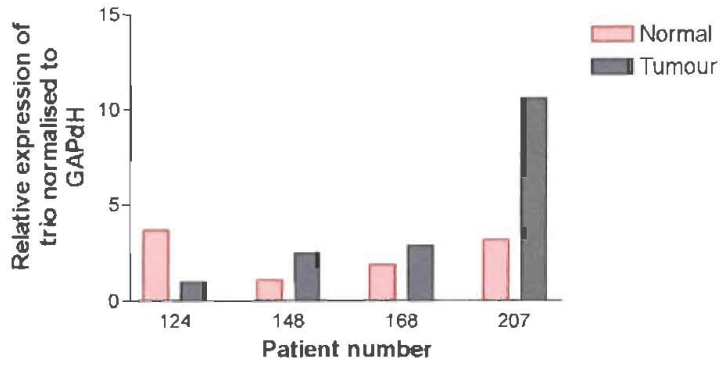


Fig. 3.8. Level of Trio expression in normal and adjacent tumour specimens from four OC patients as assessed by real-time PCR

As previously discussed, the use of adjacent normal samples for comparison in an assay of this type is problematic due to the possibility of sample contamination. Since carcinogenesis is a multistep process, microscopic examination of tissue is not sufficient to identify individual cells that are at intermediate stages of transformation. It is thus possible that normal samples may contain a relatively high proportion of cancerous cells and vice versa. An alternative approach is obtaining samples from unpaired, unsymptomatic normal subjects. While obtaining biopsies from such a sample group would be difficult, the possibility of obtaining tissue from cadavers is being investigated, although this option has its own set of associated problems.



## 3.4 Summary

Although only a small sample was tested, the results suggest that Trio may be overexpressed in a subset of OC patients. Due to several complications, we were unable to fulfill the aims of determining Trio levels in a large number of OC patients and the effect of exogenously expressed Trio on cells in vitro. However, should transient transfection of OSCC cell lines become a possibility, it would be

very interesting to see the effect of an RNAi-based knockout of Trio in KYSE520, which expresses Trio mRNA at relatively high levels.

# CHAPTER 4

## Abl-related gene (ARG) expression and potential use of Gleevec™ and 17-Allylamino Geldanamycin (17-AAG) as chemotherapeutic agents

### 4.1 Introduction

Since OC patients have such a low survival rate, it is desirable to develop more effective chemotherapies to combat this disease. Although the exact function of ARG is unknown, it has been shown to be upregulated in a number of neoplasias (Zhang *et al.*, 2003), and microarray analysis has revealed that the sequenced open reading frame is also overexpressed in OC (Wamunyokoli, 2002). It may therefore be a useful target for chemotherapy. Gleevec™ (Novartis Pharma, Switzerland) is reported to inhibit the function of this protein tyrosine kinase. 17-AAG targets Heat shock protein 90 (Hsp90), and thereby also results in inactivation of a variety of cellular kinases. In order to establish the potential value of Gleevec and 17-AAG as a chemotherapeutic agents against OC, their growth inhibitory effects on OSCC cell lines were investigated.

#### 4.1.1 Abl-related gene and gene products

The ARG gene was first identified in 1986 by Kruh *et al.*, due to its close homology to other members of the Abelson family of tyrosine kinases. By probing placental DNA with a v-Abl probe, under conditions of low stringency, a 12.5kb fragment was identified, cloned and sequenced. Northern blot analysis allowed detection of a 12kb transcript, and confirmed that the open reading frame was in fact a functional gene. The gene was localised to chromosome 1q24-25 (Kruh, 1986). A schematic representation of the protein domains of ARG is shown in figure 4.1. ARG shows notable similarity to the c-Abl tyrosine kinase in its kinase domain, and to a lesser extent in the SH2 and SH3 domains. The amino- and

carboxy-terminal residues show divergence which may be related to distinctive functions of the proteins (Kruh *et al.*, 1990).

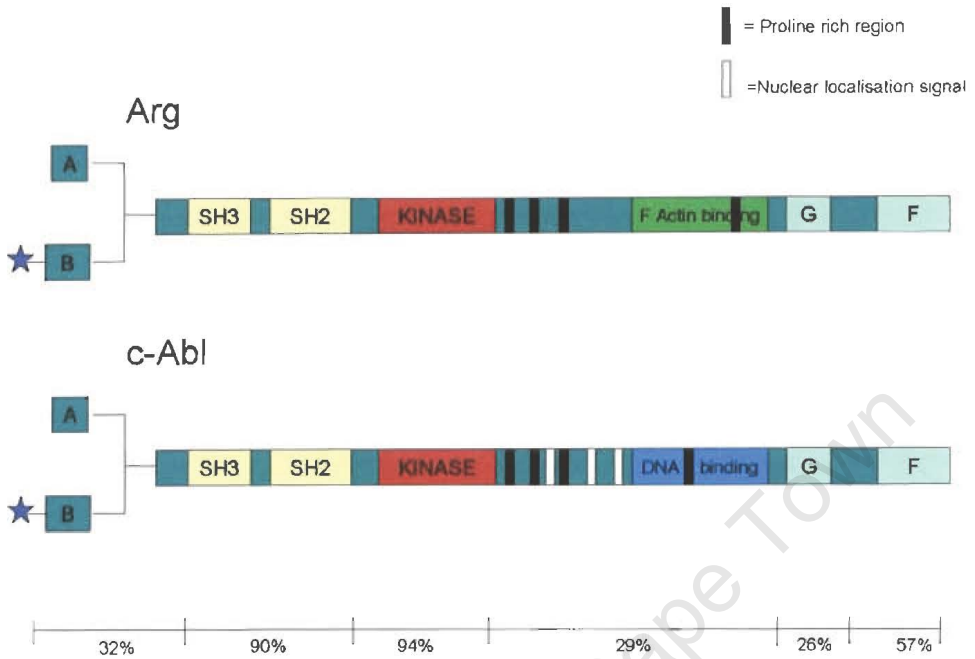


Fig. 4.1. Representation of human ARG tyrosine kinase showing percentage homology to human c-Abl. SH2 and SH3 are Src homology domains, involved in protein-protein interactions. The two C terminal domains function in binding and bundling of filamentous (F) and globular (G) actin, and the F domain of both proteins contains a nuclear export signal motif. The alternate unmyristolated (A) or myristolated (B) N terminal domains are shown (adapted from Pendergast, 2001).



Although ARG is expressed at high levels in the brain, both ARG and c-Abl are expressed in a wide variety of tissues (Perego *et al.*, 1992). Another similarity between c-Abl and ARG is the fact that both are expressed as two different transcripts, that result from alternative splicing. The transcripts are designated 1A and 1B, and differ at the 5' end of the transcript. They encode two proteins that differ at the amino termini (Kruh *et al.*, 1990). In both c-Abl and ARG, the 1A form of the protein is not myristolated, whereas the 1B forms have been found to be myristolated at Gly-2, facilitating interaction with the cell membrane. However, mutation of this glycine residue had no effect on the subcellular localisation of ARG (Wang and Kruh, 1996). In immunofluorescent experiments to determine

the subcellular localisation of ARG, there was no difference in the localisation of ARG1A, ARG1B or the ARG mutant (G2A). All three forms were located in the cytoplasm, with no nuclear staining, apart from an increased staining intensity around the periphery of the nucleus. This could indicate a possible interaction with the nuclear membrane. This finding was confirmed by subcellular fractionation experiments, in which it was discovered that both ARG1B and the nonmyristolated mutant could be detected in small quantities in the nuclear fraction. Only the phosphorylated form seemed to associate with the nucleus (Wang and Kruh, 1996).

The exact function(s) of ARG are as yet unclear, but it has been implicated in events as diverse as cell migration, DNA repair, postsynaptic assembly of the neuromuscular junction, development and differentiation, and the initiation of the apoptotic response to oxidative stress (Kain and Klemke, 2001; Li *et al.*, 2002; Finn *et al.*, 2003; Adler *et al.*, 2000; and Cao *et al.*, 2001 respectively). The role of Abl in growth cone motility and axonogenesis is well documented (Lanier and Gertler, 2000). The close homology between Abl and ARG first lead to the hypothesis that ARG may have similar functions. In fact, although the C terminal domains of the two proteins are more divergent than their N termini, ARG does have two actin binding domains at its C terminus that are analogous to those of c-Abl (Van Etten *et al.*, 1994 ) (see figure 4.1). Wang *et al.* (2001) found that ARG cooperatively bound F-actin. It was also reported that ARG would assemble F-actin filaments into high molecular weight bundles, and that this activity was dependent on the presence of both actin binding domains and a third proximal domain (amino acids 688-1182). A similar interaction was observed *in vivo* by transfection of swiss 3T3 cells with fluorescently labeled ARG. Expression of ARG occurred predominantly in actin-rich structures at the lamellipodia of transfected cells (Wang *et al.*, 2001). This suggests that ARG is involved in cell motility and the formation of focal adhesion complexes.

While ARG plays an important, if not clearly defined, role in cell migration, it also seems to be involved in growth and development, especially of the nervous system. In a mouse model, deletion of ARG caused behavioural defects. It would appear that c-Abl has some compensatory effect in the absence of ARG, because double mutant (c-Abl$^{-/-}$, ARG$^{-/-}$) embryos died from defects in neural tube development associated with disordered F-actin bundles (Koleske *et al.*, 1998).

ARG has been implicated in two types of gastrointestinal cancer. Higher levels of ARG kinase expression in gastric cancer, while having no effect on overall patient survival, have been shown to be associated with the invasiveness of the cancer (Wu *et al.*, 2003). A study of colorectal cancer patients revealed that ARG expression was higher in carcinoma patients when compared to either normal mucosa or adenoma (Chen *et al.*, 1999). Cells cultured from a patient with acute myelogenous leukaemia were found to express a fusion protein arising from a translocation between ARG and ETV6. The fusion protein comprised all the functional domains of ARG including the tyrosine kinase domain, and may be implicated in the unique differentiation capabilities of this cell line (Iijima *et al.*, 2000). It seems that ARG may be an appropriate target for anticancer therapies, and that specific inhibition of its activity may reduce cells' ability to move and metastasise, as well as disrupting signaling pathways that stimulate growth and differentiation.



### 4.1.2 Protein tyrosine kinases as targets for rational drug design

The involvement of protein tyrosine kinases in cancer has been recognised for roughly 20 years. It was discovered that animal tumour viruses often encoded tyrosine kinases, and these genes were subsequently overexpressed in cancer tissue. *In vitro* studies confirmed that they could indeed act as oncogenes, and that inhibition of tyrosine kinases in cultured cells had antiproliferative effects. This therapeutic approach was not tried *in vivo*, because of concerns that a general inhibition of all tyrosine kinases could have detrimental effects. The

challenge lay in identifying tyrosine kinase inhibitors (TKIs) that would act specifically on the subset of kinases that are directly involved in perpetuating the tumour phenotype. Ideal targets for rational drug design should also represent early molecular pathogenic changes, that are detectable before the advanced stages of cancer development (Druker, 2002). Some selective inhibitors have been identified, mainly by high throughput screening of a multitude of coumpounds. Two of the most notable successes in TKIs are Herceptin®, a monoclonal antibody directed against the Her-2/neu receptor tyrosine kinase used in the treatment of breast cancer, and Gleevec™ (STI571) originally designed to inhibit the Bcr-Abl fusion protein tyrosine kinase associated with chronic myelogenous leukemia (CML) (Reviewed in Sawyers, 2002). Drugs that indirectly inhibit the action of tyrosine kinases may also be of therapeutic benefit. Two such examples are Geldanamycin and 17-AAG.

### 4.1.3 Mode of action of Gleevec

One of the characteristics of CML is a genetic translocation between the tyrosine kinase Abl and the breakpoint cluster region (BCR). This results in the expression of the Bcr-Abl fusion protein at abnormal levels with constitutive tyrosine kinase activity. Since tyrosine kinase signaling pathways are frequently involved in regulating cell growth, division and metabolism, cell growth becomes becomes dysregulated, contributing to the neoplastic phenotype (Druker, 2002). Gleevec™ (shown in fig. 4.2) was developed as an inhibitor of this oncoprotein, since it competes with ATP for the active site in the kinase domain (Buchdunger *et al.*, 2002). It has been shown to be highly effective in the treatment of CML, and recent studies have also revealed considerable activity against a number of other tyrosine kinases.

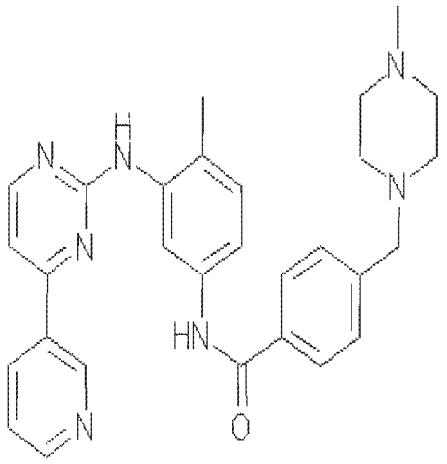

Fig. 4.2. Molecular structure of Gleevec™

Favourable results have been observed in the treatment of gastrointestinal stromal tumour (GIST), where the drug apparently targets the abnormally expressed c-Kit receptor tyrosine kinase (Zhang *et al.*, 2003). Gleevec™ also shows in vitro activity against non-small cell lung cancer (Zhang *et al.*, 2003), small cell lung cancer (Krystal *et al.*, 2000), medullary thyroid carcinoma (Cohen *et al.*, 2002), and osteosarcoma (McGary *et al.*, 2002). The range of tyrosine kinase targets of Gleevec are summarised in Table 2.1, which also shows the $EC_{50}$ for each enzyme (modified from Buchdunger *et al.*, 2002). This table highlights the selectivity of the drug for a small subset of tyrosine kinases. Some of these tyrosine kinases are frequently transcriptionally upregulated in cancer tissue.

Table 4.1. Specificity of Gleevec for various Tyrosine kinases. Concentrations that give a 50% reduction in cellular kinase activity ($EC_{50}$ concentrations) are given (modified from Buchdunger *et al.*, 2002).

| **Kinase** | **$EC_{50}$ (μM)** |
|---|---|
| v-Abl Abelson murine leukemia viral oncoprotein | 0.1-0.3 |
| BCR-Abl oncoprotein | 0.25 |
| TEL-Abl translocation product | 0.35 |
| TEL-ARG translocation product | 0.5 |
| Platelet derived growth factor receptor (PDGFR) | 0.1 |
| TEL-PDGFR translocation product | 0.15 |
| Kit (Stem cell factor receptor) | 0.15 |
| Angiogenic receptor of Vascular endothelial growth factor (KDR) | >10 |
| Insulin receptor | >100 |
| v-Src sarcoma viral oncoprotein | >10 |
| Janus kinase 2 (Jak-2) | >100 |

Two studies have investigated the effect of Gleevec in combination with other commonly used anti-cancer drugs such as cisplatin (*cis*-diamminedichloroplatinum or CDDP). Cisplatin, shown in figure 4.3, is a small molecule that interacts with DNA in such a way as to inhibit replication and transcription. It can also induce apoptosis (reviewed in Siddik, 2003).

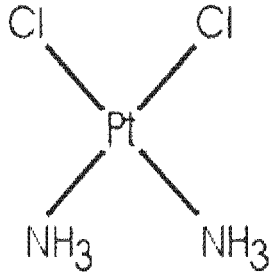


Fig. 4.3. Molecular structure of cisplatin (CDDP)

In vitro studies on non-small cell lung cancer, and human kidney cell lines revealed that Gleevec potentiates the antiproliferative effects of cisplatin (Zhang *et al.*, 2003). However, Krystal *et al.* (2000) carried out a similar study involving treatment of small cell lung cancer cells with Gleevec™, in combination with carboplatinum (a cisplatin analogue) and etoposide. They reported that there was no increase in cytotoxicity when the drugs were co-administered. One of the aims of this research is to treat cells with a combination of Gleevec™ and cisplatin at $EC_{50}$ values to determine whether this treatment approach could hold benefit for OC patients.

Two pitfalls currently associated with the chemotherapeutic use of Gleevec, are the development of resistance, and the exclusion of mast cells from the tumour. Resistance has been observed to develop in leukaemia patients with prolonged use of the drug. This occurs typically through amplification of the BCR-ABL translocated gene, or mutations in the kinase domain (Campbell *et al.*, 2002; Roche-Lestienne *et al.*, 2002). Furthermore, Gleevec inhibits the entry of mast cells into the tumour, thereby preventing the action of mast cell heparin, a powerful anticoagulant. Exclusion of heparin from the tumour has been seen to result in peri-tumoural clotting in solid tumours in mice, as well as increased tumour growth rate (Samoszuk and Corwin, 2003).

### 4.1.4 Mode of action of 17-AAG

17-AAG is a structural analogue of geldanamycin (molecular structure is shown in figure 4.4), a naturally occurring benzoquinone ansamycin antibiotic produced by *Streptomyces hygroscopicus*. It targets the molecular chaperone Hsp90. Hsp90 is responsible for stabilizing a variety of intracellular proteins and ensuring that they fold into the correct tertiary structure. By binding to the active site, 17-AAG prevents Hsp90 from interacting with its client proteins by inhibiting its intrinsic ATPase activity. The unchaperoned, misfolded proteins are subsequently ubiquitinated and targeted for proteasomal degradation (reviewed in Maloney and Workman, 2002).

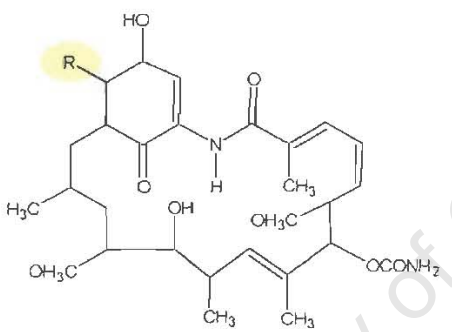


Fig. 4.4. Molecular structure of geldanamycin [R= $CH_3O$] and 17-AAG [R= $H_2C=CHCH_2NH$]

Several of the proteins which Hsp90 chaperones are involved in signalling pathways leading to cell cycle progression and the prevention of apoptosis. Hsp90 may also play a role in stabilizing oncoproteins that are chimaeric or mutated in such a way that their expression enhances the malignant phenotype. Examples of such proteins are mutated p53, Bcr-Abl, HER2/neu (ErbB2) and the transcription factor Hypoxia-inducible factor-1α (HIF1-α) (Isaacs *et al.*, 2002; reviewed in Neckers, 2002). This makes Hsp90 an attractive target for chemical inhibition since it is indirectly crucial to a number of cancer signalling pathways. 17-AAG is currently in phase I clinical trials and has shown promising initial results.

The potent antitumour activity of 17-AAG has been studied and described in a variety of cancers. In the human leukaemia cell line HL60, 17-AAG induces apoptisis at concentrations below 10μM by reducing the levels of several

intracellular kinases. These include Akt, c-Raf-1, and c-Src, all of which play a role in pathways leading to cell proliferation and survival (Nimmanapalli *et al.*, 2003). Similar studies in colon adenocarcinoma cell lines have revealed another cohort of proliferation-related kinases that are destabilised, including N-ras, Ki-Ras, c-Akt and c-Raf-1. It simultaneously prevented ERK-1/2 and c-Akt from being phosphorylated (Hostein *et al.*, 2001). Colon cancer cells did not show altered gene expression profiles following treatment with 17-AAG, but levels of some other proteins such as Hsp70, Keratin 8 and Keratin 18 were deregulated (Clarke *et al.*, 2000). 17-AAG not only depletes the cell of non-receptor kinases and serine-threonine kinases, but also steroid hormone receptors, which are a very important target of breast cancer therapy. Bagatell *et al.* (2001), have shown both in vitro and in vivo, that 17-AAG successfully reduced levels of progesterone receptor and reduced tumorigenicity of breast cancers. Another favourable effect of 17-AAG observed in non-small cell lung cancer (NSCLC) is its ability to markedly reduce metastasis. The disruption of motility-related proteins like matrix-metalloproteinase 9 (MMP9) and vascular endothelial growth factor (VEGF) are thought to underlie this effect (Nguyen *et al.*, 2000).

Several studies have investigated the effects of combining 17-AAG treatment with other chemotherapeutic agents. In combination with paclitaxel, a synergistic effect was observed, resulting in a five to 22-fold increase in apoptosis in NSCLC cell lines (Nguyen *et al.*, 2000). However, 17-AAG antagonised the cytotoxic effect of cisplatin in colon adenocarcinoma, resulting in lower levels of apoptosis than either drug administered individually. This is thought to be a result of differential caspase activation (Vasilevskaya *et al.*, 2003).

Given the potent anticancer effects of Gleevec and 17-AAG in a range of cancers, we proposed to test their activity against OC cell lines, and investigate their effect on the phosphorylation status of ARG. The specific aims of this research were:

- To determine the effect of the tyrosine kinase inhibitor Gleevec™ on the proliferation of OC cell lines
- To determine the effect of the Hsp90 inhibitor 17-AAG on the proliferation of OC cell lines and normal human fibroblasts
- To determine the effect of both of these drugs in combination with each other or the anti-cancer drug cisplatin
- To assess the effect that treatment with either Gleevec or 17-AAG has on the overall phosphotyrosine status of the cell, and thereby establish whether tyrosine kinase inhibition plays an important role in the effect of these drugs on the cells in vitro

## 4.2 Methodology

### 4.2.1 MTT assay

The MTT assay (Mosmann, 1983) is a colorimetric assay of cell proliferation. It is based on the reduction of the yellow tetrazolium salt, 3-(4,5-dimethylthiazol-2-yl)-2,5-diphenyl tetrazolium bromide (MTT), to purple formazan crystals by metabolically active cells. The amount of purple colour can be quantified by reading the absorbance of light at an appropriate wavelength. In combination with observations of cells on a microscopic level for signs of cell death, it gives a good indication of cytotoxicity.

OSSC cell lines were cultured as described in Appendix 1. Cells were plated into 96 well plates at the density shown in table 4.2, in a volume of 90μl per well. The cells were incubated at 37°C overnight to facilitate cell adherence prior to addition of test compound.

Table 4.2. Number of cells plated per well of a 96 well plate for MTT assay

| Cell line | No. of cells plated per well |
|---|---|
| WHCO1 | 3000 |
| WHCO3 | 3000 |
| WHCO5 | 3000 |
| WHCO6 | 3000 |
| DMB | 3000 |
| F1107 | 3000 |
| KYSE30 | 6000 |
| KYSE70 | 6000 |
| KYSE180 | 6000 |
| KYSE520 | 6000 |

The drugs were solubilised in DMSO, to make 50mM (cisplatin), or 10mM stocks (Gleevec and 17-AAG) that were stored at –20°C. Control cells were treated with DMSO alone. A media blank lane was left to determine background absorbance levels. Four replicate wells were treated at each drug concentration.

Cells were incubated in the presence of the test compound for 48hr at 37°C before being viewed under a phase contrast light microscope and examined for morphological changes. 10μl of MTT reagent (Roche, Mannheim) was added to each well, and the plates were incubated for a further four hours at 37°C. 100μl of solubilisation solution (Roche, Mannheim) was added and cells were returned to 37°C incubator overnight. Plates were then read on a 96well plate reader (Anthos 2001) at 595nm. Absorbance readings were analysed using Prism software to determine the $EC_{50}$ values for each cell line. $EC_{50}$ concentrations refers to that concentration which results in a response halfway between the maximum and baseline, thus giving a value that can be compared between different drugs and different cell lines.

For combination treatments, the same basic protocol was followed, but cells were treated at their $EC_{25}$ concentration of each of the drugs individually (17-AAG, cisplatin and Gleevec) and in combination.

### 4.2.2 Cell counting experiments

Cells were plated in 6 or 96 well plates at the densities reported in previous chapters, and treated with Gleevec at a final concentration of 5μM and 10μM (0.33% DMSO) for 48 hours. After treatment, media was collected, and adherent cells were washed with PBS and collected in trypsin by repeated aspiration. The cells were all pelleted by centrifugation for 5 minutes at maximum speed in a Spinnette benchtop centrifuge (IEC), and resuspended in 100μl of PBS. 10μl of this suspension was mixed with 0.4% Trypan blue (Merck), and immediately placed on a haemocytometer. Non-viable cells stained blue, and were counted separately from live cells, which excluded Trypan blue, to determine the percentage viability of the counted cells.

### 4.2.3 Western blot analysis

Western blot to detect phosphorylated tyrosines was carried out essentially as described in Weisberg and Griffin (2000), with modifications. WHCO1, WHCO5, and WHCO6 cells were plated at a density of 1.5 x $10^6$ cells per dish in 35mm dishes, allowed to adhere overnight, and subjected to treatment with either 17-AAG at $EC_{50}$ concentration, or Gleevec at 10μM. Control cells were treated with DMSO at a final concentration of 0.1%. Following a 6 hour incubation with the drug, cells in the media were pelleted as previously, and adherent cells were rinsed in PBS and collected in radioimmunoprecipitation assay (RIPA) buffer including phosphatase inhibitors, 0.1M Sodium fluoride (Merck) and 1mM Sodium orthovanadate (Sigma). The pellet of cells was also resuspended in this buffer. Cells and buffer were kept on ice at all times to prevent protein degradation. The protein solution was then incubated on ice for 25 minutes with vortexing every five minutes, and centrifuged at 12000 RCF in a Heraeus Sepatech Biofuge (model 13R). Protein was quantitated using the BCA Protein Assay Reagent (Pierce), and 50μg was loaded on a 7.5% polyacrylamide gel

(Gallagher, 1999) and run for 3 hours at 30mA. Proteins were transferred to ECL nylon membrane (Amersham Pharmacia Biotech) for 2 hours at 200mA. The membrane was blocked in 5% fat-free milk powder for 1 hour at room temperature, and incubated in anti-Phosphotyrosine primary antibody (Oncogene) at a dilution of 1:100 at 4°C overnight. It was then rinsed and incubated in goat anti-mouse HRP-linked secondary antibody (Bio-Rad) at a dilution of 1:5000 for 1 hour at room temperature. Antibody binding was detected using the Supersignal detection reagent (Pierce).

## 4.3 Results and discussion

### 4.3.1 MTT Assays

MTT assays were performed in order to determine the responsiveness of OSCC cell lines to the anticancer drugs Gleevec and 17-AAG. It was found that, while most cells were sensitive to low concentrations of 17-AAG, they were much less sensitive to Gleevec, which had a very weak effect at concentrations as high as 20μM. The MTT curves are shown in figure 4.5 and 4.6.

The stock concentrations of the different drugs were different, and so control cells were treated with different amounts of DMSO for each treatment. This accounts for variation in the absorbance of untreated cells, despite plating at constant density.

The $EC_{50}$values for each drug, as determined from the curves, are summarised in table 4.3, as well as the $EC_{25}$ values, which were calculated using the equation below, substituting (bottom + 75%(top – bottom)) for y and solving for x:

$$y = \text{bottom} + \frac{\text{top} - \text{bottom}}{1 + 10^{[(\log EC_{50} - x) \times \text{hillslope}]}}$$

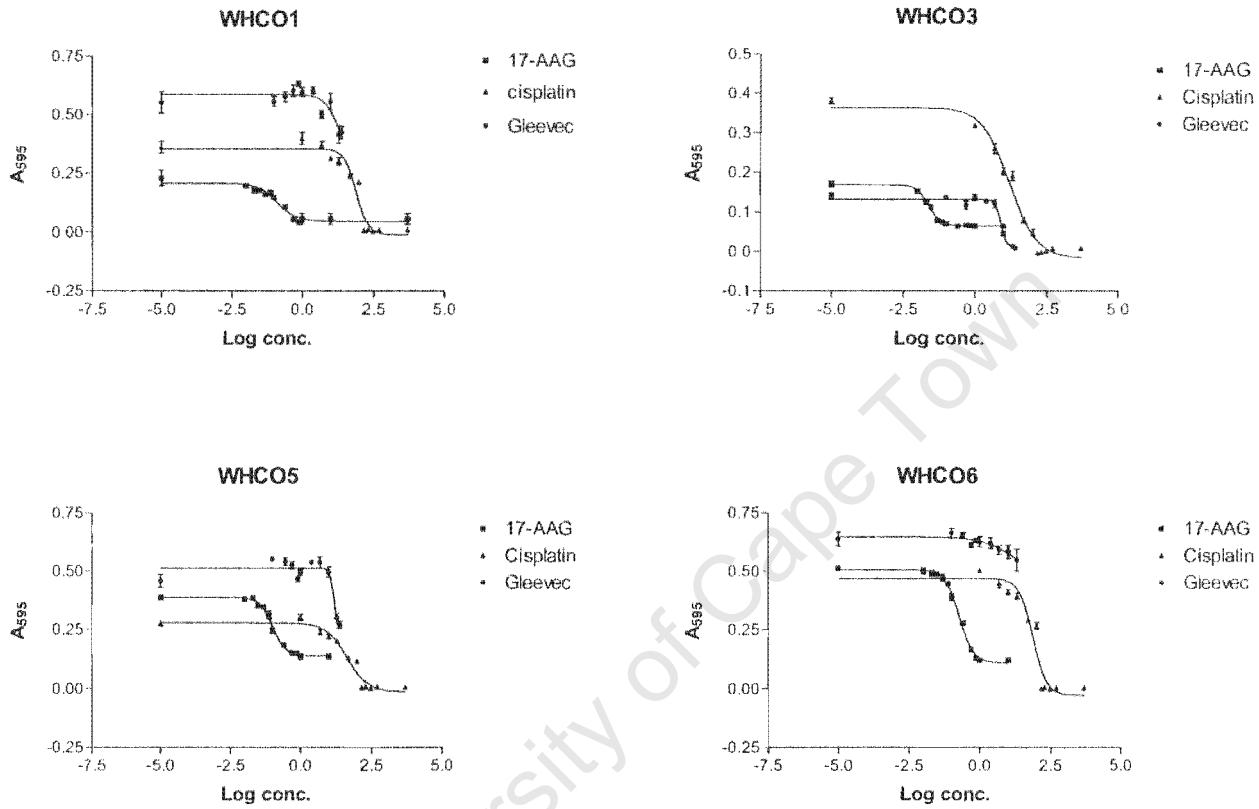




Fig. 4.5. Effect of 17-AAG, cisplatin and Gleevec on WHCO OSCC cell lines determined by MTT assay. Cells were plated in 96 well plates and treated with varying concentrations of drug for 48 hours. Each point represents the average of four replicate wells. Triangles represent cisplatin, circles represent Gleevec, and squares represent 17-AAG.

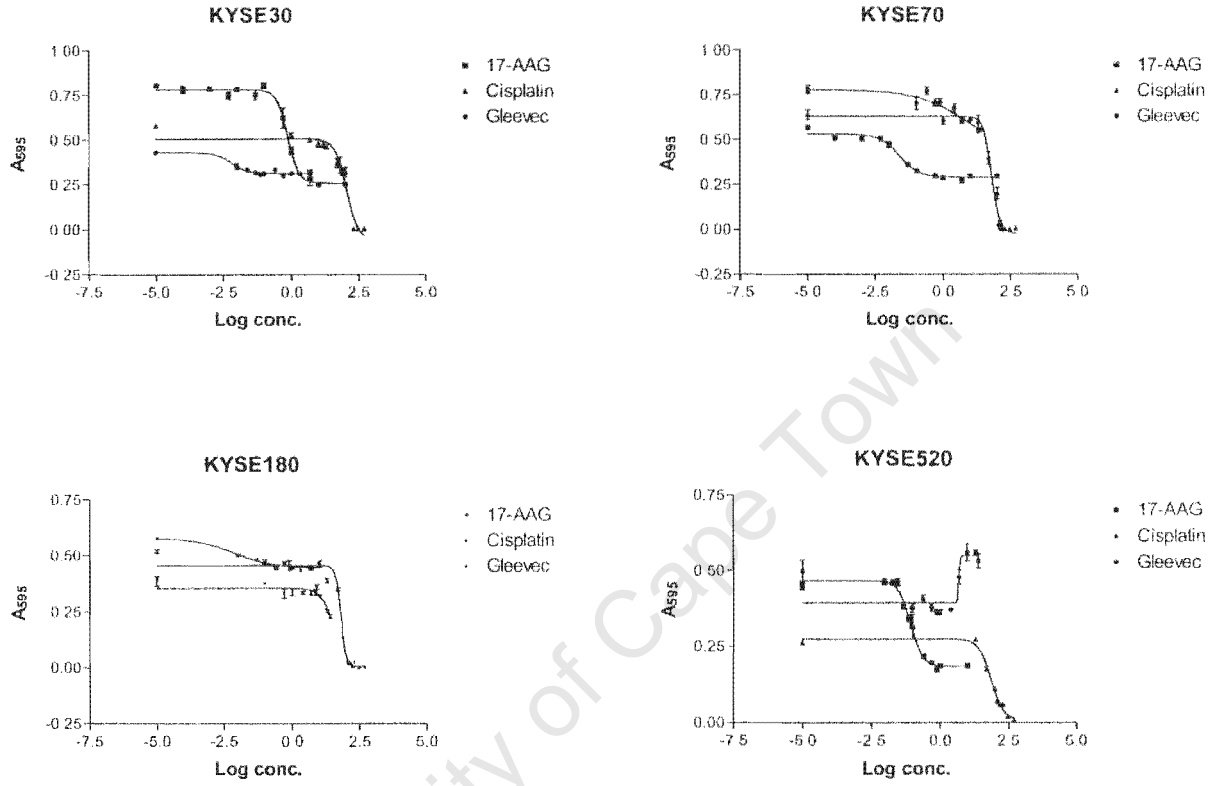


Fig. 4.6. Sensitivity of KYSE OSCC cell lines to 17-AAG, cisplatin and Gleevec, determined by MTT assay. Cells were plated in 96 well plates and treated with varying concentrations of drug for 48 hours. Each point represents the average of four replicate wells. Triangles represent cisplatin, circles represent Gleevec, and squares represent 17-AAG.

Table 4.3. Summary of $EC_{50}$ and $EC_{25}$ values for 8 OSCC cell lines (all values in μM). Where $EC_{50}$ value was incalculable because of very high concentration required (indicated by NA), value in $EC_{25}$ column indicates concentration at which drug was administered for drug combination experiments

| Cell line | 17-AAG | | Cisplatin | | Gleevec | |
|---|---|---|---|---|---|---|
| | $EC_{50}$ | $EC_{25}$ | $EC_{50}$ | $EC_{25}$ | $EC_{50}$ | $EC_{25}$ |
| WHCO1 | 0.1291 | 0.3 | 81.39 | 48 | NA | 10 |
| WHCO3 | 0.02452 | 0.014 | 15.95 | 5 | 8.218 | 6.5 |
| WHCO5 | 0.103 | 0.06 | 45.27 | 18 | NA | 10 |
| WHCO6 | 0.1896 | 0.1 | 73.66 | 40 | NA | 10 |
| KYSE30 | 0.7443 | 0.45 | 110.5 | 65 | NA | 10 |
| KYSE70 | 0.02489 | 0.01 | 63.73 | 44 | NA | 10 |
| KYSE180 | 0.0095 | 0.0014 | 63.89 | 50 | NA | 10 |
| KYSE520 | 0.08774 | 0.05 | 72.50 | 41 | NA | 10 |

All of the OSCC cell lines were sensitive to 17-AAG, with $EC_{50}$ concentrations below 1μM. In order to determine whether the drug was specifically selective for cancer cells, or exhibited cytotoxic effects on all types of cells, MTT assays were also performed on normal human fibroblasts. The DMB and F1107 cell lines, isolated from skin epithelium were used for this experiment. The MTT curves shown below (figure 4.7) show that 17-AAG did have an anti-proliferative effect on the fibroblasts. It gave $EC_{50}$ values of 0.001μM and 0.006μM for DMB and F1107 respectively.

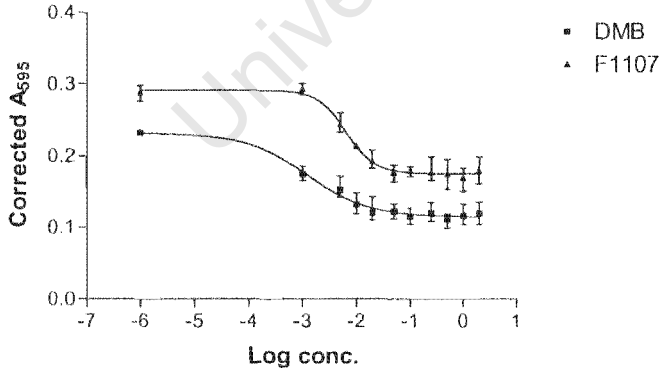


Fig. 4.7. Effect of 17-AAG on normal human fibroblast cell growth. DMB and F1107 cells were plated in 96 well plates and treated with varying concentrations of 17-AAG in quadrupilcate. After 48 hours of drug treatment the effect of 17-AAG on cell proliferation was measured by MTT assay.

Since the Gleevec was resuspended in DMSO, the maximum concentration that could be administered to the cells before the effect of the solvent became evident was 20μM. Since most cell lines showed very little response to Gleevec, $EC_{50}$ values could not be accurately calculated, and further treatments in combination with other drugs were simply done at 10μM.

Although Gleevec seemed to have little effect on the growth of the OSCC cell lines, we have demonstrated that similar concentrations of Gleevec significantly inhibited the growth of K562 cells. The human chronic myeloid leukaemia cell line, K562, has been reported to be sensitive to Gleevec (Weisberg and Griffin, 2000). An MTT assay was performed on these cells with varying concentrations of Gleevec, and gave an $EC_{50}$ value of 0.1408μM (as shown in figure 4.8), which is comparable to the value reported by Weisberg and Griffin (2000). Since this was lower than the $EC_{50}$ values of the OSCC cell lines, we concluded that the lack of response to Gleevec treatment by OSCC cell lines was indeed due to low sensitivity, and not due to reduced activity of the Gleevec used.



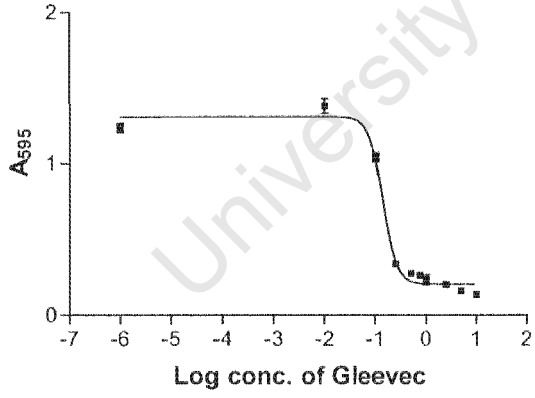


Fig. 4.8. MTEffect of Gleevec on K562 cell growth. Cells were treated with varying concentrations of Gleevec for 48 hours after which, cell proliferation was measured by MTT assay.

For the KYSE520 cells, treatment with Gleevec repeatedly resulted in increased absorbance at 595nm. However, microscopic observations of the treated cells

failed to show any obvious increase in cell number compared to untreated cells. It was, however, important to confirm quantitatively that the increase in absorbance was not due to increased proliferation of the cells. It has been reported that one of the pitfalls of the MTT assay is the induction of higher than normal mitochondrial activity by certain agents, although this is not indicative of increased cell growth (Bernhard *et al.*, 2003). In the next section, cells were manually counted using a haemocytometer to directly determine the effect of Gleevec on the proliferation of KYSE520 cells.

### 4.3.2 Cell counting experiments

Although MTT assays showed increased absorbance in KYSE520 cells treated with Gleevec, a direct cell count using a haemocytometer revealed that treatment of KYSE520 with increasing concentrations of Gleevec resulted in a decrease in cell number (shown in figure 4.9).

There was no significant increase in the number of non-viable cells counted, as identified by trypan blue staining (data not shown). This indicates that Gleevec caused reduced cell proliferation, rather than a toxic effect, with simultaneous increase in mitochondrial metabolic activity.

The results seen for KYSE520 raised questions concerning the apparently relatively weak antiproliferative effects of Gleevec treatment observed in the other cell lines, and whether this was also due to an increased metabolic rate of the mitochondria. Therefore, similar cell counting experiments were performed on 2 other cell lines: KYSE70 and KYSE180. These cells were plated into 35mm dishes and treated with varying concentrations of Gleevec for 48 hours, before being trypsinised and counted using a haemocytometer.

A

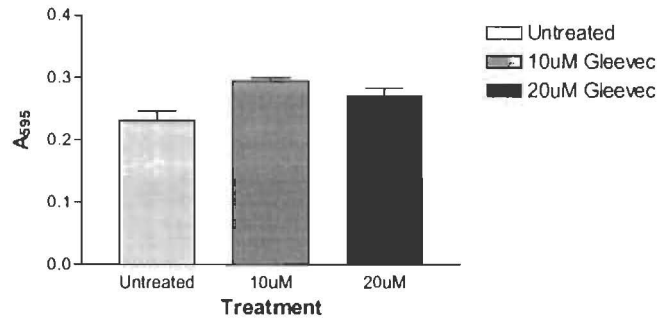


B

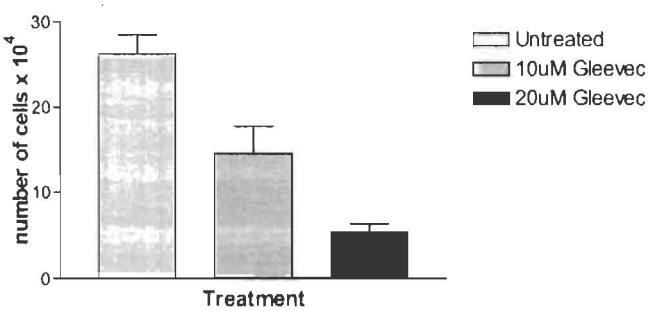


Fig. 4.9. Comparison of effect of Gleevec treatment on KYSE520 measured by (A) MTT assay and (B) Cell counting. Cells were treated with varying concentrations of Gleevec. MTT assay represents the average of four replicate wells, while cell counting data reflects the average of three replicate 35mm dishes.



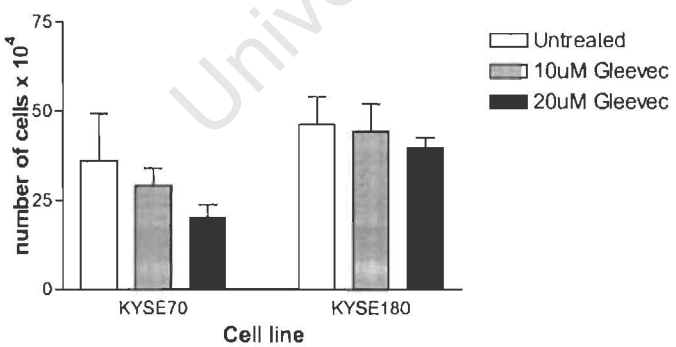


Fig. 4.10. Effect of Gleevec on cell number for two OSCC cell lines. Cells were treated with varying concentrations of Gleevec in 35mm dishes in triplicate. After 48hours of treatment, cells were trypsinised and counted directly using a haemocytometer.

The graph in figure 4.10 illustrates the results of cell proliferation assays for KYSE 70 and 180. A slight drop in cell number is observed, which is consistent with MTT curves (figure 4.5 and 4.6). Once again, no significant increase in the proportion of non-viable cells was observed. It was concluded that the weak effects of Gleevec determined by the MTT assay were an accurate reflection of resistance of OSCC cell lines to the drug, rather than the induction of increased mitochondrial activity, except in KYSE520, where Gleevec increased the cellular metabolic rate.

### 4.3.3 Drug combination treatments

In order to determine the effects of simultaneous treatment of OSCC cells lines with different drugs, cells were plated in 96 well plates and treated with each drug individually at $EC_{25}$ concentration, or a combination of drugs, each at $EC_{25}$. Cell proliferation, measured by MTT assay indicated that treatment of cells with combinations of drugs did not produce any noticeable synergism in any of the cell lines tested (figure 4.11); nor was there any antagonistic effect, but most of the interactions proved to be approximately additive.

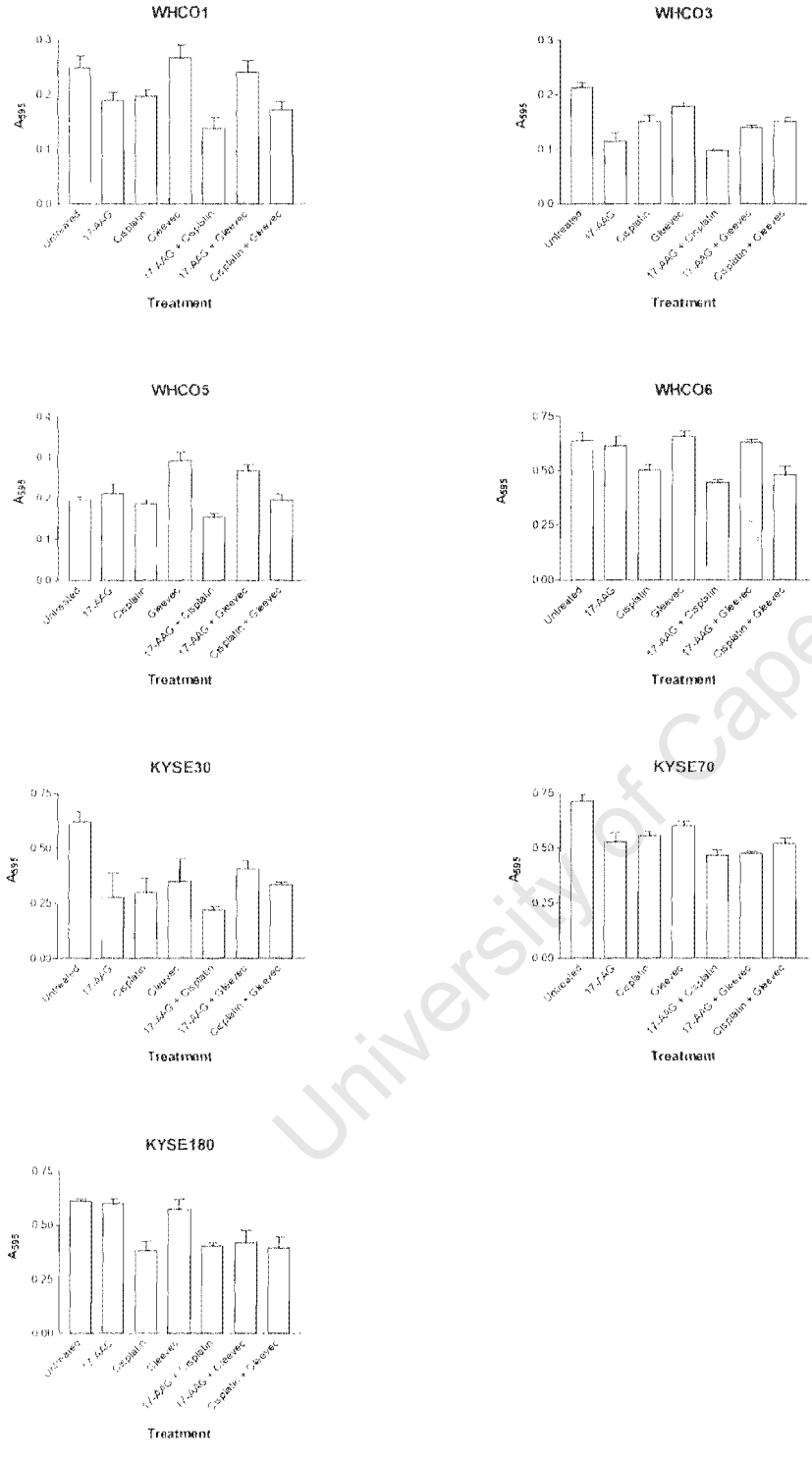




Fig. 4.11. Effect of drug combinations on cell metabolism of 8 OSCC cell lines as measured by MTT assay. Cells were plated in 96 well plates, and treated with drugs for 48 hours. Each point represents the average of four replicate wells.

### 4.3.4 Western blot analysis

Western blot analysis was carried out to determine the overall levels of tyrosine phosphorylation in untreated cells compared to those treated with Gleevec or 17-AAG. It was hoped to deduce whether tyrosine kinases were significantly inhibited by either drug. The results of the Western blot experiment are shown in figure 4.12 below. Coomassie staining of the protein gel after transfer showed that there was equal loading of protein in each lane (data not shown).

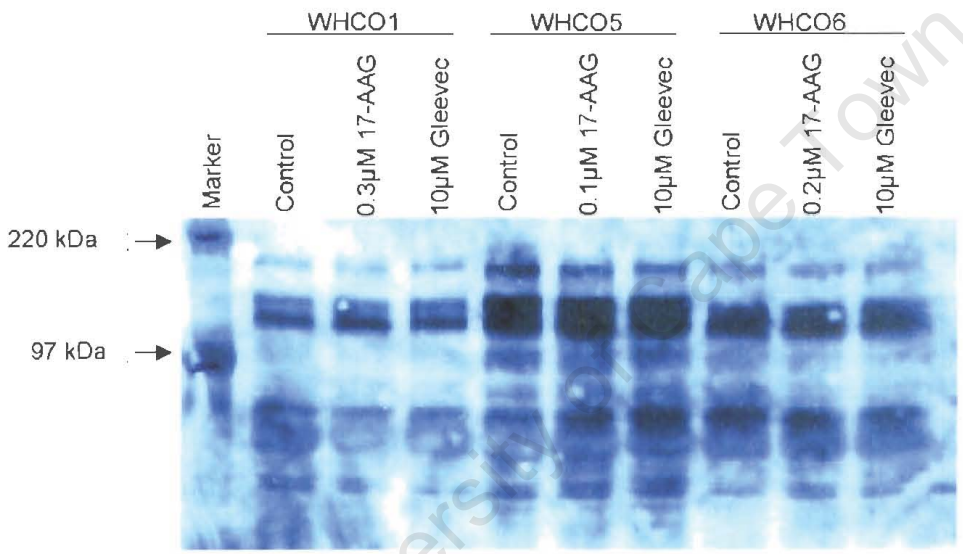




Fig. 4.12. Western blot of cell line protein extracts with anti-Phosphotyrosine antibody. Cells were treated with 10μM Gleevec or 17-AAG at $EC_{50}$ concentration for 6 hours prior to protein collection in RIPA buffer with phosphatase inhibitors. 50μg of each cell lysate was electrophoresed on a 7.5% polyacrylamide gel and transferred to membrane.

The Western blot shows that there was no significant inhibition of tyrosine phosphorylation by 17-AAG at $EC_{50}$, or Gleevec at 10μM. Gleevec had very little effect on cell proliferation, and it could therefore be argued that no change in phosphorylation should be expected. However the results for 17-AAG were surprising since it has causes a substantial reduction in cell proliferation at this concentration. There are three possible explanations for this result: the treatment time could be inappropriate to detect changes in kinase activity; the drug could have lost its potency due to freeze thawing or exposure to light; or the effect on

cell proliferation observed on treatment with 17-AAG could be mediated by proteins other than tyrosine kinases.

The first explanation seems unlikely in view of results in the literature. Changes in phosphorylation are typically demonstrated over a short time (e.g. 2 hours for Gleevec on K562 cells; Weisberg and Griffin, 2000). In order to preclude the possibility of the drug becoming ineffective, an MTT assay was performed using the same aliquots of 17-AAG as were used prior to protein extraction. The MTT assay clearly showed a reduction in cell metabolism after 48 hours for all three cell lines (see figure 4.13). It was concluded that loss of drug potency was not responsible for the lack of change in tyrosine phosphorylation levels.

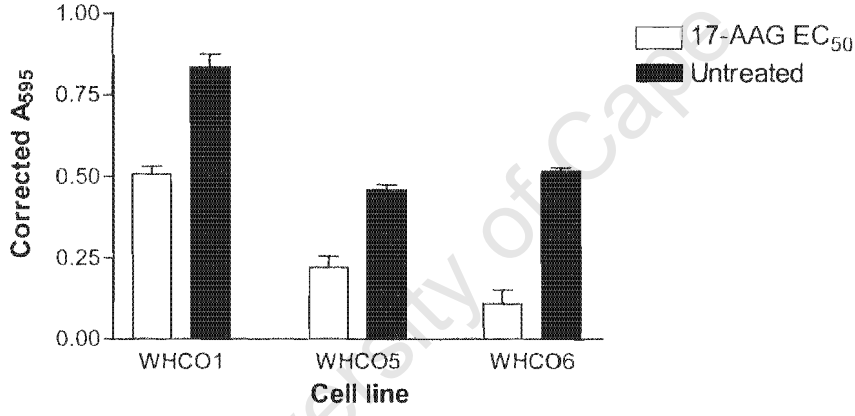


Fig. 4.13. MTT assay results to confirm potency of 17-AAG used in Western blot. Cells were tested in 96 well plate format with the same aliquots of 17-AAG as used for Western blot experiment. Error bars represent SEM of 8 replicate wells.



It was therefore concluded that the mechanism by which 17-AAG inhibited cell growth did not involve decreased expression of tyrosine kinases due to inhibition of Hsp90. There are reports in the literature of decreases in the levels of serine-threonine kinases such as Akt and Raf1 (Nimmanapalli *et al.*, 2003); as well as mutant p53, Hif1-α, MMP9 and telomerase (Blagoskonny *et al.*, 1995; Gradin *et al*, 1996; Nguyen *et al.*, 2000 and Villa *et al.*, 2003 respectively). Attenuation of these proteins could also be responsible for the reduction in cell growth observed.

## 4.4 Summary

The 8 OSCC cell lines were relatively resistant to Gleevec ($EC_{50}$ values mostly greater than 10μM), but exhibited a favourable response to 17-AAG at concentrations in the 0.001- 0.2μM range. For some of the cell lines, treatment with Gleevec resulted in decreased cell proliferation, with increased mitochondrial metabolism. Neither 17-AAG nor Gleevec exhibited a synergistic effect in combination with cisplatin. The combined effect of 17-AAG and Gleevec together was additive.

# CHAPTER 5

## Conclusions and future perspectives

This project has yielded a number of interesting findings which warrant further investigation. Our results strongly suggest that RARß2 expression is reduced in tumour tissue in a subset of OC patients by hypermethylation of the promoter region of this gene. The most valuable outcome of the study regarding RARß2 expression in OC, would be the development of an early detection assay for the disease. This may involve methylation specific PCR of DNA from peripheral blood, as described in the literature for other cancer markers (Wong *et al.*, 1999; Zou *et al.*, 2002). However, in order to be sufficiently accurate, it would be advisable to use a mixture of primers, since methylation may occur in different regions of the promoter in different patients. This technique should also be considered for use in combination with other markers of cancer development such as p16 and p15. Future work should include sodium bisulfite genomic sequencing on DNA from tumour and normal samples without cloning. This should be carried out on a large number of samples to give an indication of the frequency at which hypermethylation occurs in the overall population of OC patients. This could indicate the potential benefit to be gained from therapies that involve demethylation of DNA, using agents such as 5-Aza-dC.

Should results of further experiments indicate that hypermethylation of the RARß2 promoter is not involved in decreased expression of the gene in vivo, it would be interesting to investigate several other mechanisms which may play a role. These include altered histone acetylation patterns, as reported in breast and lung cancer (Sirchia *et al.*, 2002; Suh *et al.*, 2002 respectively). This can be detected by performing ChIP assays with antibodies specific for acetylated histones. An alternative experimental approach is treatment of cell lines with histone deacetylase inhibitors, such as Trichostatin A, to prevent deacetylation of histones, and measure levels of gene induction.

The finding that Trio may be overexpressed in cancer tissue may indicate that Trio is an important regulator of cancer cell metastasis. Before further

experimentation is done, it would be best to confirm that Trio expression is elevated in cancer compared to normal in a large sample of OC patients, which this initial study failed to accomplish. This would require a more specific anti-Trio antibody than the one used in this study, for immunohistochemical staining of archived tissue sections. This is probably a preferable method to real time PCR, since the tissue sections needed for immunohistochemistry are available. Real time PCR would require collection of a large number of samples, and these have to be treated very carefully to ensure RNA of high quality.

We propose that the development of stably transfected OSCC cells with Trio RNAi would allow one to determine the role that this protein plays in metastasis. Its effects could be quantitated by means of assays for surrogate markers of metastasis such as cell adhesion and matrigel invasion. Besides genetic downregulation of Trio protein, chemical prevention of protein activity may be of interest, and could hold potential therapeutic benefits for patients as an anti-metastatic drug. An inhibitor of the Trio-GEF2 domain, TRIPα, has been identified by high-throughput screening of peptide aptamers (Schmidt *et al.*, 2002). Although this is the domain that controls the RhoA signalling pathway leading to cell retraction, rather than cell motility, similar inhibitors of GEF1 may be identified by a similar procedure. This could prove an important way to reduce cancer cell motility and metastasis.

Probably the most significant result obtained from this project is the potent anti-proliferative effect of the Hsp90 inhibitor 17-AAG on OSCC cell lines. It would be interesting to continue this line of research by determining the precise molecular effect of the drug. This would involve conducting apoptosis assays, and flow cytometry to identify possible cell cycle blocks. Testing the drug in combination with a wider range of currently used chemotherapeutic agents, such as 5-fluorouracil, may also be valuable. Further investigation in vivo would entail treating induced tumours in nude mice, to identify any unforeseen complications associated with the use of this drug before commencing clinical trials. The identification of proteins indirectly inactivated by 17-AAG (via Hsp90), would make a significant contribution to our understanding of genes necessary for the

survival and proliferation of OC cells. This information may allow future targeting of these proteins in the effort to combat this disease.

The effect of Gleevec on OSCC cell lines was disappointing, given its reported inhibition of ARG, and the novel finding that this tyrosine kinase is upregulated in OC. However, recent research in pancreatic cancer indicates that Gleevec has a similarly weak effect in this disease (Li *et al.*, 2003). Four cell lines were tested in this study, and their $EC_{50}$ values ranged from 17- 35μM. It has also been reported that despite being highly efficacious in the treatment of gastrointestinal stromal tumours, Gleevec did not benefit patients with other soft tissue sarcomas (Verweij *et al.*, 2003). It seems unlikely that Gleevec will have any clinical application in the treatment of OC.

However, given the extremely severe nature of oesophageal cancer, and the negligible rate of patient survival, it is essential to follow up any possibility of improved therapy or detection methods. Further research into differentially expressed genes involved in OC is therefore strongly advised.

## APPENDIX 1: ROUTINE LABORATORY PROCEDURES

### 1.1. Safety Precautions

When working in the lab, standard safety precautions were observed. These included wearing gloves when working with infectious agents such as bacteria, or human tissue which could potentially be contaminated with viral carcinogens. Sharps and hazardous chemicals such as phenol and ethidium bromide were disposed of in appropriate containers.

When working with radioactive material, all working surfaces and equipment were checked with a Geiger counter before and after any work. Work was carried out behind a perspex screen and exposure was limited as much as possible. Disposal of radioactive tips and waste was carried out according to the safety regulations to prevent contamination of the environment.



### 1.2. Cell culture

*Cell Lines*

The differentiation status of the primary tumour from which different OSCC cell lines were established, are summarised in table A1.1 below.

Table A1.1. Characteristics of OSCC cell lines (Veale and Thornley, 1989; Shimada *et al.*, 1997)

| Cell line | Differentiation Status |
|---|---|
| WHCO1 | Moderate |
| WHCO3 | Moderate |
| WHCO5 | Moderate |
| WHCO6 | Moderate |
| KYSE30 | Well |
| KYSE70 | Poor |
| KYSE180 | Well |
| KYSE520 | Moderate |

Cells were cultured in a Queue incubator at 37°C, 5% $CO_2$, changing media 2 to 3 times per week. The different types of media used for different cell lines are summarised in table A1.2 below.

Table A1.2. Media requirements of cell lines

| Cell line | Media | % Fetal calf serum | Freezing medium |
|---|---|---|---|
| WHCO1, WHCO3, WHCO5, WHCO6 | DMEM | 10% | 90% culture medium +10% DMSO |
| KYSE30, KYSE70, KYSE180, KYSE520 | DMEM | 5% | 20% culture medium + 70% foetal calf serum + 10% DMSO |
| SiHa, HeLa | MEM | 10% | 90% culture medium + 10% DMSO |
| ME180 | McCoy's 5A | 10% | 90% culture medium + 10% DMSO |
| SK-N-SH, MDA-MB-231 | DMEM | 10% | 90% culture medium + 10% DMSO |
| K562 | RPMI | 10% | 90% culture medium + 10% DMSO |
| DMB, F1107 | DMEM | 10% | 90%culture medium + 10% DMSO |

The media was supplemented with 1% penicillin/streptomycin solution, except for 1 week before performing a mycoplasm test. When cells reached approximately 80% confluency, they were trypsinised and passaged. Cells of the KYSE series were centrifuged to remove trypsin before being replated.

For long-term storage in liquid nitrogen, cells were trypsinised, centrifuged to pellet, and resuspended in the freezing medium indicated in Table A1.2. The cells were dispensed into cryovials in 1ml aliquots. These were frozen slowly at –70°C overnight before transferral to liquid nitrogen.

Mycoplasm testing was carried out at least 2 to 3 times per year to check that the cells were free of contamination. Prior to testing, cells were cultured for at least 1 week in media without antibiotic supplements. The cells were then trypsinised, spun out of the trypsin and resuspended in antibiotic free-media. A drop of this suspension was placed onto a sterile coverslip in a 60mm dish, and allowed to adhere at 37°C. After approximately 5 hours, 3ml of media was added to the dish, which was further incubated overnight. The mycoplasm check was carried out by Ingrid Baumgarten (Chemical Pathology, UCT), by performing a Hoechst stain and examining the cells under a fluorescent microscope.



## 1.3. Cloning

Where long term storage of probes was necessary, these were cloned into bacteria and stored as frozen cultures at –70°C. Cloning was also employed for DNA fragments that were to be sequenced.

*Preparation of competent cells*

5ml of Luria broth (LB) was inoculated with 50µl of frozen stock of *Eschericia coli* XL1 cells, and incubated overnight at 37°C with shaking at 200rpm in a Controlled Environment Incubator Shaker (Series 25) (New Brunswick Scientific Co., NJ). 200ml of LB was inoculated with 200µl of overnight culture, and this was incubated as previously. The OD of the culture was monitored until it reached 0.4- 0.6 (600nm), at which point cells were pelleted by spinning at 2000rpm in a Beckman benchtop centrifuge (4°C). All but 2ml of the medium was decanted, and cells were resuspended in the remaining supernatant. Five volumes of ice cold $CaCl_2$ (50mM) was added, and cells were incubated on ice for 1.5 hours. Cells were spun very slowly (~800rpm) for 2 minutes and all but 3ml of the supernatant was removed by aspiration. An equal volume of $CaCl_2$-

glycerol-PIPES solution was added, and the cells were dispensed into 200µl aliquots in eppendorfs before being stored at –70°C.

*Ligation*

PCR products were cut out of a gel and purified using spin columns (QIAquick gel extraction kit, QIAGEN). The DNA was quantitated and combined with the vector DNA in a molar ratio of 3:1, with T4 DNA ligase and sd$H_2O$ to a final volume of 10µl. The mixture was incubated overnight at 4°C.

*Transformation of competent cells*

2µl of the ligation mixture was placed into a 1ml eppendorf on ice, to which was added 50µl of competent cells. The cells were then incubated on ice for 20 minutes before a 50s heat shock in a 42°C waterbath. Tubes were returned to ice for 2 minutes, and 950µl of SOC medium was added. Cells were allowed to recover for 1.5 hours at 37°C as previously with shaking (~150rpm). 100µl of each transformation reaction was plated onto duplicate LB-Amp plates, and incubated overnight at 37°C. Blue-white selection was carried out, where appropriate, by adding 20µl of 50mg/ml X-gal and 100µl of 0.1M IPTG to the surface of the plate, smearing to cover entire surface and allowing to dry, before plating cells.



*Screening for inserts*

Colonies were screened for the presence of an insert either by (i) isolation of the plasmid DNA followed by restriction enzyme digestion to check for a band of the expected size (12 units *EcoR*I per 5µl DNA at 37°C overnight) or (ii) colony PCR using primers specific for the insert of interest.

*Plasmid preparation*

Colonies were inoculated into 5ml LB + 50µg/ml Ampcillin and cultured overnight. Cells were pelleted by spinning at 2000rpm for 5 minutes. The supernatant was

decanted and cells resuspended in 200µl GTE solution. 2µl RNase A was added and incubated for 5 minutes at room temperature. Fresh NaOH/SDS solution was prepared and 400µl was added. Tubes were placed on ice for 5 minutes. This solution was transferred to a 1ml eppendorf and 300µl of potassium acetate solution was added. Tubes were votexed and placed on ice for 5 minutes before a 3 minute spin in a Eppendorf microfuge (5414S) to pellet cell debris and chromosomal DNA. Supernatant was removed and the spin step repeated. 0.8ml of 95% ethanol was added, and the tubes were left at room temperature for 2 minutes to allow the plasmid DNA to precipitate. Plasmid DNA was pelleted by spinning for 2 minutes at top speed in a Heraeus Sepatech Biofuge (model 13R). The pellet was then washed with 70% ethanol and resuspended in TE buffer or sd$H_2O$.

## 1.4. DNA Extraction and Analysis

*Extraction of DNA from cultured cells*

Cells grown in a 35- 60mm dish were washed with cold PBS, and lysed with 1ml of lysis buffer collected into a 1ml eppendorf. This solution could be stored at –20°C before processing, or processed immediately. 55µl of Proteinase K (10mg/ml) was added and tubes were incubated at 65°C for 15 minutes to inactivate endogenous DNases, before overnight incubation at 50°C. The solution was extracted with 500µl of phenol: chloroform: isoamylalcohol (IAA) (25:24:1), spun briefly to facilitate phase separation, and the top phase was transferred to a clean eppendorf tube. Extraction with chloroform: IAA (24:1) was carried out in the same way. 50µl of 3M sodium acetate and 1ml of ice cold absolute ethanol were added, and precipitation was carried out at –20°C for 20 minutes- overnight. DNA was pelleted by a 10 minute centrifugation at top speed in a Heraeus Sepatech centrifuge (model 13R), and washed in 70% ethanol to remove excess salts. The pellets were air dried and resuspended in TE or sd$H_2O$.

*Spectrophotometric analysis of Nucleic acids*

Quantitation of nucleic acids was performed in a Beckman DU 650 spectrophotometer. Absorbance was measured at 260nm and 280nm. The ratio of 260: 280 was used to indicate the purity of nucleic acid, and whether there was significant contamination by protein or phenol.

*Standard electrophoresis of Nucleic acids*

RNA gels were prepared in a fume hood by dissolving 1g agarose in 85ml DEPC water and 10 ml 10x MOPS. This solution was cooled to 60°C and 5.4ml of 12.3M formaldehyde and 2μl ethidium bromide were added. When set, the gel was placed in a tank and covered with 1x MOPS buffer. 10μl of formaldehyde loading buffer was added to the sample to be elecrophorectically separated (usually 1- 15μg). The sample was heated to 55°C for 15 minutes before loading. The gel was run at 50V for approximately 1 hour, depending on the migration of the dye.

For Northern blotting, gels were photographed and washed twice for 20 minutes in 10x SSC. The gel was placed inverted on a stack of paper towel that had been completely soaked in 10x SSC and had all air bubbles removed in a pyrex dish. Wet Hybond-$N^+$ nylon transfer membrane (Amersham Pharmacia Biotech) was placed on top of the gel and air bubbles were carefully removed by rolling with a pipette. Two pieces of Whatman paper were placed on top and again, air bubble were carefully removed. All of the exposed tissue paper was covered with cling wrap, and a stack of dry paper towel was placed on top, pressed down by a weight on a piece of glass. The entire dish was covered with cling wrap and allowed to transfer for 17- 18 hours at room temperature. The blot was then rinsed, dried, and RNA was immobilised by UV crosslinking or baking at 80°C for 3 hours. Blots were stored at 4°C in a dessicator.

DNA samples to be run on a gel were made up to 10ul and mixed with 2μl of 6x loading dye before being loaded on a 2% agarose gel containing 0.2μg/ml

ethidium bromide in 1x TAE or TBE. Voltage of 60- 90V was applied for 30- 90 minutes depending on desired migration of the loading dye.

*Table of Primers*

| Gene | Product | Sequences | Reference |
|---|---|---|---|
| RARß2 | 721bp from mRNA | 5'- AGA GTT TGA TGG AGT TGG GTG GAC -3'<br>5'- GCT GGC AGA GTG AAG GGA AAG TTT -3' | Widschwendter *et al.*, 2000 |
| LDL-R | 276bp from mRNA | 5'- CAA TGT CTC ACC AAG CTC TG -3'<br>5'- TCT GTC TCG AGG GGT AGC TG -3' | Widschwendter *et al.*, 2000 |
| RARß2 | 330bp from exon 5 | 5'- GGC TTT TAG CTG GCT TGT CTG –3'<br>5'- TGA GCA GTG TGC CGA TGC TG –3' | Sommer, *et al.*, 1999 |
| 18S rRNA | 148bp from mRNA | 5'- GTA ACC CGT TGA ACC CCA TT –3'<br>5'- CCA TCC AAT CGG TAG TAG CG –3' | Uray *et al.*, 2002 |
| RARß promoter P2 and part of exon 5 | 710bp from DNA- first round of nested PCR | 5'- GTA TAG AGG AAT TTA AAG TGT GGG TTG GG –3'<br>CCT ATA ATT AAT CCA AAT AAT CAT TTA CC –3' | Widschwendter *et al.*, 2000 |
| | 635bp from DNA- second round of nested PCR | 5'- GTA GG(C/T) GGA ATA TTG TTT TTT AAG TTA AG –3'<br>5'- AAT CAT TTA CCA TTT TCC AAA CTT ACT C –3' | Widschwendter *et al.*, 2000 |
| RARß promoter P2 methylated | 146bp from $Na_2S_2O_5$ treated DNA | 5'- TCG AGA ACG CGA GCG ATT CG –3'<br>5'- GAC CAA TCC AAC CGA AAC GA –3' | Kuroki *et al.*, 2003 |

| | | | |
|---|---|---|---|
| RARß promoter P2 unmethylated | 146bp from $Na_2S_2O_5$ treated DNA | 5'- TTG AGA ATG TGA GTG ATT TGA –3'<br>5'- AAC CAA TCC AAC CAA AAC AA –3' | Kuroki *et al.*, 2003 |
| ß-actin | 650bp from genomic DNA | 5'- TGA CGG GGT GAC CCA CAC TGT GCC CAT CTA –3'<br>5'- CTA GAA GCA TTT GCG GTG GAC GAT GGA GGG –3' | Matsha, *et al.*, 2002 |
| Trio exon 4 | 445bp from DNA | 5'- GGC CTT ACC AAA GTA GTT GAT CC –3'<br>5'- GCT TCA GCT TCC TCA CAT GC –3' | Designed using Primer 3 software (Rosen and Skaletsky, 2000) |
| GAPdH for real time PCR | 225bp from cDNA | 5'-AAG GTC GGA GTC AAC GGA TT-3'<br>5'-CTC CTG GAA GAT GGT GAT GG-3' | Engelbrecht, *et al.*, 2003 |
| Trio exon 4 for real time PCR | 200bp from cDNA | 5'- GGC CTT ACC AAA GTA GTT GAT CC –3'<br>5'- CGA GCC CCC TCT AAA TCC T-3' | Designed using Primer 3 software (Rosen and Skaletsky, 2000) |

## REFERENCES


Adler CE, Miyoshi-Akiyama T, Aleman LM, Tanaka M, Smith JM, Mayer BJ. Abl family kinases and Cbl cooperate with the Nck adaptor to modulate Xenopus development. J Biol Chem. 2000; 275:36472-8.

Altucci L, Gronemeyer H. The promise of retinoids to fight against cancer. Nat Rev Cancer. 2001; 1:181-93.

Bachman KE, Park BH, Rhee I, Rajagopalan H, Herman JG, Baylin SB, Kinzler KW, Vogelstein B. Histone modifications and silencing prior to DNA methylation of a tumor suppressor gene. Cancer Cell. 2003; 3:89-95.

Bagatell R, Khan O, Paine-Murrieta G, Taylor CW, Akinaga S, Whitesell L. Destabilization of steroid receptors by heat shock protein 90-binding drugs: a ligand-independent approach to hormonal therapy of breast cancer. Clin Cancer Res. 2001; 7:2076-84.

Bah E, Hall AJ, Inskip HM. The first 2 years of the Gambian National Cancer Registry. Br J Cancer. 1990; 62:647-50.

Bateman J, Van Vactor D. The Trio family of guanine-nucleotide-exchange factors: regulators of axon guidance. J Cell Sci. 2001; 114:1973-80.

Baylin SB, Bestor TH. Altered methylation patterns in cancer cell genomes: cause or consequence? Cancer Cell. 2002;; 1:299-305.

Baylin SB, Herman JG. DNA hypermethylation in tumorigenesis: epigenetics joins genetics. Trends Genet. 2000;16:168-74.

Bayo S, Parkin DM, Koumare AK, Diallo AN, Ba T, Soumare S, Sangare S. Cancer in Mali, 1987-1988. Int J Cancer. 1990; 45:679-84.

Bernhard D, Schwaiger W, Crazzolara R, Tinhofer I, Kofler R, Csordas A. Enhanced MTT-reducing activity under growth inhibition by resveratrol in CEM-C7H2 lymphocytic leukemia cells. Cancer Lett. 2003; 1:193-9.

Blagosklonny MV, Toretsky J, Neckers L. Geldanamycin selectively destabilizes and conformationally alters mutated p53. Oncogene. 1995; 11:933-9.

Blot WJ. Esophageal cancer trends and risk factors. Semin. Oncol. 1995; 21: 403.

Brand *et al.*, Identification of a second human retinoic acid recpetor. Nature 1988; 332: 850- 853

Buchdunger E, O'Reilly T, Wood J. Pharmacology of imatinib (STI571). Eur J Cancer. 2002; 38 Suppl 5:S28-36.

Bustin SA. Quantification of mRNA using real-time reverse transcription PCR (RT-PCR): trends and problems. J Mol Endocrinol. 2002;29:23-39.

Campbell LJ, Patsouris C, Rayeroux KC, Somana K, Januszewicz EH, Szer J. BCR/ABL amplification in chronic myelocytic leukemia blast crisis following imatinib mesylate administration. Cancer Genet Cytogenet. 2002;139:30-3.

Cao C, Leng Y, Li C, Kufe D. Functional interaction between the c-Abl and Arg protein-tyrosine kinases in the oxidative stress response. J Biol Chem. 2003; 278:12961-7

Cerione RA, Zheng Y. The Dbl family of oncogenes. Curr Opin Cell Biol. 1996; 8:216-22.

Chakravarti N, Mathur M, Bahadur S, Shukla NK, Rochette-Egly C, Ralhan R. Expression of RARalpha and RARbeta in human oral potentially malignant and neoplastic lesions. Int J Cancer. 2001; 91:27-31.

Chambon P. A decade of molecular biology of retinoic acid receptors.
FASEB J. 1996;10:940-54.

Chen WS, Kung HJ, Yang WK, Lin W. Comparative tyrosine-kinase profiles in colorectal cancers: enhanced arg expression in carcinoma as compared with adenoma and normal mucosa. Int J Cancer. 1999; 83:579-84.

Chen LI, Sommer KM, Swisshelm K. Downstream codons in the retinoic acid receptor beta -2 and beta -4 mRNAs initiate translation of a protein isoform that disrupts retinoid-activated transcription. J Biol Chem. 2002; 277:35411-21.

Clarke PA, Hostein I, Banerji U, Stefano FD, Maloney A, Walton M, Judson I, Workman P. Gene expression profiling of human colon cancer cells following inhibition of signal transduction by 17-allylamino-17-demethoxygeldanamycin, an inhibitor of the hsp90 molecular chaperone. Oncogene. 2000;19: 4125-33.

Cohen MS, Hussain HB, Moley JF. Inhibition of medullary thyroid carcinoma cell proliferation and RET phosphorylation by tyrosine kinase inhibitors. Surgery. 2002;132:960-6.

Costello JF, Fruhwald MC, Smiraglia DJ, Rush LJ, Robertson GP, Gao X, Wright FA, Feramisco JD, Peltomaki P, Lang JC, Schuller DE, Yu L, Bloomfield CD, Caligiuri MA, Yates A, Nishikawa R, Su Huang H, Petrelli NJ, Zhang X, O'Dorisio MS, Held WA, Cavenee WK, Plass C. Aberrant CpG-island methylation has non-random and tumour-type-specific patterns. Nat Genet. 2000; 24:132-8.

Day NE. The geographic pathology of cancer of the oesophagus. Br. Med. Bull 1984; 40: 329-334

Debant A, Serra-Pages C, Seipel K, O'Brien S, Tang M, Park SH, Streuli M. The multidomain protein Trio binds the LAR transmembrane tyrosine phosphatase, contains a protein kinase domain, and has separate rac-specific and rho-specific guanine nucleotide exchange factor domains. Proc Natl Acad Sci U S A. 1996; 93:5466-71.

de Bolla AR, Shave RM, Fagg SL, Heald K, Hughes MA, Wallace DM, Edwards PD. The influence of retinoic acid receptor (RAR) status of bladder tumours on the course of the disease. Br J Urol. 1985; 57:676-9.

de The H, Marchio A, Tiollais P, Dejean A. Differential expression and ligand regulation of the retinoic acid receptor alpha and beta genes. EMBO J. 1989; 8:429-33.

Dietzsch, E, Parker MI. Infrequent somatic deletion of the 5' region of the COL1A2 gene in oesophageal squamous cell cancer patients. Clin. Chem. Lab Med 2002; 40: 941-945

Druker BJ. STI571 (Gleevec) as a paradigm for cancer therapy. Trends Mol Med. 2002; 8:S14-8.

Estrach S, Schmidt S, Diriong S, Penna A, Blangy A, Fort P, Debant A. The Human Rho-GEF trio and its target GTPase RhoG are involved in the NGF pathway, leading to neurite outgrowth. Curr Biol. 2002; 12:307-12.

Evron E, Dooley WC, Umbricht CB, Rosenthal D, Sacchi N, Gabrielson E, Soito AB, Hung DT, Ljung B, Davidson NE, Sukumar S. Detection of breast cancer cells in ductal lavage fluid by methylation-specific PCR. Lancet. 2001; 357:1335-6.

Farber E. The multistep nature of cancer development. Cancer Res. 1984; 44:4217-23.

Finn AJ, Feng G, Pendergast AM. Postsynaptic requirement for Abl kinases in assembly of the neuromuscular junction. Nat Neurosci. 2003; 6:717-23.

Gallagher, SR. *Current Protocols in Molecular Biology*. 1999. Unit 10.2A, Supl. 47. John Wiley and Sons, Massachusetts, USA.

Glickman, JN. Section II: Pathology and pathologic staging of esophageal cancer. Sem. Thoracic and Cardiovascuilar Surg. 2002; 15: 167-179

Gradin K, McGuire J, Wenger RH, Kvietikova I, fhitelaw ML, Toftgard R, Tora L, Gassmann M, Poellinger L. Functional interference between hypoxia and dioxin signal transduction pathways: competition for recruitment of the Arnt transcription factor. Mol Cell Biol. 1996; 16:5221-31.

Greenblatt MS, Bennett WP, Hollstein M, Harris CC. Mutations in the p53 tumor suppressor gene: clues to cancer etiology and molecular pathogenesis. Cancer Res. 1994; 54:4855-78.

Hamilton SR, Aaltonen LA. (editors). *World Health Organisation Classification of Tumours. Pathology and genetics of tumours of the digestive system.* 2000. IARC Press, Lyon, France.

Hanahan D, Weinberg RA. The hallmarks of cancer. Cell. 2000; 100: 57-70.

Hendricks, D., and Parker MI. Oesophageal cancer in Africa. IUBMB Life 2002; 53: 263-268.

Hollstein MC, Smits AM, Galiana C, Yamasaki H, Bos JL, Mandard A, Partensky C, Montesano R. Amplification of epidermal growth factor receptor gene but no evidence of ras mutations in primary human esophageal cancers. Cancer Res. 1988; 48:5119-23.

Hollstein, MC, Peri L, Manard AM, Welsh JA, Montesano R, Metcalf RA, Bak, M, Harris CC. Genetic analysis of human esophageal tumors from two high incidence geographic areas: frequent p53 base substitutions and absence of *ras* mutations. Cancer Research 1991; 51: 4102-6.

Hoogendoorn B, Coleman SL, Guy CA, Smith K, Bowen T, Buckland PR, O'Donovan MC. Functional analysis of human promoter polymorphisms. Hum Mol Genet. 2003; 12:2249-54.

Hostein I, Robertson D, DiStefano F, Workman P, Clarke PA. Inhibition of signal transduction by the Hsp90 inhibitor 17-allylamino-17-demethoxygeldanamycin results in cytostasis and apoptosis. Cancer Res. 2001; 61:4003-9.

Houle B, Rochette-Egly C, Bradley WE. Tumor-suppressive effect of the retinoic acid receptor beta in human epidermoid lung cancer cells. Proc Natl Acad Sci U S A. 1993; 90:985-9.

Iijima Y, Ito T, Oikawa T, Eguchi M, Eguchi-Ishimae M, Kamada N, Kishi K, Asano S, Sakaki Y, Sato Y. A new ETV6/TEL partner gene, ARG (ABL-related gene or ABL2), identified in an AML-M3 cell line with a t(1;12)(q25;p13) translocation. Blood. 2000; 95: 2126-31.

Isaacs JS, Jung YJ, Mimnaugh EG, Martinez A, Cuttitta F, Neckers LM. Hsp90 regulates a von Hippel Lindau-independent hypoxia-inducible factor-1 alpha-degradative pathway. J Biol Chem. 2002; 277:29936-44.

Ivanova T, Petrenko A, Gritsko T, Vinokourova S, Eshilev E, Kobzeva V, Kisseljov F, Kisseljova N. Methylation and silencing of the retinoic acid receptor-beta 2 gene in cervical cancer. BMC Cancer. 2002; 2:4.

Jiang W, Zhang YJ, Kahn SM, Hollstein MC, Santella RM, Lu SH, Harris CC, Montesano R, Weinstein IB. Altered expression of the cyclin D1 and retinoblastoma genes in human esophageal cancer. Proc Natl Acad Sci U S A. 1993; 90: 9026-30.

Jutterman R, Li E, Jaenisch R. Toxicity of 5-aza-2'-deoxycytidine to mammalian cells is mediated primarily by covalent trapping of DNA methyltransferase rather than DNA demethylation. Proc. Natl. Acad. Sci. USA 1994 91:11797-11801

Kain KH, Klemke RL. Inhibition of cell migration by Abl family tyrosine kinases through uncoupling of Crk-CAS complexes. J Biol Chem. 2001; 276:16185-92.

Karpf AR, Jones DA. Reactivating the expression of methylation silenced genes in human cancer. Oncogene. 2002; 21:5496-503.

Katayama A, Mafune K, Tanaka Y, Takubo K, Makuuchi M, Kaminishi M. Autopsy findings in patients after curative esophagectomy for esophageal carcinoma. J Am Coll Surg. 2003; 196:866-73.

Khuri FR, Lotan R, Kemp BL, Lippman SM, Wu H, Feng L, Lee JJ, Cooksley CS, Parr B, Chang E, Walsh GL, Lee JS, Hong WK, Xu XC. Retinoic acid receptor-beta as a prognostic indicator in stage I non-small-cell lung cancer. J Clin Oncol. 2000; 18:2798-804.

Kim NW. Clinical implications of telomerase in cancer. Eur J Cancer. 1997; 33:781-6.

Kim R, Weissfeld JL, Reynolds JC, Kuller LH. Etiology of Barrett's metaplasia and esophageal adenocarcinoma. Cancer Epidemiol Biomarkers Prev. 1997; 6:369-77.

Kleinberg, L., Knisely JP, Heitmiller R, Zahurak M, Salem R, Burtness B, Heath EI, Fotastiere AA. Mature survival results with preoperative cisplatin, protracted infusion 5-fluorouracil, and 44-Gy radiotherapy for esophageal cancer. International Journal of Oncology and Biological Physiology 2003; 56: 328- 34.

Koleske AJ, Gifford AM, Scott ML, Nee M, Bronson RT, Miczek KA, Baltimore D. Essential roles for the Abl and Arg tyrosine kinases in neurulation. Neuron. 1998; 21:1259-72.

Kruh GD, King CR, Kraus MH, Popescu NC, Amsbaugh SC, McBride WO, Aaronson SA. A novel human gene closely related to the abl proto-oncogene. Science. 1986; 234:1545-8.

Kruh GD, Perego R, Miki T, Aaronson SA. The complete coding sequence of arg defines the Abelson subfamily of cytoplasmic tyrosine kinases. Proc Natl Acad Sci U S A. 1990; 87:5802-6.

Krystal GW, Honsawek S, Litz J, Buchdunger E. The selective tyrosine kinase inhibitor STI571 inhibits small cell lung cancer growth. Clin Cancer Res. 2000; 6:3319-26.

Kukreja J, Jaklitsch MT. Section IV: selective use of neoadjuvant therapy. Semin Thorac Cardiovasc Surg. 2003; 15:187-96.

Kumar S, Dimri K, Datta NR, Rastogi N, Lal P, Das KJ, Ayyagari S. Safety and efficacy of concurrent cisplatin and radiotherapy in inoperable or metastatic squamous cell esophageal cancer. Acta Oncol. 2002; 41:457-62.

Kuroki T, Trapasso F, Yendamuri S, Matsuyama A, Alder H, Mori M, Croce CM. Allele loss and promoter hypermethylation of VHL, RAR-beta, RASSF1A, and FHIT tumor suppressor genes on chromosome 3p in esophageal squamous cell carcinoma. Cancer Res. 2003; 63:3724-8.

Lam, AK. Molecular biology of esophageal squamous cell carcinoma. Crit. Rev. Onc./ Heamatol. 2002; 33: 71- 90.

Laird PW. The power and the promise of DNA methylation markers. Nat Rev Cancer. 2003; 3:253-66.

Lanier LM, Gertler FB. From Abl to actin: Abl tyrosine kinase and associated proteins in growth cone motility. Curr Opin Neurobiol. 2000; 10:80-7.

Lewin,B. *Genes VI*. 1997. Oxford University Press, New York

Li RM, Lu YK, Chen HY, Gu YZ, Yang J, Hu JQ. Late results of surgical treatment in esophageal carcinoma and factors influencing prognosis. Chin Med J (Engl). 1981; 94:729-32.

Li Y, Shimizu H, Xiang SL, Maru Y, Takao N, Yamamoto K. Arg tyrosine kinase is involved in homologous recombinational DNA repair. Biochem Biophys Res Commun. 2002; 299:697-702.

Li J, Kleeff J, Guo J, Fischer L, Giese N, Buchler MW, Friess H. Effects of STI571 (gleevec) on pancreatic cancer cell growth. Mol Cancer. 2003; 2:32.

Lieb M, Rehmat S. 5-Methylcytosine is not a mutation hot spot in nondividing Escherichia coli. Proc Natl Acad Sci U S A. 1997; 94:940-5

Liebl EC, Forsthoefel DJ, Franco LS, Sample SH, Hess JE, Cowger JA, Chandler MP, Shupert AM, Seeger MA. Dosage-sensitive, reciprocal genetic interactions between the Abl tyrosine kinase and the putative GEF trio reveal trio's role in axon pathfinding. Neuron. 2000; 26:107-18.

Linden PA, Sugarbaker DJ. Section V: techniques of esophageal resection. Semin Thorac Cardiovasc Surg. 2003; 15:197-209.

Livak KJ, Schmittgen TD. Analysis of relative gene expression data using real-time quantitative PCR and the 2(-Delta Delta C(T)) Method. Methods. 2001; 25:402-8.

Lotan R, Xu XC, Lippman SM, Ro JY, Lee JS, Lee JJ, Hong WK. Suppression of retinoic acid receptor-beta in premalignant oral lesions and its up-regulation by isotretinoin. N Engl J Med. 1995; 332:1405-10.

Lotan R. Retinoids in cancer chemoprevention. FASEB J. 1996; 10:1031-9.

Lotan Y, Xu XC, Shalev M, Lotan R, Williams R, Wheeler TM, Thompson TC, Kadmon D. Differential expression of nuclear retinoid receptors in normal and malignant prostates. J Clin Oncol. 2000; 18:116-21.

Lu SH, Hsieh LL, Luo FC, Weinstein IB. Amplification of the EGF receptor and c-myc genes in human esophageal cancers. Int J Cancer. 1988; 42:502-5.

Maloney A, Workman P. HSP90 as a new therapeutic target for cancer therapy: the story unfolds. Expert Opin Biol Ther. 2002; 2:3-24.

Mandard AM, Hainaut P, Hollstein M. Genetic steps in the development of squamous cell carcinoma of the esophagus. Mutat Res. 2000; 462:335-42.

Marasas WF. Discovery and occurrence of the fumonisins: a historical perspective. Environ Health Perspect. 2001; 109 Suppl 2:239-43.

Matsha T, Erasmus R, Kafuko AB, Mugwanya D, Stepien A, Parker MI; CANSA/MRC Oesophageal Cancer Research Group. Human papillomavirus associated with oesophageal cancer. J Clin Pathol. 2002; 55:587-90.

McGary EC, Weber K, Mills L, Doucet M, Lewis V, Lev DC, Fidler IJ, Bar-Eli M. Inhibition of platelet-derived growth factor-mediated proliferation of osteosarcoma cells by the novel tyrosine kinase inhibitor STI571. Clin Cancer Res. 2002; 8:3584-91.

Medley QG, Buchbinder EG, Tachibana K, Ngo H, Serra-Pages C, Streuli M. Signaling between focal adhesion kinase and trio. J Biol Chem. 2003; 278:13265-70.

Meltzer SJ. The molecular biology of esophageal carcinoma. Recent Results Cancer Res. 1996;142:1-8.

Mettlin C, Graham S, Priore R, Marshall J, Swanson M. Diet and cancer of the esophagus. Nutr Cancer. 1981; 2:143-7.

Mosmann T, Rapid colorimetric assay for cellular growth and survival: application to proliferation and cytotoxicity assays. J Immuno Methods. 1983; 65: 55- 63.

Mqoqi N, Kellet P, Madhoo J, Sitas F. *Incidence of histologically diagnosed cancer in South Africa 1996- 1997.* 2003, National Health Laboratory Service, Johannesburg.

Mugwanya D, Stepien A, Targonska IBJ, Kafuko A, Mdondolo N. The Umtata polulation based cancer registry (1996- 1999). Oesophageal Cancer Consortium conference Abstracts. 2001.

Nagpal S, Zelent A, Chambon P. RAR-beta 4, a retinoic acid receptor isoform is generated from RAR-beta 2 by alternative splicing and usage of a CUG initiator codon. Proc Natl Acad Sci U S A. 1992; 89:2718-22.

Nakachi K, Imai K, Hoshiyama Y, Sasaba T. The joint effects of two factors in the aetiology of oesophageal cancer in Japan. J Epidemiol Community Health. 1988; 42:355-64.

Neckers L. Hsp90 inhibitors as novel cancer chemotherapeutic agents. Trends Mol Med. 2002; 8(4 Suppl):S55-61

Ng HH and Bird A. DNA methylation and chromatin modification. Curr Opin Genet Dev. 1999; 9: 158- 163.

Nguyen DM, Desai S, Chen A, Weiser TS, Schrump DS. Modulation of metastasis phenotypes of non-small cell lung cancer cells by 17-allylamino 17-demethoxy geldanamycin. Ann Thorac Surg. 2000; 70:1853-60.

Nimmanapalli R, O'Bryan E, Kuhn D, Yamaguchi H, Wang HG, Bhalla KN. Regulation of 17-AAG-induced apoptosis: role of Bcl-2, Bcl-XL, and Bax downstream of 17-AAG-mediated down-regulation of Akt, Raf-1, and Src kinases. Blood. 2003; 102:269-75.

O'Brien SP, Seipel K, Medley QG, Bronson R, Segal R, Streuli M. Skeletal muscle deformity and neuronal disorder in Trio exchange factor-deficient mouse embryos. Proc Natl Acad Sci U S A. 2000; 97:12074-8.

Pacella-Norman R, Urban MI, Sitas F, Carrara H, Sur R, Hale M, Ruff P, Patel M, Newton R, Bull D, Beral V. Risk factors for oesophageal, lung, oral and laryngeal cancers in black South Africans. Br J Cancer. 2002; 86:1751-6.

Pendergast AM. The Abl family kinases: mechanisms of regulation and signaling. Adv Cancer Res. 2002; 85:51-100.

Perego R, Ron D, Kruh GD. Arg encodes a widely expressed 145 kDa protein-tyrosine kinase. Oncogene. 1991; 6:1899-902. Erratum in: Oncogene 1992; 7:607.

Qiu H, Zhang W, El-Naggar AK, Lippman SM, Lin P, Lotan R, Xu XC. Loss of retinoic acid receptor-beta expression is an early event during esophageal carcinogenesis. Am J Pathol. 1999; 155:1519-23.

Rideout WM 3rd, Coetzee GA, Olumi AF, Jones PA. 5-Methylcytosine as an endogenous mutagen in the human LDL receptor and p53 genes. Science. 1990; 249:1288-90.

Robertson KD, Jones PA. DNA methylation: past, present and future directions. Carcinogenesis. 2000; 21:461-7.

Roche-Lestienne C, Soenen-Cornu V, Grardel-Duflos N, Lai JL, Philippe N, Facon T, Fenaux P, Preudhomme C. Several types of mutations of the Abl gene can be found in chronic myeloid leukemia patients resistant to STI571, and they can pre-exist to the onset of treatment. Blood. 2002; 100:1014-8.

Rochette-Egly C, Lutz Y, Saunders M, Scheuer I, Gaub MP, Chambon P. Retinoic acid receptor gamma: specific immunodetection and phosphorylation. J Cell Biol. 1991; 115:535-45.

Rozen S, Skaletsky HJ. Primer3 on the WWW for general users and for biologist programmers. In: Krawetz S, Misener S (eds) *Bioinformatics Methods and Protocols: Methods in Molecular Biology*. 2003. Humana Press, Totowa, NJ, pp 365-386.

Sambrook J, Fritsch EF, Maniatis T. Molecular Cloning: A Laboratory Manual, 2nd edition. 1989. Cold Springs Harbor Laboratory Press, New York.

Samoszuk M, Corwin MA. Acceleration of tumor growth and peri-tumoral blood clotting by imatinib mesylate (Gleevec). Int J Cancer. 2003; 106:647-52.

Sawyers CL. Rational therapeutic intervention in cancer: kinases as drug targets. Curr Opin Genet Dev. 2002; 12:111-5.

Schmidt S, Diriong S, Mery J, Fabbrizio E, Debant A. Identification of the first Rho-GEF inhibitor, TRIPalpha, which targets the RhoA-specific GEF domain of Trio. FEBS Lett. 2002; 523:35-42.

Seipel K, Medley QG, Kedersha NL, Zhang XA, O'Brien SP, Serra-Pages C, Hemler ME, Streuli M. Trio amino-terminal guanine nucleotide exchange factor domain expression promotes actin cytoskeleton reorganization, cell migration and anchorage-independent cell growth. J Cell Sci. 1999; 112:1825-34.

Seipel K, O'Brien SP, Iannotti E, Medley QG, Streuli M. Tara, a novel F-actin binding protein, associates with the Trio guanine nucleotide exchange factor and regulates actin cytoskeletal organization. \J Cell Sci. 2001; 114:389-99.

Shen JC, Rideout WM 3rd, Jones PA. The rate of hydrolytic deamination of 5-methylcytosine in double-stranded DNA. Nucleic Acids Res. 1994; 22:972-6.

Sherr CJ. Cancer cell cycles. Science. 1996; 274:1672-7.

Shimada Y, Imamura M, Wagata T, Yamaguchi N, Tobe T. Characterization of 21 newly established esophageal cancer cell lines. Cancer. 1992; 69:277-84. Erratum in: Cancer 1992; 70:206.

Shintani M, Okazaki A, Masuda T, Kawada M, Ishizuka M, Doki Y, Weinstein IB, Imoto M. Overexpression of cyclin DI contributes to malignant properties of esophageal tumor cells by increasing VEGF production and decreasing Fas expression. Anticancer Res. 2002; 22:639-47.

Siddik ZH. Cisplatin: mode of cytotoxic action and molecular basis of resistance. Oncogene. 2003; 22:7265-79.

Sirchia SM, Ren M, Pili R, Sironi E, Somenzi G, Ghidoni R, Toma S, Nicolo G, Sacchi N. Endogenous reactivation of the RARbeta2 tumor suppressor gene epigenetically silenced in breast cancer. Cancer Res. 2002; 62:2455-61.

Sitas F, Bezwoda WR, Levin V, Ruff P, Kew MC, Hale MJ, Carrara H, Beral V, Fleming G, Odes R, Weaving A. Association between human immunodeficiency virus type 1 infection and cancer in the black population of Johannesburg and Soweto, South Africa. Br J Cancer. 1997; 75:1704-7.

Smiraglia DJ, Rush LJ, Fruhwald MC, Dai Z, Held WA, Costello JF, Lang JC, Eng C, Li B, Wright FA, Caligiuri MA, Plass C. Excessive CpG island hypermethylation in cancer cell lines versus primary human malignancies. Hum Mol Genet. 2001;10:1413-9.

Sommer KM, Chen LI, Treuting PM, Smith LT, Swisshelm K. Elevated retinoic acid receptor beta(4) protein in human breast tumor cells with nuclear and cytoplasmic localization. Proc Natl Acad Sci U S A. 1999; 96:8651-6.

Suh YA, Lee HY, Virmani A, Wong J, Mann KK, Miller WH Jr, Gazdar A, Kurie JM. Loss of retinoic acid receptor beta gene expression is linked to aberrant histone H3 acetylation in lung cancer cell lines. Cancer Res. 2002; 62:3945-9.

Sun SY, Lotan R. Retinoids and their receptors in cancer development and chemoprevention. Crit Rev Oncol Hematol. 2002; 41:41-55.

Szyf M, Detich N. Regulation of the DNA methylation machinery and its role in cellular transformation. Prog Nucleic Acid Res Mol Biol. 2001;69:47-79.

Toulouse A, Morin J, Pelletier M, Bradley WE. Structure of the human retinoic acid receptor beta 1 gene. Biochim Biophys Acta. 1996; 1309:1-4.

Uray IP, Connelly JH, Thomazy V, Shipley GL, Vaughn WK, Frazier OH, Taegtmeyer H, Davies PJ. Left ventricular unloading alters receptor tyrosine kinase expression in the failing human heart. J Heart Lung Transplant. 2002; 21:771-82.

Ursic-Vrscaj M, Kovacic J, Poljak M, Marin J. Association of risk factors for cervical cancer and human papilloma viruses in invasive cervical cancer. Eur J Gynaecol Oncol. 1996;17:368-71.

Van Etten RA, Jackson PK, Baltimore D, Sanders MC, Matsudaira PT, Janmey PA. The COOH terminus of the c-Abl tyrosine kinase contains distinct F- and G-actin binding domains with bundling activity. J Cell Biol. 1994;124:325-40. Erratum in: J Cell Biol 1994;124:865.

Vasilevskaya IA, Rakitina TV, O'Dwyer PJ. Geldanamycin and its 17-allylamino-17-demethoxy analogue antagonize the action of Cisplatin in human colon adenocarcinoma cells: differential caspase activation as a basis for interaction. Cancer Res. 2003; 63:3241-6.

Veale RB, Thornley AL. Increased single class low-afinity EGF receptors expressed by human oesophageal squamous cell carcinoma cell lines. S Afr J Sci. 1989; 85: 375- 379.

Verweij J, van Oosterom A, Blay JY, Judson I, Rodenhuis S, van der Graaf W, Radford J, Le Cesne A, Hogendoorn PC, di Paola ED, Brown M, Nielsen OS. Imatinib mesylate (STI-571 Glivec, Gleevec) is an active agent for gastrointestinal stromal tumours, but does not yield responses in other soft-tissue sarcomas that are unselected for a molecular target. Results from an EORTC Soft Tissue and Bone Sarcoma Group phase II study. Eur J Cancer. 2003; 39:2006-11.

Villa R, Folini M, Porta CD, Valentini A, Pennati M, Daidone MG, Zaffaroni N. Inhibition of telomerase activity by geldanamycin and 17-allylamino, 17-demethoxygeldanamycin in human melanoma cells. Carcinogenesis. 2003; 24:851-9.

Wamunyokoli FAW. Differentially expressed genes in oesophageal cancer. 2002. PhD Thesis, UCT.

Wang B, Kruh GD. Subcellular localization of the Arg protein tyrosine kinase. Oncogene. 1996; 13:193-7.

Wang Y, Miller AL, Mooseker MS, Koleske AJ. The Abl-related gene (Arg) nonreceptor tyrosine kinase uses two F-actin-binding domains to bundle F-actin. Proc Natl Acad Sci U S A. 2001; 98:14865-70.

Weisberg E, Griffin JD. Mechanism of resistance to the ABL tyrosine kinase inhibitor STI571 in BCR/ABL-transformed hematopoietic cell lines. Blood. 2000; 95:3498-505.

Widschwendter M, Berger J, Hermann M, Muller HM, Amberger A, Zeschnigk M, Widschwendter A, Abendstein B, Zeimet AG, Daxenbichler G, Marth C. Methylation and silencing of the retinoic acid receptor-beta2 gene in breast cancer. J Natl Cancer Inst. 2000; 92:826-32.

Wong IH, Lo YM, Zhang J, Liew CT, Ng MH, Wong N, Lai PB, Lau WY, Hjelm NM, Johnson PJ. Detection of aberrant p16 methylation in the plasma and serum of liver cancer patients. Cancer Res. 1999; 59:71-3.

Wu CW, Li AF, Chi CW, Huang CJ, Huang CL, Lui WY, Lin WC. Arg tyrosine kinase expression in human gastric adenocarcinoma is associated with vessel invasion. Anticancer Res. 2003; 23:205-10.

Xu XC, Ro JY, Lee JS, Shin DM, Hong WK, Lotan R. Differential expression of nuclear retinoid receptors in normal, premalignant, and malignant head and neck tissues. Cancer Res. 1994; 54:3580-7.

Xu XC, Sneige N, Liu X, Nandagiri R, Lee JJ, Lukmanji F, Hortobagyi G, Lippman SM, Dhingra K, Lotan R. Progressive decrease in nuclear retinoic acid receptor beta messenger RNA level during breast carcinogenesis. Cancer Res. 1997; 57:4992-6.

Xu XC. Detection of altered retinoic acid receptor expression in tissue sections using in situ hybridization. Histol Histopathol. 2001;16:205-12.

Yoshida K, Kyo E, Tsuda T, Tsujino T, Ito M, Niimoto M, Tahara E. EGF and TGF-alpha, the ligands of hyperproduced EGFR in human esophageal carcinoma cells, act as autocrine growth factors. Int J Cancer. 1990; 45:131-5.

Yoshida R, Nakajima M, Nishimura K, Tokudome S, Kwon JT, Yokoi T. Effects of polymorphism in promoter region of human CYP2A6 gene (CYP2A6*9) on expression level of messenger ribonucleic acid and enzymatic activity in vivo and in vitro. Clin Pharmacol Ther. 2003; 74:69-76.

Zelent A, Mendelsohn C, Kastner P, Krust A, Garnier JM, Ruffenach F, Leroy P, Chambon P. Differentially expressed isoforms of the mouse retinoic acid receptor beta generated by usage of two promoters and alternative splicing. EMBO J. 1991;10:71-81.

Zeschnigk M, Lich C, Buiting K, Doerfler W, Horsthemke B. A single tube PCR test for the diagnosis of Angelman and Prader-Willi syndrome based on allelic methylation differences at SNRPN locus. Eur J Human Genetics. 1997; 5:94- 98.

Zhang P, Gao WY, Turner S, Ducatman BS. Gleevec (STI-571) inhibits lung cancer cell growth (A549) and potentiates the cisplatin effect in vitro. Mol Cancer. 2003; 2:1.

Zhuang Y, Faria TN, Chambon P, Gudas LJ. Identification and Characterization of Retinoic Acid Receptor beta(2) Target Genes in F9 Teratocarcinoma Cells. Mol Cancer Res. 2003; 1:619-30.

Zou HZ, Yu BM, Wang ZW, Sun JY, Cang H, Gao F, Li DH, Zhao R, Feng GG, Yi J. Detection of aberrant p16 methylation in the serum of colorectal cancer patients. Clin Cancer Res. 2002; 8:188-91.